

# Optical dissection of amygdalar network dynamics related to stress, anxiety, and pharmacological treatment

Dissertation  
der Fakultät für Biologie  
der Ludwig-Maximilians-Universität München

vorgelegt von  
Florian Hladky



München, 7. November 2013

1. Gutachter: Prof. Rainer Landgraf

2. Gutachter: Prof. George Boyan

Tag der mündlichen Prüfung: 10. April 2014

“Nevertheless the difference in mind between man and the higher animals, great as it is, certainly is one of degree and not of kind. We have seen that the senses and intuitions, the various emotions and faculties, such as love, memory, attention, curiosity, imitation, reason, etc., of which man boasts, may be found in an incipient, or even sometimes in a well-developed condition, in the lower animals.”

(Darwin, 1871), *Descent of Man*, page 105

## Zusammenfassung

Zum limbischen System gehören Gehirnregionen, die unter anderem an der Verarbeitung von Informationen beteiligt sind, die mit Angst und Furcht in Verbindung gebracht werden können. Zu diesem System gehören der Hippokampus, der mediale präfrontale Kortex und die Amygdala. Die neuronalen Netzwerke des limbischen Systems modulieren im Anschluss an diese Informationsverarbeitung unter anderem die Stressreaktion durch ihre Interaktion mit dem Nucleus paraventricularis des Hypothalamus, dessen Neurone "Corticotropin-releasing hormone" (CRH) ausschütten. CRH stimuliert die Produktion von Kortikosteroiden in der Glandula adrenalis, die das Verhalten, das Immunsystem und den Energiehaushalt beeinflussen.

Die neuronalen Netzwerke des limbischen Systems und die Hirnregionen mit denen sie interagieren sind an der Pathophysiologie von Angststörungen beteiligt. Dieser Zusammenhang wurde in Tiermodellen gezeigt, indem die elektrische Aktivität bestimmter Regionen des limbischen Systems mit Angst- und Furcht-assoziiertem Verhalten korreliert werden konnte. Eine wichtige Rolle hierbei spielt die laterale (LA) und basolaterale (BLA) Amygdala.

In diesem Kontext gibt es aus neurobiologischer Sicht eine Wissenslücke zwischen der Aktivität und Plastizität einzelner Neurone und den damit verbundenen Veränderungen des gesamten Netzwerkes als Prozessierungseinheit. Der Grund hierfür ist teilweise das unvollständige Wissen über den Aufbau der entsprechenden neuronalen Netzwerke.

Für die Untersuchung der Aktivität und Plastizität von anatomisch klar definierten Netzwerken der LA und BLA wurde ein *in vitro* "Voltage-sensitive dye imaging" (VSDI)-basiertes Messverfahren in Hirnschnitten von Mäusen entwickelt und die gewonnenen Daten unter Verwendung eines eigens programmierten Algorithmus analysiert. Damit konnte gezeigt werden, dass innerhalb des neuronalen Netzwerkes der LA unter Verwendung desselben elektrischen Stimulationsprotokolls (hochfrequente Stimulation (HFS)), das bekannt dafür ist neuronale Plastizität zu induzieren, gegensätzliche und räumlich voneinander getrennte Veränderungen in der Aktivitätsstärke hervorgerufen werden können. Auf diesem Befund aufbauend wurde untersucht ob Mediatoren der Stressreaktion diese Art der Plastizität beeinflussen. Es wurde beobachtet, dass CRH das Verhältnis von HFS-vermittelter

Potenzierung und Depression der Aktivität in der LA konzentrationsabhängig in Richtung der Potenzierung verschiebt. Darüber hinaus konnte gezeigt werden, dass "Corticotropin-releasing hormone receptor type 1" (CRHR1) an diesem Effekt beteiligt ist.

Ähnliche Befunde ergab die Applikation von Kortikosteron unter Verwendung dieses experimentellen Ansatzes. Es konnte sowohl in der LA, als auch in der BLA gezeigt werden, dass dieses Stresshormon die basale neuronale Netzwerkaktivität erhöht. Außerdem wurde die Potenzierung der Netzwerkaktivität durch Kortikosteron erhöht. In einer weiteren Experimentserie wurde die Stärke der Netzwerkpotenzierung in Gehirnschnitten von Mäusen miteinander verglichen, die sich in Bezug auf ihr Angstverhalten unterscheiden. Es konnte gezeigt werden, dass das neuronale Netzwerk der BLA in Hirnschnitten von ängstlichen Mäusen stärker durch HFS potenziert wird, als das Netzwerk der BLA von Mäusen, die weniger Angst zeigen.

Abschließend wurden unterschiedliche Klassen von Pharmazeutika (Selektive Serotonin-Wiederaufnahmehemmer (SSRIs), Serotonin-Noradrenalin-Wiederaufnahmehemmer (SNRIs), Trizyklische Antidepressiva (TCAs) und Antipsychotika) im Hinblick auf ihren Einfluss auf die basale Netzwerkaktivität der LA und BLA untersucht. Die Ergebnisse zeigten, dass diese Substanzklassen die Netzwerkaktivität in der LA und BLA abschwächen.

In der Zusammenschau all dieser Befunde konnte ein Zusammenhang zwischen Stress und erhöhter Aktivität in einer Gehirnregion hergestellt werden, die mit Furcht im Zusammenhang steht. Außerdem konnte eine Verbindung zwischen einem ängstlichen Verhaltensphänotypen und einer netzwerkspezifischen Informationsverarbeitung dargelegt werden. Darüber hinaus konnten neue Erkenntnisse bezüglich des Wirkungsprofils von verschiedenen Klassen von Pharmazeutika (SSRIs, SNRIs, TCAs und Antipsychotika) auf der Ebene der Regulation der Aktivität von neuronalen Netzen gewonnen werden. Diese Befunde können dazu beitragen die Wissenslücke zwischen der Aktivität von Neuronen bzw. neuronalen Netzen und Furcht bzw. Angst zu schließen.

## Abstract

The limbic system comprises brain structures that are involved in the processing of information related to fear and anxiety. This system contains the hippocampus, the medial prefrontal cortex and the amygdala. Downstream of this information processing, limbic circuits modulate, among others, the stress responses via their interaction with the paraventricular nucleus of the hypothalamus. Subsequently, neurons of this nucleus release corticotropin-releasing hormone (CRH), which in turn enhances the production of corticosteroids by the adrenal glands. This affects behaviour, the immune response and energy homeostasis.

The limbic brain nuclei and their output targets can be associated to the pathophysiology of anxiety disorders. This involvement has been shown by use of animal models, where the activity of distinct subfields of the limbic system could be correlated with occurrence of fear- and anxiety-like behaviour. The lateral (LA) and basolateral (BLA) nuclei of the amygdala display such changes in activity upon the expression of associated behaviour.

On the neurobiological level, a gap of knowledge exists between changes in the activity and plasticity of single neurons and the concomitant changes of the network as a whole processing unit. This gap is partially due to the incomplete knowledge of the neuronal circuitry.

To investigate network activity and plasticity in these nuclei *in vitro*, a voltage-sensitive dye imaging assay in conjunction with advanced data processing was developed for mouse brain slices, reliably containing distinct parts of the LA and BLA. By this means, we showed that these neuronal networks respond spatially segregated to the same plasticity-inducing stimulus (i.e. high-frequency stimulation (HFS)) in opposite ways. Based on these findings, the effect of mediators of the stress responses was investigated on network plasticity. CRH, in a concentration-dependent manner, reshaped the LA responses induced by HFS by shifting the balance between potentiation and depression in the direction of potentiation. Furthermore, we demonstrated that corticotropin-releasing hormone receptor type 1 (CRHR1) is involved in mediating these plastic changes.

The application of corticosterone within the same paradigm has shown that this stress hormone increases the strength of basal neuronal network activity and the magnitude of potentiation in the LA and BLA. Furthermore, the use of brain slices

from inbred mouse lines that differ with respect to their anxiety-related behaviour revealed that the strength of network potentiation is increased in the BLA of animals showing high anxiety-related behaviour. Finally, distinct classes of pharmaceuticals (selective serotonin reuptake inhibitors (SSRIs), serotonin noradrenalin reuptake inhibitors (SNRIs), tricyclic antidepressants (TCAs), and antipsychotics) were used to investigate their putative role in the regulation of the activity in the LA and BLA, and it could be shown that these substances are capable of dampening LA and BLA network activity.

To conclude, this study provides evidence for a link between stress and an increased cue-responsiveness of a fear-mediating brain structure and also links a pathological and stable anxious phenotype with differences in the memory-encoding capacity of this system. Furthermore, it gives insights into the method of action of distinct classes of commonly used pharmaceutical components (SSRIs, SNRIs, TCAs, and antipsychotics) on a neuronal network level. These data might help to further bridge the knowledge gap between neuronal network activity and fear- and anxiety-related behaviour.

## Contents

	Page no.
<b>1. Introduction</b>	<b>1</b>
<b>1.1 The limbic system in the mammalian brain</b>	<b>1</b>
<b>1.2 The brain circuitry of fear and anxiety</b>	<b>1</b>
<b>1.3 The HPA axis</b>	<b>3</b>
<b>1.4 Psychiatric disorders that are related to fear and anxiety</b>	<b>4</b>
1.4.1 Mouse models of anxiety disorders	5
<b>1.5 The amygdala</b>	<b>7</b>
1.5.1 Overview of anatomical subdivisions of the amygdala	8
1.5.2 Anatomical organization of amygdalar key nuclei	9
1.5.3 Functional connectivity within amygdalar key nuclei	10
1.5.3.1 Neuronal plasticity	14
1.5.3.2 Mediators of the stress responses and their influence on neuronal network activity and plasticity in the LA and BLA	16
1.5.3.3 Pharmacological intervention	17
<b>1.6 Working hypothesis</b>	<b>19</b>
<b>2. Material and Methods</b>	<b>20</b>
<b>2.1 Mice</b>	<b>20</b>
<b>2.2 Preparation of brain slices</b>	<b>21</b>
<b>2.3 VSDI</b>	<b>22</b>
<b>2.4 Advanced data processing</b>	<b>26</b>
<b>2.5 Field potential recordings</b>	<b>29</b>
<b>3. Results</b>	<b>31</b>
<b>3.1 Development of VSDI assay</b>	<b>31</b>
<b>3.2 Investigation of neuronal network dynamics</b>	<b>36</b>
3.2.1 Field potential recordings	36
3.2.2 Monitoring of network dynamics by means of VSDI and subsequent data processing	37
3.2.2.1 Pharmacological characterization of changes in network dynamics	41
3.2.3 Investigation of the effect of CRH on network activity and dynamics in the LA and BLA	44
3.2.3.1 Involvement of CRHR1 in CRH-induced changes in network activity and dynamics in the LA and BLA	48

3.2.4 Investigation of the effect of Cort on network activity and dynamics in the LA and BLA	52
3.2.5 Comparison of network dynamics in amygdalar slices obtained from HAB and NAB mice	54
<b>3.3 Pharmaceutical treatment</b>	<b>55</b>
<b>4. Discussion</b>	<b>59</b>
<b>4.1 Slicing procedure and qualitative/quantitative investigation of signal propagation within the amygdalar neuronal network</b>	<b>59</b>
<b>4.2 Investigation of neuronal network dynamics</b>	<b>61</b>
4.2.1 Verification of induction protocol	61
4.2.2 Detection of amygdalar network dynamics by means of VSDI and data processing of VSDI movies	61
4.2.2.1 Pharmacological characterization of changes in network dynamics	63
4.2.3 Effect of CRH on LA and BLA network activity and dynamics	64
4.2.3.1 Dissection of the involvement of CRHR1 in the observed changes in network activity and dynamics	67
4.2.4 Effect of Cort on LA and BLA network activity and dynamics	69
4.2.5 Differences in network dynamics in the LA and BLA of HAB/NAB mice	70
<b>4.3 Pharmaceutical treatment</b>	<b>71</b>
<b>5. Conclusion</b>	<b>75</b>
<b>6. References</b>	<b>76</b>
<b>7. Appendix 1</b>	<b>90</b>
<b>8. Abbreviations</b>	<b>92</b>
<b>9. List of figures</b>	<b>95</b>
<b>10. Publications</b>	<b>98</b>
<b>11. Curriculum Vitae</b>	<b>99</b>
<b>12. Danksagung</b>	<b>100</b>
<b>13. Erklärung</b>	<b>101</b>

## **1 Introduction**

### **1.1 The limbic system in the mammalian brain**

In the 1930s, brain regions thought to be involved in the processing and expression of emotions were put together in one brain circuitry, named the "limbic system" (Adolphs, 2010). The mammalian limbic system can be described as a processing linkage between subcortical structures such as the hypothalamus, the periaqueductal gray, and nuclei of the brain stem on the one hand, and cortical regions such as sensory or motor cortices on the other hand (Adolphs, 2010). The regions frequently referred to as part of the limbic system include the hippocampus, the amygdala, the insula and the medial prefrontal cortex (Adolphs, 2010; Price and Drevets, 2010; Stein and Steckler, 2010; Cisler and Olatunji, 2012).

In the following, emphasis will be put on these limbic structures in the context of being part of a brain circuitry mediating fear and anxiety (Aggleton, 2000; LeDoux, 2007; Stein and Steckler, 2010; Adolphs, 2013).

### **1.2 The brain circuitry of fear and anxiety**

As stated above, the limbic circuitry is part of brain structures that mediate fear and anxiety comprises the amygdala, the hippocampus, the insula, and the medial prefrontal cortex.

Figure 1.2.-1 depicts this network together with some known input and output pathways. Although studies describing parts of the functional connectivity within this system have been published (Szinyei et al., 2000; Kim et al., 2011; Orsini et al., 2011), directions of information flow were intentionally excluded from this scheme to put emphasis that full knowledge of functional interconnections has not been completely deciphered.

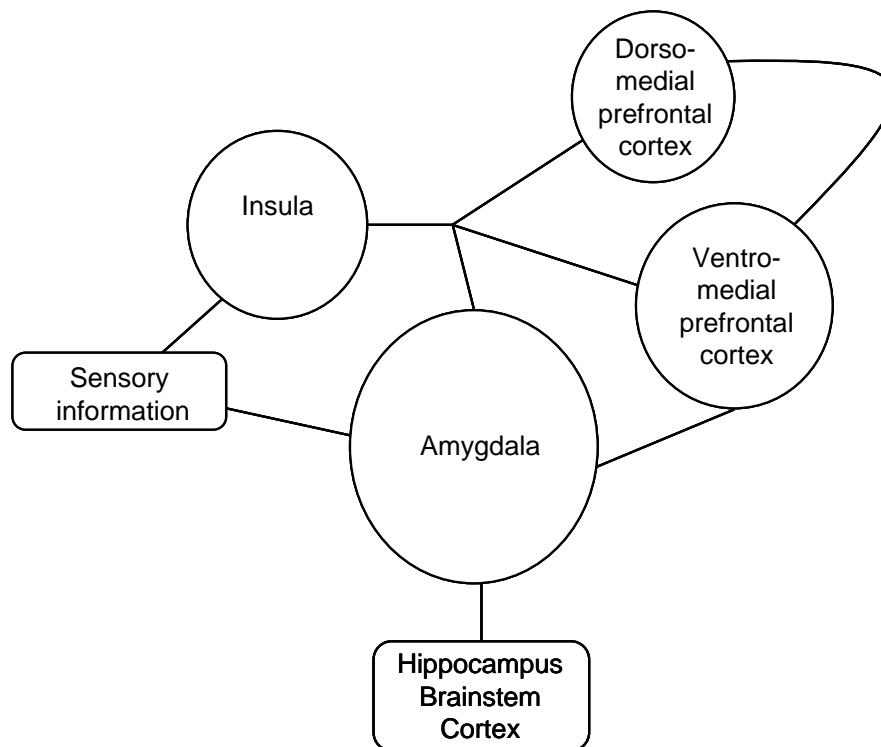


**Figure 1.2.-1. Basic scheme of the limbic brain system with known connectivity as indicated through black lines.** adapted from Stein and Steckler (2010)

Sensory afferences arising from thalamic nuclei and association cortices terminate in the amygdala and insula (LeDoux, 1991; LeDoux, 2007; Stein and Steckler, 2010). Within the amygdala, the respective signals are processed in the lateral (LA) and basolateral (BLA) nucleus (LeDoux, 1991; Szinyei et al., 2000; LeDoux, 2007; Stein and Steckler, 2010). After integration of diverse limbic inter- and intra-circuit information, the amygdala projects to the hippocampus (Andersen et al., 2007), the periaqueductal gray (LeDoux, 2007), the brainstem (Veening et al., 1984), the hypothalamus (Sah et al., 2003), striatal structures, such as the bed nucleus of the stria terminalis (Walker et al., 2009) or the ventral striatum (LeDoux, 2007), and regions of the cortex (Aggleton, 2000; LeDoux, 2007). From a functional point of view, these projections may be attributed to further signal processing (Johansen, et al., 2012), storage of information which can be related to fear memory (Ramirez, et al., 2013), contributions to the control of the bodily expression of fear (LeDoux, 2007) or anxiety (Cryan and Holmes, 2005), and the regulation of the stress responses (Fink, 2006).

The insula can be linked to the processing of sensory information related to negative emotions and also to the regulation of the autonomous nervous system in response to emotion-related stimuli (Adolphs, 2010; Stein and Steckler, 2010).

The dorsal and ventral parts of the medial prefrontal cortex are involved in the regulation of intra-limbic processing, which in turn is related to fear and fear memory (Morgan and LeDoux, 1995; Sotres-Bayon and Quirk, 2010; Mountney et al., 2011). This includes signal modulation through “higher” cognitive processes (Stein and Steckler, 2010) within the dorso-medial prefrontal cortex, which influences the activity of the amygdala via signalling through the ventro-medial prefrontal cortex (Baratta et al., 2008; Stein and Steckler, 2010).

The limbic brain circuitry interacts with the hypothalamus (Fink, 2006) via the amygdala (Price, 2003; Andersen et al., 2007), the hippocampus (Andersen, 2007), and the medial prefrontal cortex (Radley, 2009). Within this framework, cognitive processes related to fear and anxiety influence a brain nucleus mediating the stress responses via the activation of the hypothalamic-pituitary-adrenal (HPA) axis (Fink, 2006; Mountney, 2011; Adolphs, 2013).

### **1.3 The HPA axis**

The hypothalamus receives inputs, among other brain structures, from the limbic circuitry and is involved in the initiation of the stress responses. The parvocellular part of the paraventricular nucleus (PVN) contains corticotropin-releasing hormone (CRH) and arginine vasopressin (AVP) synthesizing neurons (Fink, 2006). CRH, via corticotropin-releasing hormone receptor type 1 (CRHR1), and AVP, via the V1b receptor, stimulate the release of adrenocorticotrophic hormone (ACTH) from the anterior pituitary (Papadimitriou and Priftis, 2009; Refojo and Holsboer, 2009). In addition, CRH from PVN neurons is released centrally and influences the production of CRH within other brain structures e.g. the central amygdala (CeA), thereby shaping the overall stress responses of the brain (Roozendaal et al., 2002; Shekhar et al., 2005; Fink, 2006). The release of ACTH, in turn, stimulates the release of adrenal steroids (Refojo and Holsboer, 2009). These include cortisol in humans and corticosterone (Cort) in rodents (Fink, 2006).

Besides exerting a negative feedback on hypothalamic CRH secretion, adrenal steroids also influence behaviour, the immune response, and energy homeostasis (Fink, 2006); for further details regarding CRH and Cort in a brain-circuit specific manner see chapter: 1.5.3.2.

#### **1.4 Psychiatric disorders that are related to fear and anxiety**

Fear can be seen as a state that results from a confrontation of an organism with a situation threatening its homeostasis (Damasio and Carvalho, 2013). As a consequence, the organism tries to escape this situation to avoid damage and to reduce the anxious feeling (Adolphs, 2013; Damasio and Carvalho, 2013). Anxiety, in contrast to fear, represents a state of an organism awaiting putative threatening situations (Adolphs, 2013).

When suffering from anxiety disorders, the anxious feeling persists without being ever confronted with the threatening situation, which seriously impacts on the individual (Cryan and Holmes, 2005).

According to the DSM IV criteria for humans, anxiety disorders include (Stein and Steckler, 2010):

Agoraphobia with or without history of panic disorder

Social phobia

Simple phobia

Panic disorder

Generalized anxiety disorder

Obsessive compulsive disorder

Posttraumatic stress disorder

Acute stress disorder

Substances used to treat these psychiatric conditions are e.g. citalopram, venlafaxine, and clomipramine (Benkert and Hippus, 2011).

For more information about pharmacotherapy, see chapter: 1.5.3.3

In psychiatric research, animal models are widely used to correlate neurobiological endophenotypes with a defined anxiety-like behavioural phenotype (Cryan and Holmes, 2005). By that, researchers aim to gain insights into the mechanisms that contribute to the development of these psychiatric diseases (Bourin et al., 2007).

### 1.4.1 Mouse models of anxiety disorders

The development of mouse models offers an animal model that is accessible to genetic tools (Cryan and Holmes, 2005; Bourin et al., 2007; Maren, 2008; Neumann et al., 2011). Conditioned models are commonly established by using pavlovian fear conditioning, where a neutral stimulus (conditioned stimulus (CS)), such as a tone or certain contextual cues, is paired with an aversive stimulus (unconditioned stimulus (US)), such as a foot shock. After conditioning and subsequent fear memory formation, the animals show fear-related behaviour, e.g. freezing, upon presentation of CS (Rodrigues et al., 2004; Apergis-Schoute et al., 2005; Cryan and Holmes, 2005). By use of this paradigm, researchers are able to investigate the modulation of acquired fear memory, thereby possibly mimicking the oblivion of an acquired fearful experience. It could be shown that, after conditioning, single and repeated presentation of the CS is capable of decreasing the freezing response of the animal (Myers and Davis, 2007; Quirk et al., 2010). The creation of unconditioned models can be achieved either by selection of animals upon a behavioural phenotype within a clearly defined paradigm and subsequent inbreeding of these mice (Cryan and Holmes, 2005; Bourin et al., 2007; Krömer et al., 2005), or via genetic manipulation (van Gaalen et al., 2002; Cryan and Holmes, 2005).

An example of an unconditioned mouse model is the high vs. normal anxiety-related behaviour (HAB/NAB) mouse model. Mice are selected according to their behaviour on the elevated-plus maze, where the time spent on the open arms is used as the selection criterion for subsequent bi-directional breeding within the groups (Krömer, et al., 2005; Bourin et al., 2007). Employing this mouse model in conjunction with fear conditioning has shown that HAB mice display a higher degree of freezing in comparison to NAB mice in a contextual fear conditioning paradigm (Yen et al., 2012).

Another example of unconditioned mouse models is transgenic mice. Advances within these approaches allow the generation of conditional knock-out mouse lines to overcome the problem of compensatory genetic mechanisms, which may complicate the causal linkage between the inactivated gene and the observed alteration in behaviour (Cryan and Holmes, 2005).

This technique has been successfully applied to selectively knock-out CRHR1 and to link CRHR1 expression in glutamatergic neurons in forebrain structures, including the hippocampus and the amygdala, with anxiety-related behaviour (Refojo et al., 2011). The authors showed that these knock-out mice exhibited more entries into the lit compartment of the dark-light box and a higher locomotor activity (Refojo et al., 2011). Since the dark-light box paradigms based on the assumption that more entries into the lit compartment reflect a less anxious state of the animal (Cryan and Holmes, 2005), the authors provided evidence that CRHR1 is involved in the mediation of anxiety-associated behaviour (Refojo et al., 2011).

Unconditioned models can be used to study anxiety, whereas conditioned ones to examine fear and fear memory formation (Cryan and Holmes, 2005; LeDoux, 2007) with respect to the specific contribution of distinct brain circuits and underlying neurobiological mechanisms.

A limbic brain structure significantly involved in many aspects of fear, fear memory, and anxiety is the amygdala (Davis et al., 1994; Aggleton, 2000; Blair et al., 2001; Sah et al., 2003; Rainnie et al., 2004; Cryan and Holmes, 2005; Shekhar et al., 2005; LeDoux, 2007; Gallagher et al., 2008; Maren, 2008; Ehrlich et al., 2009; Johansen et al., 2010; Johansen et al., 2011; Kim et al., 2011; Johansen et al., 2012; Mahan and Ressler, 2012; Pare and Duvarci, 2012; Damasio and Carvalho, 2013). In the following chapter, emphasis will be put on this region with anatomical and functional aspects.

## 1.5 The amygdala

### Anatomical considerations

The amygdala is a brain structure that lies in the anterior-medial portion of each temporal lobe (Aggleton, 2000). It was first described in the early 19<sup>th</sup> century by Burdach (Sah et al., 2003). Since then, its anatomical organization was investigated in more detail, resulting in the view that the amygdala can be subdivided in approximately 13 nuclei and cortical regions that are interconnected for the processing of sensory and polymodal information (Aggleton, 2000; Sah et al., 2003). Although this consensus exists, there is also another view, in which nuclei of the amygdala are not an entity but extensions of the cortex and the striatum (LeDoux, 2007). The present study is based on the view that the amygdala can be subdivided in several key nuclei that are specifically interconnected to fulfil distinct roles in the integration and computation of incoming information related to emotions such as fear and anxiety (LeDoux, 2007). Unless otherwise stated, the data described in the following originate from rodent studies.

### 1.5.1 Overview of anatomical subdivisions of the amygdala

According to Paxinos (2004) and Schmitt et al. (2012), the amygdaloid complex can be subdivided as follows:

Supranuclear division of amygdala

Superficial cortical-like nuclear group

Olfactory amygdala

Anterior amygdaloid area

Nucleus of the lateral olfactory tract

Anterior cortical nucleus

Postero-lateral cortical nucleus

Amygdalo-piriform transition area

Peri-amygdaloid complex

Posterior amygdaloid nucleus

Vomeronasal cortical-like amygdala

Nucleus of the accessory olfactory tract

Postero-medial cortical nucleus

Amygdalo-hippocampal area

Bed nucleus of the accessory olfactory tract

Vomeronasal amygdala

Medial extended amygdala

Medial amygdaloid complex

Medial sub-lenticular extended amygdala

Medial subdivision of the bed nucleus of the stria terminalis

Medial division of the supra-capsular division of the bed nucleus of the stria terminalis

Intra-amygdaloid division of the bed nucleus of the stria terminalis

Extended Amygdala

Central extended amygdala

**Central amygdaloid nucleus**

Central sub-lenticular extended amygdala

Lateral division of the bed nucleus of the stria terminalis

Lateral supra-capsular division of the bed nucleus of the stria terminalis

Interstitial nucleus of the posterior limb of the anterior commissure

Latero-basal nuclear complex

**Lateral amygdala**

**Basolateral amygdaloid nucleus**

Basomedial amygdaloid nucleus

Ventral basolateral amygdaloid nucleus

Unclassified cell group

Amygdalo-striatal transition zone

Interfascicular islands

Interfascicular islands, granular part

Interfascicular islands, parvocellular part

**Intercalated masses**

Intramedullary griseum

Para-striatal nucleus

Bed nucleus of the anterior commissure

Subventricular nucleus

Fusiform nucleus

Nucleus of the commissural component of the stria terminalis

The order depicted in this column was obtained and confounded by the use of ontogenetic, histo- and immunocytochemical techniques (Paxinos, 2004; Schmitt et al., 2012). In the following, emphasis will be put on key nuclei and circuits that are known to be involved in the processing and storage of fear memories and the expression of fear and anxiety. These nuclei and cell groups appear in red and bold in the above hierarchy.

### **1.5.2 Anatomical organization of amygdalar key nuclei**

#### **Central extended amygdala**

The CeA, bordered laterally by the basolateral complex and medially by the striatum, can be subdivided from dorsal to ventral in the centrolateral nucleus (ICe) and the centromedial nucleus (mCe) (Sah et al., 2003) (Figure 1.5.2-2). From a developmental point of view, these nuclei originate from the striatum which is also reflected through their efferences and their neuronal architecture (Sah et al., 2003).

#### **Deep nuclei of the amygdala**

The LA and the BLA can be grouped within the deep nuclei group. These nuclei are located dorsally within the amygdaloid complex and are bordered laterally by the external capsule (EC) and medially by the CeA. From the dorsal to ventral axis, these nuclei are arranged from the LA to the BLA (Aggleton, 2000; Sah et al., 2003) (Figure 1.5.2-2). Embryologically and functionally, these nuclei resemble to cortical circuits (Sah et al., 2003).

#### **Intercalated masses**

The intercalated cell masses can be subdivided based on their location relative to the key nuclei of the amygdala. The lateral intercalated cells are located laterally to the LA (Ehrlich et al., 2009), whereas the medial population of intercalated cells is located between the LA/BLA and the CeA. This population of cells can further be subdivided in dorsal intercalated cells, main intercalated cells and ventral intercalated cells (Pare and Duvarci, 2012). These populations are put together in the group of “medial intercalated cells” in Figure 1.5.2-2, which was built according to: Sah et al., (2003); LeDoux (2007); Ehrlich et al., (2009); Pare and Duvarci, (2012).

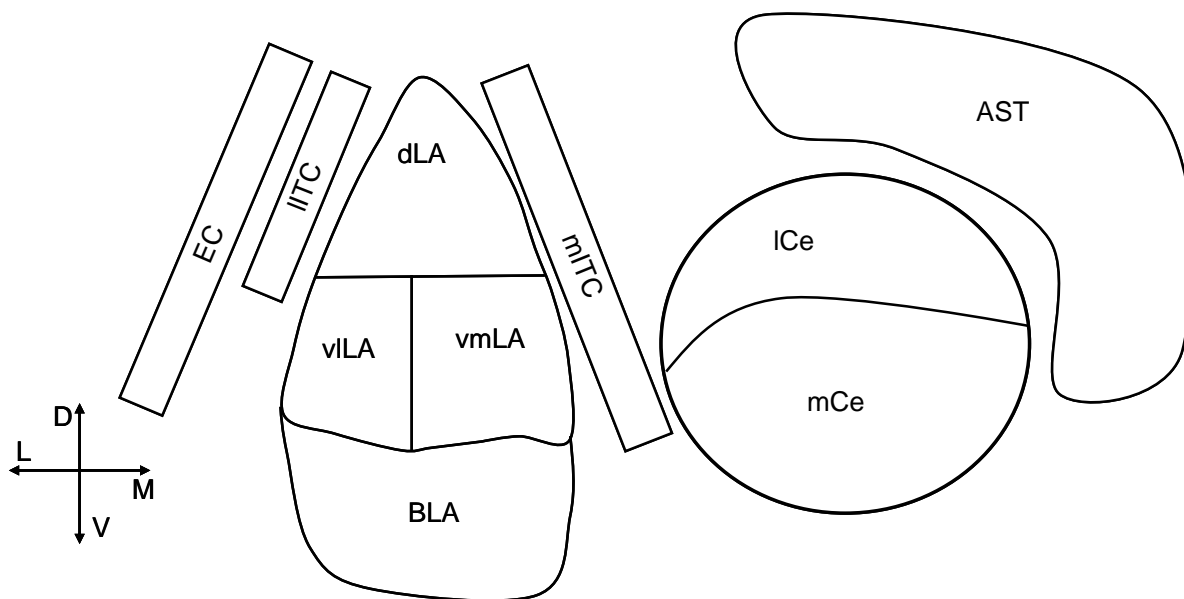


**Figure 1.5.2-2. Key nuclei, cell groups, and fibre tracts within the amygdaloid complex and their anatomical location along the dorsal/ventral and lateral/medial axes.** EC = External capsule, IITC = Lateral intercalated cells, mITC = Medial intercalated cells, dLA = Dorsal lateral amygdala, vlLA = Ventro-lateral lateral amygdala, vmLA = Ventro-medial lateral amygdala, BLA = Basolateral amygdala, ICe = Centrolateral amygdala, mCe = Centromedial amygdala, AST = Amygdalo-striatal transition area, D = dorsal, V = ventral, L = lateral, M = medial.

### 1.5.3 Functional connectivity within amygdalar key nuclei

The amygdalar neuronal network is strongly heterogeneously distributed with respect to the flow of electrical signals (LeDoux, 2007). Inter-nuclear flow of activity follows the tendency to travel from dorsal to ventral and from lateral to medial, which can also be observed on the level of axonal connectivity (Krettek and Price, 1978; Ehrlich et al., 2009; Pare and Duvarci, 2012).

The spreading of excitatory and inhibitory neuronal activity within the LA and BLA is reciprocally regulated through feedback and feedforward circuits (Ehrlich et al., 2009). Inhibitory circuits mainly contribute to this signal processing by a local intra-nuclear (Ehrlich et al., 2009) regulation of the output of their projection neurons.

The flow of excitatory and inhibitory neuronal activity was investigated within the LA in coronal and horizontal slices (Samson and Pare, 2006). This study showed that in coronal slices, excitatory responses could be detected with the highest prevalence upon application of glutamate in the direction from dorsal to ventral whereas inhibitory signalling appeared to be diffuse. In horizontal brain slices, excitation

mainly spreads from the EC towards a medial direction. Inhibitory activity could be detected within this section from medial to lateral (Samson and Pare, 2006).

Another study put emphasis on the observation that feedback inhibition along the transverse section of the LA gates the strength of excitatory activity and, by that, patterns the LA in discrete processing entities along this axis (Samson et al., 2003).

The fact that the LA, via convergence of cortical and thalamic afferences (LeDoux, 2007), is a major sensory input region, together with the above mentioned observations, exemplifies the capacity of this nucleus to modulate the direction and strength of signal propagation by a fine regulation of neuronal activity through inhibitory circuits. The dominance of excitatory signalling is emphasized by the higher number of excitatory projection neurons in comparison to the number of interneurons in the LA and BLA (Davis et al., 1994; Ehrlich et al., 2009; Orsini and Maren, 2012).

In contrast, the striatum-like CeA mainly contain inhibitory neurons (Ehrlich et al., 2009; Orsini and Maren, 2012). The ICe receives most inputs from the LA, the BLA, and intercalated cells, where they undergo intra-nuclear processing through inhibitory networks (Pare and Duvarci, 2012). Subsequently, signals are conveyed to the mCe, which in turn projects to downstream targets of the amygdala (Pare and Duvarci, 2012). Besides inputs from the ICe, the mCe also receives direct inputs from the BLA and intercalated cells (Pare and Duvarci, 2012).

Within the amygdaloid complex, the intercalated cells exert their function by inhibiting and thereby a “fine tuning” of the activity within distinct nuclei. On the one hand, these cells modulate the processing of cortical sensory inputs and, on the other hand, shape the activity of the ICe and mCe, one of the major output circuits of the amygdala (Pare and Duvarci, 2012).

Figure 1.5.3-3 depicts the known functional connectivity but also connections with so far undefined function among amygdalar key nuclei together with other brain structures. The LA appears as a functional entity, including the dorsal, ventrolateral and ventromedial nucleus in this scheme. Inputs arising from known fibre tracks such as the EC or internal capsule (IC) are indicated.

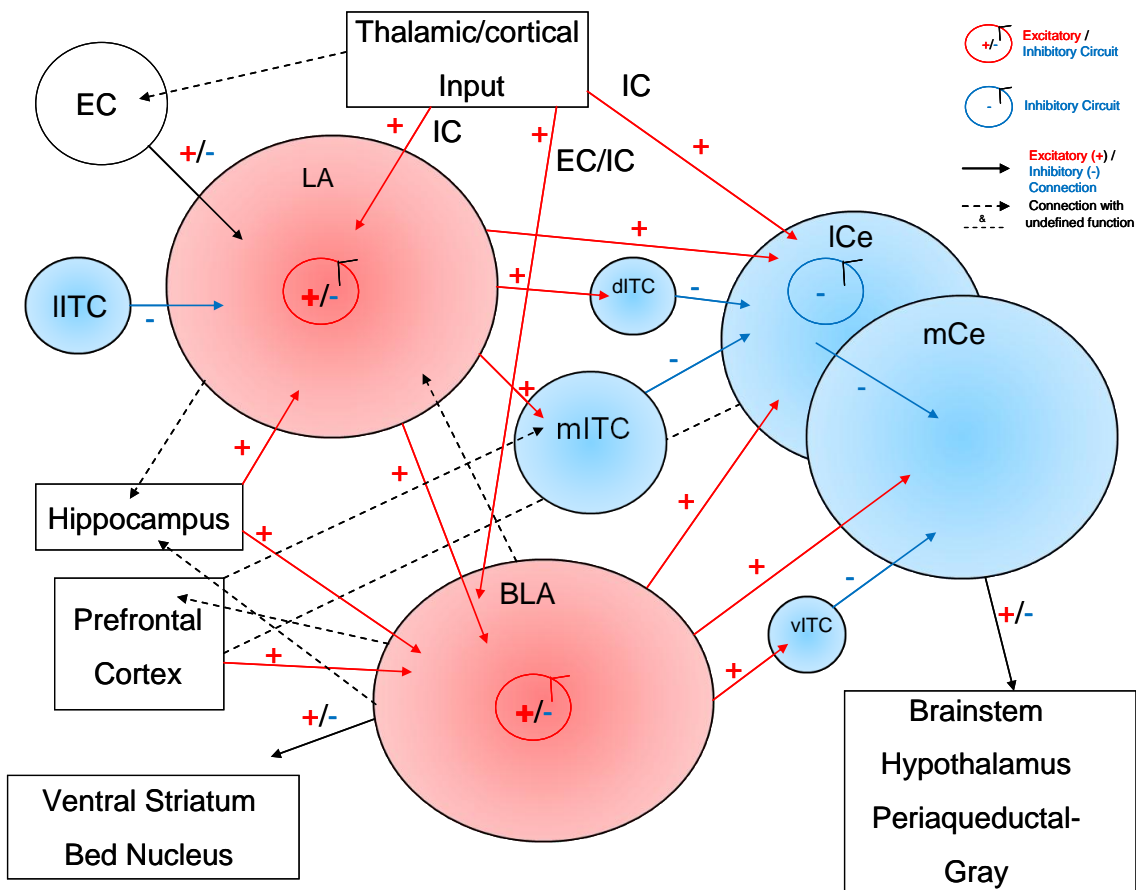


**Figure 1.5.3-3. Functional connectivity of amygdala key nuclei and cell groups.** Please note the weighted excitatory drive within the LA and BLA, which is indicated through bold "+" signs and tendencies of structures to be either excitatory (red) or inhibitory (blue). EC = External capsule, IC = Internal capsule, LA = Lateral amygdala, BLA = Basolateral amygdala, ICe = Central lateral amygdala, mCe = Centromedial amygdala, IITC = Lateral intercalated cells, dITC = Dorsal intercalated cells, mITC = Main intercalated cells, vITC = Ventral intercalated cells.

Figure 1.5.3-3 also illustrates the large portion of excitatory drive within the LA and BLA and, in contrast to that, the dominance of inhibitory circuits in the CeA and intercalated cell masses.

Figure 1.5.3-3 was prepared according to:

Veening et al. (1984); Aggleton, (2000); Kjelstrup et al. (2002); Sah et al. (2003); LeDoux, (2007); Ehrlich et al. (2009); Walker et al. (2009); Morozov et al. (2011); Tye et al. (2011); Mahan and Ressler, (2012); Pare and Duvarci, (2012).

Regarding neurotransmission, glutamate and gamma-aminobutyric acid (GABA) exert their effects within this circuitry via the activation of their respective ionotropic and metabotropic receptors (Sah et al., 2003).

It is important to mention that the computational properties of the amygdalar system with respect to input-output relationships on the level of neuronal network activity and plasticity are difficult to resolve due to the incomplete knowledge about the functional connectivity. Some studies have linked the activity within distinct amygdalar key nuclei with behaviour related to fear and anxiety. For example the optogenetic control of distinct central amygdalar nuclei revealed that the ICe is involved in the acquisition of fear memory, whereas the mCe in its behavioural expression (Ciocchi et al., 2010). Transgenic mice carrying a construct, in which a reporter gene ( $\beta$ -galactosidase) was under the control of the c-fos promoter, demonstrated that a population of glutamatergic neurons in the LA is activated by contextual fear conditioning (Wilson and Murphy, 2009). Other studies using *in vivo* single unit recordings in rats showed that after auditory fear conditioning the presentation of the CS was capable of increasing the firing rate of LA projection neurons. This phenomenon was accompanied by freezing behaviour (Repa et al., 2001; Goosens et al., 2003).

By use of a fear conditioning paradigm in rats, a contextual cue was employed as a CS. The authors observed that after CS-US pairing the neuronal activity increased upon CS presentation, and that the animals exhibited freezing behaviour (An et al., 2012).

Another study demonstrated that the anxiogenic drug yohimbine was capable of increasing the spontaneous activity of projection neurons in the BLA, as revealed by *in vivo* recordings in rat brains (Buffalari and Grace, 2009). This finding is in line with a report showing that the optogenetic activation of BLA projection neurons of mice, which terminate in the ventral hippocampus, enhances anxiety-related behaviour (Felix-Ortiz et al., 2013). Conversely, it was also shown that optogenetic activation of a subpopulation of principal neurons in the BLA of mice exerts an inhibitory influence on the activity of neurons in the mCe and LA. This activation resulted in a decreased fear response of these animals during an auditory fear conditioning paradigm (Jasnow et al., 2013).

Taking together, it is likely that an increase in neuronal activity within the LA can be related to anxiety, fear, and fear memory, whereas the activity in the BLA might differentially contribute to distinct forms of anxiety, fear, and fear memory.

In the following part, cellular mechanisms, potentially involved in the modulation of neuronal network activity and plasticity in the LA and BLA will be described.

### 1.5.3.1 Neuronal plasticity

Neurons and consequently neuronal networks exhibit the potential to undergo long lasting changes of their firing properties in response to certain stimuli, a phenomenon that is mediated by a structural remodelling of the cellular architecture. The resultant physiological changes can be seen as an adaptation to changing environments (Ho et al., 2011). With respect to the fear conditioning paradigm, the CS-US association is thought to be partially stored in the LA and BLA (Myers and Davis, 2007; Johansen et al., 2010). Extinction training after fear conditioning can weaken the acquired memory traces in these nuclei. From a functional point of view, this effect most likely results from the formation of new memories (Orsini and Maren, 2012).

Cellular mechanisms which are thought to mediate long-lasting changes in neuronal activity that accompanies fear memory formation or extinction is long-term potentiation (LTP) or long-term depression (LTD). LTP is a lasting increase in the strength of synaptic transmission, LTD a lasting decrease (McKernan and Shinnick-Gallagher, 1997; Rogan et al., 1997; Sigurdsson et al., 2007; Orsini and Maren, 2012).

### Plasticity in the LA and BLA

Sensory inputs conveyed by thalamic and cortical afferences to LA and BLA neurons about CS and US are able to induce a lasting enhancement in the strength of synaptic transmission and, thereby, to increase the strength of neuronal activity (McGaugh, 2004; Sigurdsson et al., 2007; Orsini and Maren, 2012). *In vivo* studies in rats showed that the infusion of D(-)-2-Amino-5-phosphopentanoic acid (AP 5), a N-methyl-D-aspartate (NMDA) receptor antagonist, into the amygdala, blocked the acquisition of fear memory, which is in line with the observation that activity of this ionotropic glutamate receptor is frequently essential for LTP induction (Miserendino et al., 1990; Collingridge and Bliss, 1995; Hille, 2001). NMDA receptors are calcium permeable channels, activated by the binding of glutamate but blocked at resting

membrane potential by magnesium. This  $Mg^{2+}$  block is removed upon depolarization which allows the influx of calcium ions into the postsynapse (Hille, 2001).

It has been shown that the composition of NMDA receptor subunits in principal neurons of the LA varies between synapses depending on their cortical or subcortical origin (Weisskopf and LeDoux, 1999). These differences can be related to different responses upon plasticity-inducing stimuli: GluN2A-containing NMDA receptors are involved in the induction of LTP whereas GluN2B-containing receptors in the mediation of LTD (Dalton et al., 2012). On the behavioural level, a blockade of GluN2B receptors in the amygdala impairs extinction of conditioned fear in rats (Dalton et al., 2008).

The LA and BLA also display other forms of plasticity. An example for this is the involvement of voltage-gated calcium channels (VGCCs). It was shown, both *in vivo* and *in vitro*, that interfering with calcium signalling via the application of calcium chelators or blockers of VGCCs impaired fear memory formation and induction of LTP, respectively (Orsini and Maren, 2012). The specific involvement of L-type VGCCs (L-VGCCs) in fear extinction was demonstrated by the infusion of the antagonists verapamil or nifedipine into the BLA of rats (Davis and Bauer, 2012). The downstream targets of NMDA receptor and L-VGCC activation is the regulation of intracellular calcium concentration which, in turn, modulates a variety of signalling cascades (Blair et al., 2001). These include: NO-synthase, phosphatases, protein kinase A (PKA), protein kinase B (PKB), protein kinase C (PKC), calcium/calmodulin protein kinase (CaMKII), mitogen-activated protein kinases (MAP Kinases),  $IP_3$ -signalling. Synaptic changes primarily occur on the level of exo- and endocytosis and trafficking of  $\alpha$ -amino-3-hydroxy-5-methyl-4-isoxazolepropionic acid (AMPA) receptors. Other mechanisms include: presynaptic vesicle mobilization and stabilisation of the synapse through adhesion molecules (e.g. neural cell adhesion molecules) (Lin et al., 2001; Ho et al., 2011; Johansen et al., 2011; Orsini and Maren, 2012).

### **1.5.3.2 Mediators of the stress responses and their influence on neuronal network activity and plasticity in the LA and BLA**

#### **CRH**

CRH, a 41 amino-acid long peptide, is a fast mediator of the stress responses within HPA axis regulation (Refojo and Holsboer, 2009). CRH is also involved in the regulation of fear and anxiety behaviour (Roozendaal et al., 2002; van Gaalen et al., 2002; Shekhar et al., 2005; Gallagher et al., 2008; Hostetler and Ryabinin, 2013). Besides in the PVN, CRH is also produced in the CeA and is capable of invading the LA and BLA upon its release (Roozendaal et al., 2002; Shekhar et al., 2005).

Within the brain of humans and rodents two classes of CRH receptors (CRHR1 & CRHR2) can be found in basal forebrain and brainstem circuits (Gallagher et al., 2008). These G-protein-coupled receptors exert various intracellular effects including the increase of cyclic adenosine monophosphate (cAMP) and free calcium as well as the regulation of the activity of PKA, PKB, PKC and MAP Kinases (Gallagher et al., 2008). CRHR1 messenger RNA (mRNA) is detectable in the LA and BLA, and its expression has been shown to influence anxiety-related behaviour (Refojo et al., 2011). In another *in vivo* study performed in rats, the authors could demonstrate that infusions of CRH into the LA enhance the expression of conditioned fear and attenuate fear memory formation (Isogawa et al., 2013). Roozendaal et al. (2008) showed that CRH infusions into the rat BLA facilitate memory consolidation via retention of inhibitory avoidance performance.

In a study conducted in mouse brain slices, the authors found that bath application of CRH strengthened signal propagation from the LA to the BLA via CRHR1 (Refojo et al., 2011).

#### **Corticosteroids**

Corticosteroids such as Cort are produced by the adrenal glands and released into the blood in a high extend during stressful events. They can cross the blood-brain barrier and affect distinct brain functions via binding to mineralocorticoid (MRs) and glucocorticoid (GRs) receptors (Fink, 2006). GRs exert their actions via genomic and

non-genomic effects. On the genomic level, the ligand-receptor complex in the cytoplasm translocates into the nucleus and acts as a transcription factor (Makara and Haller, 2001; Groeneweg et al., 2012). Three criteria have been defined to separate genomic from non-genomic effects: onset of the effect, independence of blockade of parts of the receptor complex, and endurance of the effect after the elimination of putative genomic targets (Makara and Haller, 2001).

Membrane-bound MRs and GRs are found in the amygdala of mice and rats, with their highest density nearby synapses, thus suggesting that they exert fast, non-genomic effects (Johnson et al., 2005; Groeneweg et al., 2012). Downstream of corticosteroid binding, signalling factors that were shown to be involved in mediating such effects include extracellular signal-regulated kinase (ERK1/2), G-proteins, cAMP, PKA, CREB, intracellular calcium concentration changes and phospholipase C (PLC). These findings originate from studies done in the hippocampus, hypothalamus, and dorsal root ganglion cell culture (Groeneweg et al., 2012).

An *in vivo* study in rats investigating the influence of Cort on the retention of contextual fear memory showed that this treatment increases freezing behaviour up to 6 days after conditioning (Thompson et al., 2004). With respect to neuronal activity, it has been shown in brain slices from rats that application of Cort enhances the excitability of BLA projection neurons by a decrease of GABAergic inhibition onto these neurons. This effect was mediated by a shift of the Cl<sup>-</sup> reversal potential (Duvarci and Pare, 2007). Another *in vitro* study using mouse brain slices demonstrated a rapid, MR-dependent increase of excitatory postsynaptic currents in the BLA upon application of Cort (Karst et al., 2010).

### 1.5.3.3 Pharmacological intervention

An important question arising from the observation that an increase in neuronal activity in the LA and partly in the BLA is linked to anxiety is whether pharmacological intervention can counteract this phenomenon (Maren and Quirk, 2004). One commonly used and, from a mechanistic point of view, well understood class of chemical compounds are benzodiazepines such as diazepam (Whiting, 2006). This positive allosteric modulator of the GABA<sub>A</sub> receptor is well suited for the treatment of pathological anxiety, as the regulation of excitation in the LA and BLA is mediated via

GABA<sub>A</sub> receptors (Sah et al., 2003). In spite of this beneficial effect, the use of benzodiazepines is accompanied by severe side effects, which include cognitive impairment and the risk of addiction (Whiting, 2006). Out of these constraints, other interventions are also indicated for the treatment of anxiety disorders and novel substances are under development. A putative novel pharmaceutical, namely N-(4-Hydroxyphenyl) arachidonylamide (AM 404), is based on the fact that the regulation of emotional processing, such as extinction of fear memories, is affected by the endocannabinoids anandamide and 2-arachidonoyl glycerol. These molecules bind to two receptors, from which cannabinoid receptor type 1 is the most widely expressed in the brain (McDonald and Mascagni, 2001). Upon binding, endocannabinoids affect excitatory and inhibitory neurotransmission. In the context of fear conditioning, endocannabinoids facilitate extinction of fear memory (de Bitencourt et al., 2013; Mechoulam and Parker, 2013). Accordingly, it was shown that AM 404, which acts as an inhibitor of endocannabinoid uptake, facilitates the extinction of contextual fear memories in rats (de Bitencourt et al., 2008).

In the currently available pharmacotherapy selective serotonin reuptake inhibitors (SSRIs), serotonin noradrenalin reuptake inhibitors (SNRIs), and tricyclic antidepressants (TCAs) are also indicated for the treatment of various anxiety disorders (Zohar and Westenberg, 2000; Vaswani et al., 2003; Katzman, 2004; Benkert and Hippus, 2011). From a functional point of view, it could be shown that chronic treatment with the SSRI citalopram impaired fear extinction. This effect was accompanied by a downregulation of the GluN2A subunit of the NMDA receptor (Burghardt et al., 2013). Another *in vitro* study revealed that the SSRI tianeptine was capable of reducing the firing frequency of action potentials of LA neurons. As shown *in vivo*, tianeptine treatment also prevented the stress-mediated increase in dendritic outgrowth in the LA and anxiety-like behaviour (Pillai et al., 2012).

It is increasingly thought, that distinct SSRIs exert an anxiolytic effect via the modulation of glutamatergic neurotransmission in limbic circuits including the BLA (McEwen et al., 2010). Out of these observations, the question arises if the regulation of neuronal activity can be observed on a circuit level, thus providing a potential neuronal network mechanism by which distinct classes of antidepressants mediate parts of their anxiolytic effects.

## 1.6 Working hypothesis

The heterogeneous neuronal networks of the LA and BLA are involved in the regulation of fear, fear memory and anxiety. This regulation is mediated by the modulation of signalling strength and several studies point towards a positive correlation between increased neuronal activity and fear, fear memory and anxiety. However, a gap of knowledge exists between the electrical activity of single neurons in the LA and BLA and the activity of the network as a whole processing unit, due to the incomplete knowledge regarding the underlying circuitry.

An approach to partly bridge this knowledge gap is the investigation of whole neuronal network activity in brain slices, containing parts of clearly defined amygdalar nuclei. In this way, network activity and plasticity in the LA and BLA can be investigated, thereby capturing the sum of cellular events in response to certain stimuli, reflected by alterations in signalling strength.

To achieve this, an assay was developed, based on voltage-sensitive dye imaging (VSDI). This technique is capable of reporting changes in neuronal activity and plasticity with a high spatial and temporal resolution (Airan et al., 2007; Stepan et al., 2012).

### **Questions addressed in the present work**

1. Is it possible to reliably investigate neuronal activity in brain slices containing distinct nuclei of the amygdala by use of VSDI?
2. Is it possible to monitor amygdalar neuronal network plasticity with VSDI?
3. Is it possible to increase the capacity of detection in the recorded VSDI signals to quantitatively and reliably capture plastic changes as response to certain stimuli?
4. Which receptors and ion channels are involved in mediating the putative changes?
5. Do mediators of the stress responses impact on neuronal network activity and plasticity in the LA and BLA?
  - 5.1. Involvement of CRH?
  - 5.2. Involvement of Cort?
6. Do brain slices from HAB/NAB mice differ in amygdalar neuronal network plasticity?
7. Are pharmaceutical components capable of influencing amygdalar neuronal network activity monitored by VSDI?

## **2 Material and Methods**

### **2.1 Mice**

Horizontal brain slices were prepared from 8-12 weeks old male C57BL/6N male mice (BI 6) (Animal breeding facility MPI of Neurobiology), CD 1 male HAB mice, CD 1 NAB mice (line maintenance at the MPI of Psychiatry) or male  $Crhr1^{loxP/loxP}$  *Camk2 $\alpha$ -Cre* (CKO) and male  $Crhr1^{loxP/loxP}$  (CTRL) mice (housed at the MPI of Psychiatry). All mice were housed under standard laboratory conditions (light cycle 12:12 hours), room temperature (22°C), air humidity (55%) with food and water ad libitum. Animals of the same sex were housed and kept together in groups of 3-5 animals. All experiments were performed in accordance with governmental guidelines for animal welfare of Upper Bavaria, Germany.

CKO and CTRL mice were provided by the research group Molecular Neurogenetics of the MPI of Psychiatry; for details, see Refojo et al. (2011). In brief: for generation of mice with a conditional *Crhr1* allele, animals were created using in utero electroporation of a modified *Crhr1* allele carried by a linearized vector within TBV2 embryonic stem cells from 129S2 mice (Kühne et al., 2012). The mice carrying a  $Crhr1^{loxP/loxP}$  allele were backcrossed for seven generations to BI 6 mice. Generation of mice in which the *Crhr1* allele was selectively deleted in forebrain glutamatergic neurons was achieved by crossing  $Crhr1^{loxP/loxP}$  mice with  $Crhr1^{loxP/loxP}$  *Camk2 $\alpha$ -Cre* mice (Minichiello et al., 1999), which were backcrossed with BI 6 mice for more than 10 generations.

CD 1 HAB/NAB mice were provided by the research group Behavioural Neuroendocrinology of the MPI of Psychiatry. In brief: these mouse strains were selected and bidirectional bred with respect to their behavioural phenotype regarding their time spent on the open arms in the elevated plus-maze paradigm (Krömer et al., 2005).

## 2.2 Preparation of brain slices

The animals were sacrificed and decapitated. The following steps were conducted in ice-cold sucrose-based artificial cerebrospinal fluid (sACSF) saturated with carbogen gas (95% O<sub>2</sub> / 5% CO<sub>2</sub>). The sACSF (pH 7.4) contained the following (in mM): 87 NaCl, 2.5 KCl, 1.25 NaH<sub>2</sub>PO<sub>4</sub>, 25 NaHCO<sub>3</sub>, 25 glucose, 75 sucrose, 7 MgCl<sub>2</sub>, 0.5 CaCl<sub>2</sub>. After decapitation the brain was quickly removed and separated into its hemispheres. For this, the scalp was removed with a scissor to expose the skull. A cut along the midline from caudal to rostral was made with a scissor and the halves of the cranium were opened with a pincer. The brain was hauled out using a rounded spatula after cutting the optical nerve. After preparation the brain was put in ice-cold, carbogenated sACSF for at least 1 min. Subsequently, the whole brain was transferred onto a sACSF saturated filter (Whatman) to trim the brain for the slicing procedure with a razor blade. This included cutting off of the cerebellum and the olfactory bulb. The brain was separated into its hemispheres by cutting along the midline and one hemisphere was afterwards put onto its cut face. The other hemisphere was stored in sACSF. A transversal cut was made at the dorsal part of one hemisphere resulting in a cut face on which the brain was glued on the vibratom holder using histoacryl glue (Braun, Aesculap). Horizontal brain slices with a thickness of 400 µm containing distinct nuclei of the amygdala were prepared using a vibratom (Microm, HM 650 V). To preserve a similar amygdaloid network among the slices, landmarks were used (see results). After slicing, the slices were kept in a holding chamber containing carbogenated sACSF for 30 min at 34°C. After this incubation, slices were transferred into a holding chamber containing carbogenated ACSF which was composed of (in mM): 125 NaCl, 2.5 KCl, 1.25 NaH<sub>2</sub>PO<sub>4</sub>, 25 Glucose, 25 NaHCO<sub>3</sub>, 1 MgCl<sub>2</sub>, 2 CaCl<sub>2</sub> (pH 7.4) (nACSF) and incubated at room temperature (22-25°C; RT).

For extracellular recordings, the slices were incubated for at least 1.5 hours in nACSF at RT.

### 2.3 VSDI

For staining, the voltage-sensitive dye (VSD) 4-(2-(6-(Dibutylamino)-2-naphthalenyl)-1-(3-sulfopropyl) pyridinium hydroxide inner salt (Di-4-ANEPPS) (dissolved in dry Dimethylsulfoxide (DMSO) to a 20.8 mM stock solution) was used. The slices were placed in a staining chamber which contained carbogenated nACSF and Di-4-ANEPPS (7.5 µg/ml; <0.1% DMSO) for 15 min at RT. After the staining procedure, the slices were incubated for at least 30 min in a carbogenated nACSF containing holding chamber at RT.

For VSDI experiments the slices were placed in the recording chamber and continuously superfused with carbogenated nACSF (3 ml/min flow rate) using a gravity perfusion system and a peristaltic pump (Ismatec). To fix the slice in the recording chamber, a grid consisting out of a platinum frame on which nylon strings were glued was put onto the slice.

To evoke neuronal activity within the LA and BLA, square pulse electrical stimuli (200 µs pulse width) were delivered via a custom made monopolar tungsten electrode (Science Products; 50 µm pole diameter) to either the EC or intra-nuclear fibres of the LA using an Iso-Stim 0.1M stimulator (npi). The stimulation electrode was positioned onto the slice using a micro manipulator. The stimulator was triggered by the MiCAM02 software via an A/D converter.

VSDI was conducted using the MiCAM02 hard- and software package (Brain Vision, Tokyo, Japan). The tandem-lens microscope was equipped with the MiCAM02-HR camera and the 2x and 1x lens at the objective and condensing side, respectively.

For excitation of Di-4-ANEPPS, a halogen lamp (Moritex, MHAB-150W) was used and its light was band-pass filtered at a wavelength of 530 nm. Emitted light was high-pass filtered (>590 nm) and captured via a charged-coupled device (CCD) camera (Figure 2.3-4).

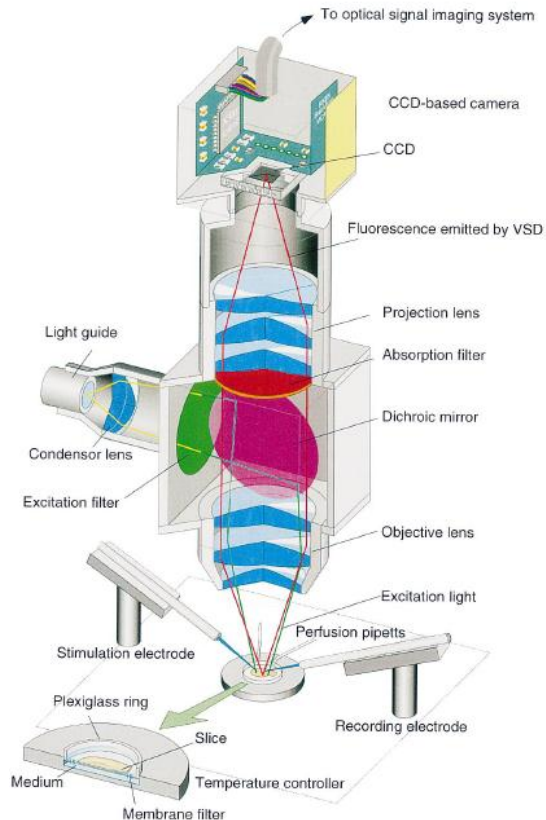


**Figure 2.3-4. Principle of VSDI.** VSDI = Voltage-sensitive dye imaging, adapted from Tominaga et al. (2000)

Acquisition parameters were 88 x 60 pixels frame size, 36.4 x 40  $\mu\text{m}$  pixel size and 2.2 ms sampling time.

For noise reduction, four acquisitions of an interval of 5 sec were averaged. This step was done in all VSDI recordings. Additionally, three acquisitions, averaged as stated above, were taken at an interval of 2 min and subsequently averaged (Figure 2.3-5).

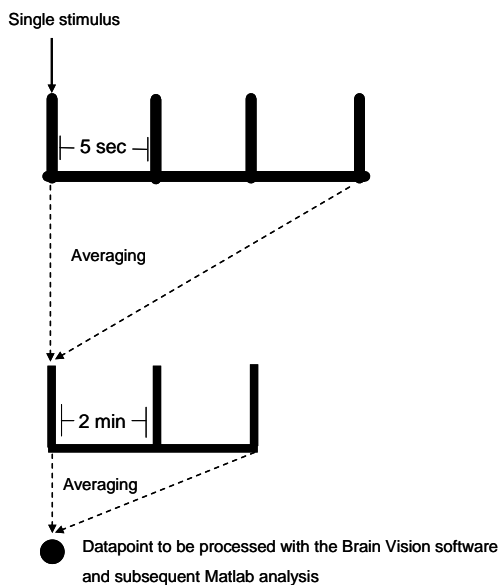


**Figure 2.3-5. Data acquisition using the Brain Vision software and averaging steps to reduce noise.**

For processing of averaged VSDI data, the relative change in fluorescence intensity  $\Delta F/F$  was calculated per pixel. Spatial and temporal smoothing was conducted by applying a 3x3x3 average filter. Quantification of VSDI signals was done using the peak of "Region of interest" (ROI)-extracted fast-depolarization mediated imaging signals (FDSs) after stimulus onset.

To minimize calculation errors due to noise, a  $\Delta F/F$  value before stimulus onset was subtracted from the value of the FDS peak amplitude (Figure 2.3-6).

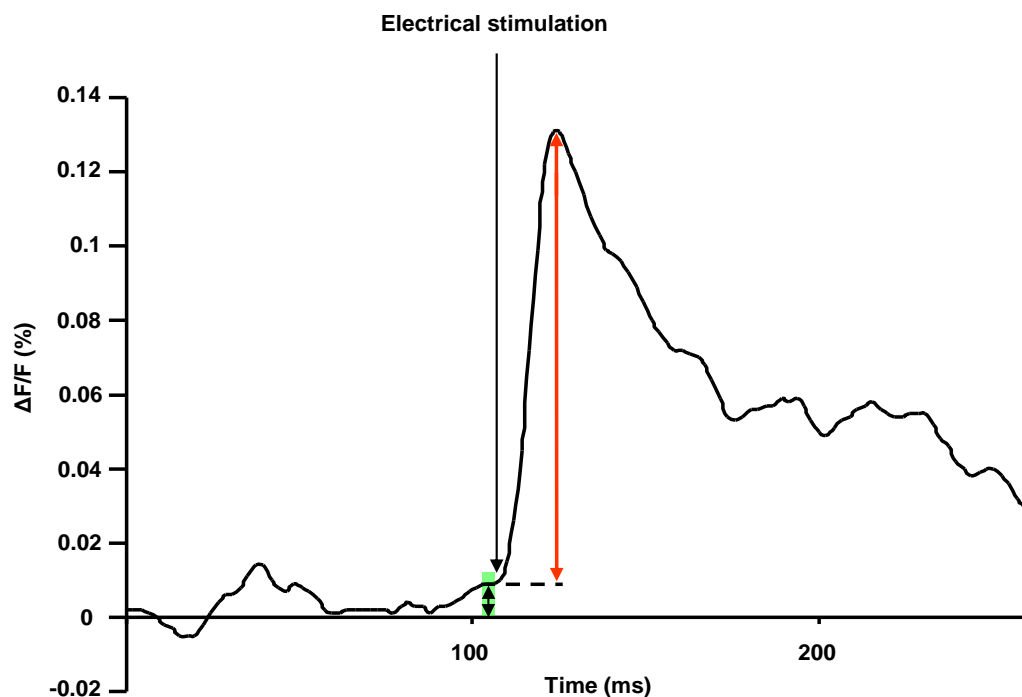


**Figure 2.3-6. Baseline correction of FDSs.** The average value of noise-induced baseline fluctuations before stimulus onset during a timeframe of 4.4 ms (green bar) is subtracted from the FDS value of the FDS peak amplitude to determine the change in fluorescence induced by electrical stimulation (red arrow).

Recordings were made after adjusting the peak amplitude of FDSs extracted by ROIs covering either the LA or the BLA to the half-maximum amplitude as exemplified in Figure 2.3-7.

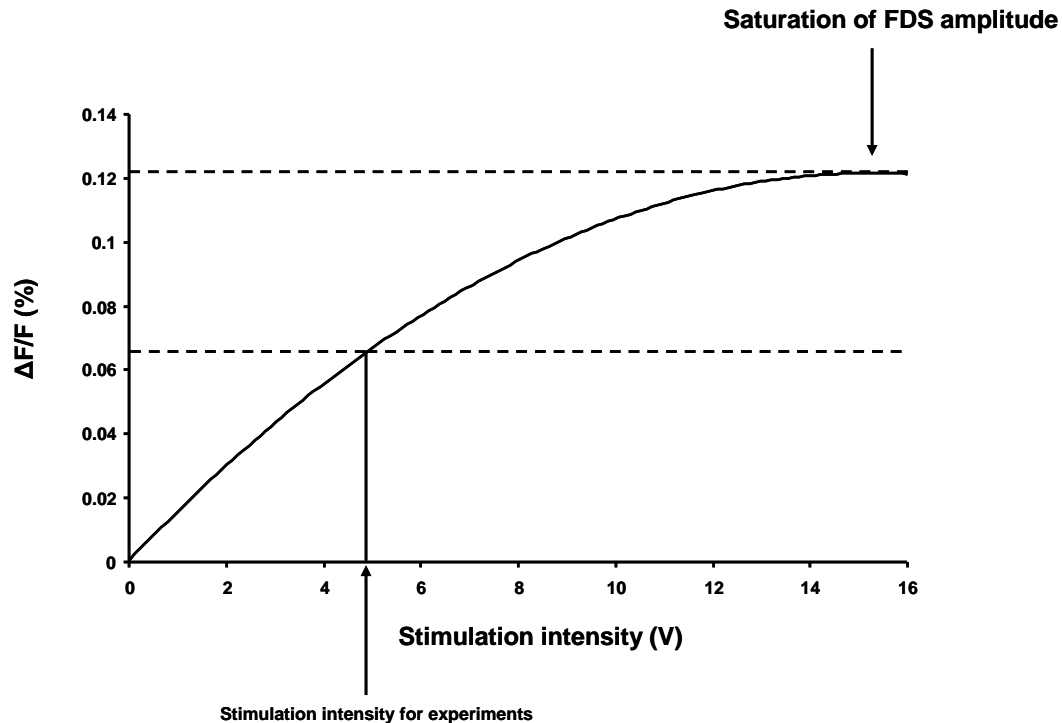


**Figure 2.3-7. Principle of the adjustment of FDSs for subsequent VSDI experiments in the LA and BLA.** For all VSDI experiments, the stimulation intensity was adjusted to reach the half-maximum amplitude of the FDS within the LA- or BLA-ROI. LA = Lateral amygdala, BLA = Basolateral amygdala, FDS = Fast depolarization-mediated signal, ROI = Region of interest, VSDI = Voltage-sensitive dye imaging.

Although  $\Delta F/F$  values differed among slices, a stimulation intensity of  $\sim 16$  V to reach saturation of the FDS amplitude was the same throughout slices. If a slice could not be saturated within this range, it was excluded from subsequent analysis. After obtaining stable baseline responses, substances were bath applied for the investigation of their effect on FDS peak amplitude or plasticity. For induction of plastic changes within the LA or BLA, two trains of stimuli (100 Hz for 1 s; HFS) separated by a 30 s interval were applied to the EC using the same stimulation intensity as used for baseline recordings. For delivering HFS through the stimulator, it was triggered using a pulse generator (Master 8, A.M.P.I).

In the analysis, two parameters were used, which are defined as follows:

#### Neuronal network activity

Responses of the VSD-stained neuronal network upon single-pulse electrical stimulation

#### Neuronal network dynamics

Responses of the VSD-stained neuronal network upon single-pulse electrical stimulation after HFS

For the investigation of network activity, reflected by the FDS amplitude, a ROI was set manually according to anatomical landmarks and quantification of VSDI signals was done using the Brain Vision Software by averaging all  $\Delta F/F$  values of the pixels within the ROI. This was done for baseline movies and movies which were acquired after application of a particular substance. All values were normalized to baseline and statistical analysis was conducted by comparing the average values of the last three datapoints after substance application or HFS to baseline. Network dynamics were investigated by data processing in Matlab (Matlab & Simulink, Version: R2007b; The Mathworks 2007). For this purpose, Brain Vision-processed VSDI movies were exported as ASCII files and subsequently imported into Matlab.

## **2.4 Advanced data processing**

### **Initial Processing**

By the import of ASCII files into Matlab, 80x66 pixel arrays, which contained the inverted differential data of Brain Vision images, were created. Specific frames from single Brain Vision movies were preselected in the Brain Vision software to be exported.

To assess the background noise, the last 20 frames before electrical stimulation were selected. The root-mean square (RMS) noise throughout these 20 consecutive frames was calculated per pixel by using:

$$x_{\text{rms}} = \sqrt{\frac{1}{n} (x_1^2 + x_2^2 + \dots + x_n^2)}$$

As threshold operation, the threefold value of RMS values was used for further processing. These operations were done over three movies and the resulting values for each pixel were averaged across these movies. In the following, this array, which contained the averaged threefold RMS values per pixel across three movies, is termed "RMSThreshold". These values corresponded to the approximately three-fold value of the standard deviation of the background noise at a particular pixel. The RMSThreshold was used to reliably distinguish between sites which display a stimulation induced depolarization before HFS and sites within the movies, only exhibiting noise. For this purpose 25 frames, which were acquired directly after stimulus onset, were extracted from the baseline movies. To compensate for noise, the frame before stimulus onset was extracted and its single-pixel values were subtracted from the corresponding pixel values of post-stimulus frames. Afterwards, a maximum intensity projection over all frames was computed to capture the FDS. The resultant array contained the maximum single-pixel values of  $\Delta F/F$  with a time period of 55 ms after stimulus onset (see results, Figure 3.2.2-16). Maximum single pixel values which displayed a value  $> \text{RMSThreshold}$  were set to 1, whereas pixels with values  $\leq \text{RMSThreshold}$  were set to 0. All baseline movies were processed in this way and as a final step multiplied by each other. The resultant array was used as an "Active Site Filter", new designed for each slice (see results, Figure 3.2.2-15, Figure 3.2.2-14C). By multiplication of the Active Site Filter with the corresponding arrays of the movies, pixels, to be further processed were selected.

For the analysis of network dynamics within a particular slice, 25 frames after stimulus onset were extracted from the baseline movies and all movies after HFS, and processed for baseline fluctuations and maximum intensity to capture the FDS over time. The Active Site Filter was applied to all of these arrays. Afterwards, baseline arrays were averaged and all arrays were divided by this array. This resulted in arrays which contain the relative changes in network response before and after HFS over all active sites across the maximum change of  $\Delta F/F$  over time. The resulting spatial resolution corresponded to the distance of the single light sensors in the CCD camera; i.e.  $36.4 \times 40 \mu\text{m}$  (see results, Figure 3.2.2-14D, E).

To restrict single-pixel values to the LA or BLA, ROIs were set according to anatomical landmarks. Array values within the LA or BLA were set to 1 whereas all values outside the LA or BLA were set to 0. The resultant array was multiplied with all processed arrays.

### **Value Extraction**

To reliably detect only sites, which either displayed potentiation or depression of neuronal activity after HFS, filters were designed. The parameter to define continuous potentiation or depression at one site was its persistence between minutes 30 and 42 after HFS. Therefore, pixels which showed a potentiation or a depression with respect to  $\Delta F/F$  that lasted over the last three processed movies were used for subsequent analysis.

Both filters were designed in a two-step procedure. For filtering of continuously potentiated sites, all single pixel values  $\leq 1$  were set to 0, whereas those exhibiting a value  $> 1$  were set to 1. This was done for the last three arrays of  $\Delta F/F$ , thereby spanning the time period of minutes 30-42 after HFS. The three resultant arrays were multiplied by each other, creating an array that served as filter to detect potentiated sites over time. This filter in turn was multiplied with all processed arrays and only sites, which were included in the resultant arrays, were termed sites where potentiation occurred.

The same procedure was carried out for sites of depression, with exception of the initial two steps. In the first step, all single pixels that showed a value  $\geq 1$  were set to 0. After that, all pixels displaying a value  $> 0$  were set to 1.

If these filters were applied and a slice did not show sites of continuous potentiation or depression, it was excluded from some of the following extraction steps.

The extraction of several parameters was done after the processing steps. This included the extraction and averaging of relative values of all potentiated or depressed sites. Additionally the number of potentiated or depressed sites was quantified. To take into account both the strength of plasticity and the number of plastic sites, the total strength of all potentiated or depressed sites was determined by summing up the single percentage values of potentiation or depression.

If a slice did not show continuous potentiation or depression, the number of potentiated or depressed sites was defined as zero. For the other two analysis

parameters, values of relative change or total change were excluded from further analysis.

For the analysis of network dynamics in the BLA, only parameters of potentiation were analysed.

## **2.5 Field potential recordings**

For field potential recordings, slices were transferred to the recording chamber mounted on a vibration-cushioned table (TMC, Peabody). The slices were continuously superfused with carbogenated nACSF. All devices were grounded and the setup was located within a faraday cage (TMC, Peabody) to minimize electric noise. Slices were fixed by means of a grid and the stimulation electrodes, as well as the recording electrode, were positioned into the neuronal tissue using micromanipulators (PCS 400, EXFO, Burleigh). The recording electrodes had an open-tip resistance of 0.8-1.1 M $\Omega$ . The electrodes were pulled from borosilicate glass capillaries (GC 150TF-10 (Harvard Apparatus)) using DMZ Universal puller (Zeitz) and filled with nACSF. Square pulse electrical stimuli (50  $\mu$ s pulse width) were applied using the Iso-Stim 0,1M stimulator (npi). The Master 8 stimulator was used to trigger the stimulator to apply HFS. For single-pulse electrical stimulation and recording of signals at an interval of 15 s, the Pulse 8 software (HEKA Electronic) was used to trigger the stimulator through an A/D converter (HEKA Electronic). Signals were low-pass filtered at 1 kHz and sampled at 5 kHz.

Since the signals recorded within the LA can reflect both excitatory field postsynaptic potentials and action potentials, the peak amplitude of the potential deflection was used as quantitative of activity instead of the slope (Kulisch et al., 2011).

Recordings were performed in the LA upon stimulation of the EC. Baseline field potential responses were adjusted to half maximum of the field potential amplitude and after obtaining stable responses over 20 min, HFS was applied. The responses after HFS were recorded for 45 min.

The maximum field potential amplitude was analysed using the Pulse 8 software.

Afterwards, 4 recordings were averaged to 1 data point. Recordings were normalized to baseline responses.

## Chemicals

Substances were diluted and applied via the perfusion system or diluted in the staining chamber for VSDI staining. In all cases in which chemicals were solved in DMSO, the same amount of DMSO was added to the nACSF for baseline recordings. For details regarding chemicals, see appendix 1.

## Statistics

All values are given as mean  $\pm$  SEM. Statistical analysis was performed using the two-tailed unpaired/paired t-test, the Mann-Whitney Rank Sum test, the Wilcoxon Signed Rank test, the One-Way ANOVA followed by Bonferroni *post hoc* test or the One-Way ANOVA on ranks followed by Dunn's test. Data were tested on ranks as stated above, if the respective normality or equal variance test failed.

Data sets were tested using the Grubb's test with a p-value of 0.05 for significant outliers. Differences were considered significant if  $p < 0.05$  (\* $p < 0.05$ , \*\* $p < 0.01$ , \*\*\* $p < 0.001$ ).

Statistical analysis was done by use of Sigma Stat or Graph pad Quickcalcs, which was accessed via: [www.graphpad.com/quickcalcs/Grubbs1.cfm](http://www.graphpad.com/quickcalcs/Grubbs1.cfm)

## 3 Results

### 3.1 Development of VSDI assay

#### Slicing protocol and pharmacological characterization of VSDI signals

Unless otherwise stated, in the following, brain slices from BI 6 mice were used for experiments. For the investigation of network activity and dynamics within the LA and BLA, 400  $\mu\text{m}$ -thick horizontal brain slices were cut. To obtain reliable and comparable results in all slices, a slicing protocol was developed according to anatomical landmarks. These landmarks included the lateral ventricle, the stria terminalis, and the CA1 region of the hippocampus. Since slicing was performed from ventral to dorsal, the pyramidal cell layer of the hippocampal CA1 region appeared diffuse at the level which contains the relevant neuronal network of the LA and BLA, marking the transition zone from the intermediate to the dorsal part of the hippocampus (Figure 3.1-8A). Additionally, a fibre bundle could be observed at the border from the BLA to CeA which has been described previously (von Bohlen und Halbach and Albrecht, 1998; Paxinos, 2004). The neuronal network contained in this slice preparation was used for all experiments.

Subsequent slicing in a thickness of 400  $\mu\text{m}$  resulted in a plane in which the pyramidal cell layer of the CA1 region was clearly defined, thus providing an end point for slice preparation (Figure 3.1-8B). As a reference for landmarks described above, an anatomical tracing study in the rat brain was used (von Bohlen und Halbach and Albrecht, 1998).

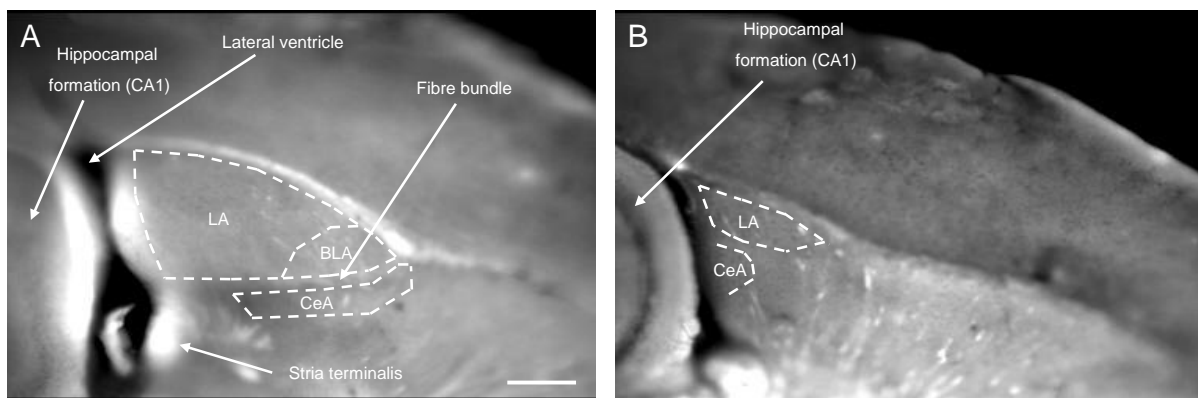


**Figure 3.1-8. Different planes of horizontal brain slices which contain distinct nuclei of the amygdaloid complex.** A, Brain slice which contains the ventral lateral amygdala, the dorsal basolateral amygdala, and the central nucleus of the amygdala. B, Brain slice which contains the lateral amygdala and the central amygdala. The planes of the slices were cut with a transversal distance of 400  $\mu\text{m}$ . Landmarks to distinguish between different levels are described in detail using arrows. LA = Lateral amygdala, BLA = Basolateral amygdala, CeA = Central amygdala, Scale bar = 400  $\mu\text{m}$ .

After the development of this slicing protocol, signal propagation was qualitatively investigated after the delivery of a single electrical stimulation pulse to the EC (Figure 3.1-9). Amygdalar neuronal network activity spread from the EC to the lateral and medial portion of LA, the BLA, and from the LA and BLA to the CeA as described previously (Sah et al., 2003; LeDoux, 2007; Pare and Duvarci, 2012).

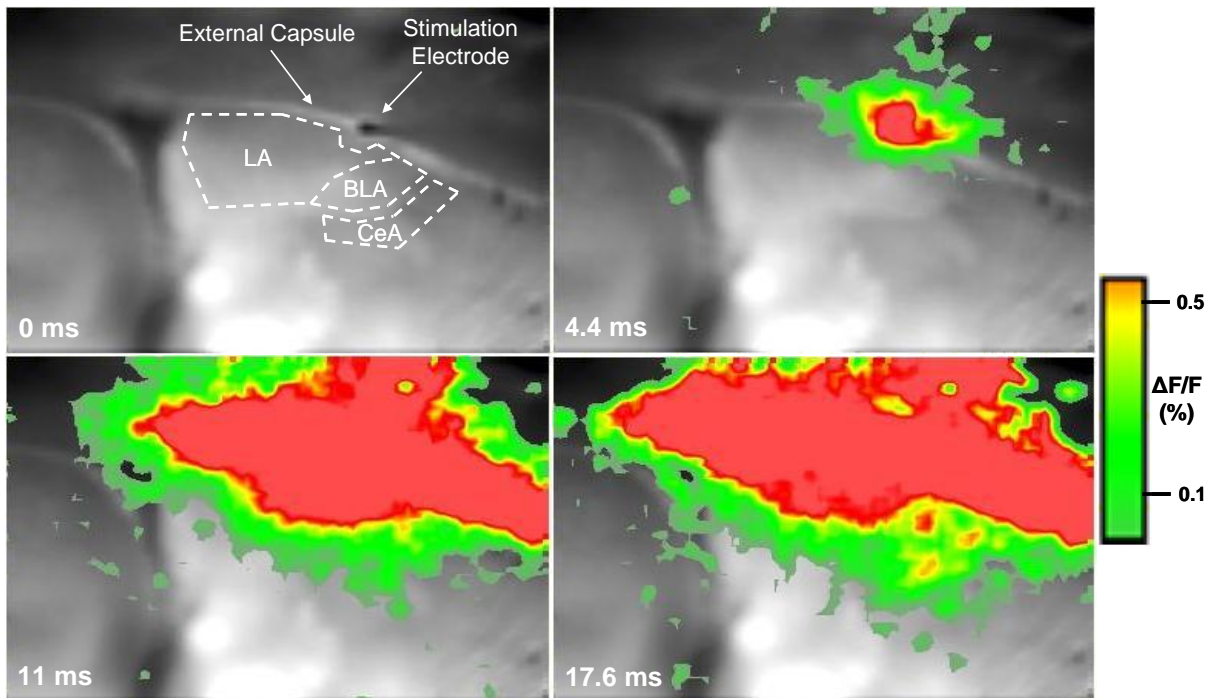


**Figure 3.1-9. Overview of amygdaloid nuclei contained in the horizontal brain slice and location of the stimulation electrode.** Time course of VSD signal propagation within the lateral, basolateral, and central nucleus of the amygdala after electrical stimulation of the external capsule. Warmer colours (see colour bar) represent stronger neuronal activity. LA = Lateral amygdala, BLA = Basolateral amygdala, CeA = Central amygdala, VSD = Voltage-sensitive dye.

Intra-LA single-pulse electrical stimulation resulted in signal propagation from the LA to the dorsal part of the BLA and the CeA within the brain slice (Figure 3.1-10). This pathway of activity flow was previously described (Pare and Duvarci, 2012).

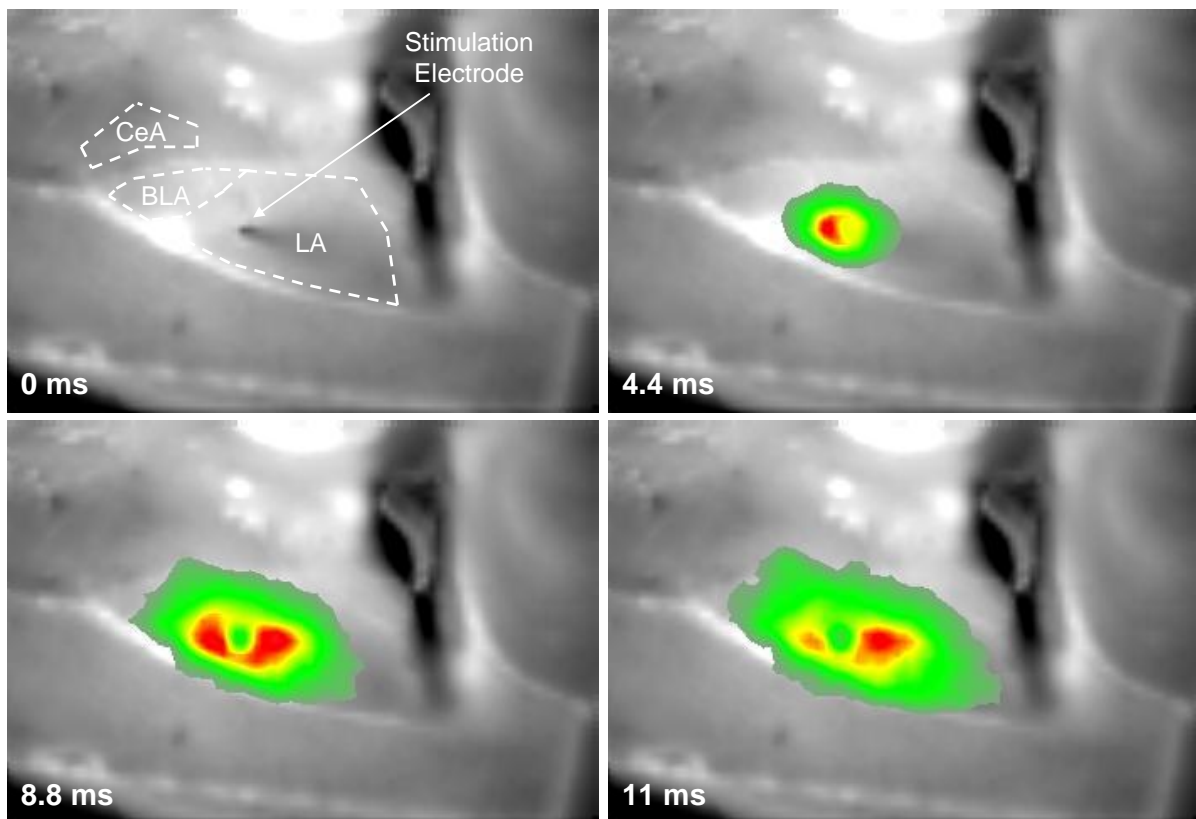


**Figure 3.1-10. Overview of amygdaloid nuclei contained in the horizontal brain slice and location of the stimulation electrode.** Time course of VSD signal propagation within the lateral, basolateral, and central nucleus of the amygdala after electrical stimulation within the lateral amygdala. LA = Lateral amygdala, BLA = Basolateral amygdala, CeA = Central amygdala, VSD = Voltage-sensitive dye.

The quantification of acquired VSDI signals is done by setting a ROI according to anatomical landmarks as previously described in the LA or BLA subfield (Figure 3.1-11A). The VSD Di-4-ANEPPS is capable of reporting de- or hyperpolarizing changes in membrane potential as alterations in fluorescence (Tominaga et al., 2000). Given this fact, one could observe, that the VSD signals had different time courses if comparing the LA with the BLA (Figure 3.1-11B). The LA signal displayed a slow hyperpolarizing component, which could be abolished by bath application of the GABA<sub>B</sub> receptor antagonist (2S)-3-[[[(1S)-1-(3,4-Dichlorophenyl)-ethyl]amino]-2-hydroxypropyl](phenylmethyl)phosphinic acid hydrochloride (CGP 55845) (5  $\mu$ M) (data not shown). This antagonist was also capable of prolonging the stimulus-evoked depolarization-mediated VSD signal in the LA and BLA FDSs.

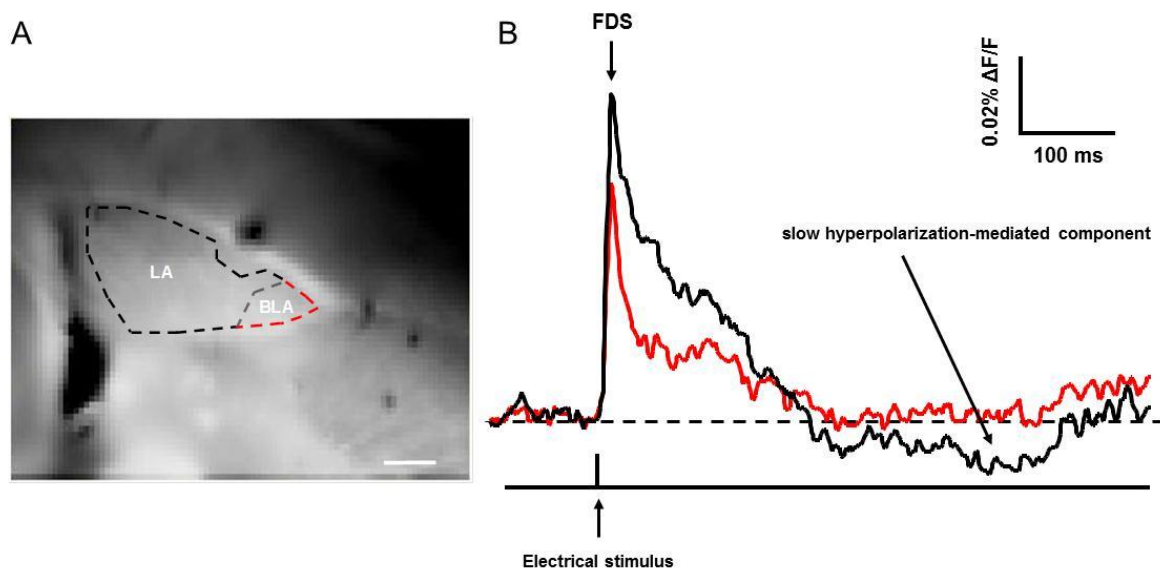


**Figure 3.1-11. Detection of VSD signal in specific ROIs after single electrical stimulation of the external capsule.** A, Dotted lines depict whole LA ROI (black) and whole BLA ROI (red) contained in the brain slice. Dotted gray line indicates the border between LA and BLA; Scale bar: 400  $\mu\text{m}$ . B, Time course of VSD signal after single stimulus onset colour coded for the LA (black) and the BLA (red). For further quantification of VSD signals the FDS is used. Please note the slow hyperpolarization-mediated component in the LA signal and its absence in the BLA signal. VSD = Voltage-sensitive dye, ROI = Region of interest, FDS = Fast depolarization-mediated signal, LA = Lateral amygdala, BLA = Basolateral amygdala.

To pharmacologically characterize the VSD signal in our slices, the FDS component of the signal was chosen and known blockers of ion channels were bath applied. The voltage-gated sodium channel blocker tetrodotoxine (TTX) (1  $\mu\text{M}$ ) was capable of abolishing the FDS, whereas 2,3-dihydroxy-6-nitro-7-sulfamoyl-benzo[f]quinoxaline-2,3-dione (NBQX) (5  $\mu\text{M}$ ) and AP 5 (50  $\mu\text{M}$ ), blockers of ionotropic glutamate receptors strongly reduced FDS amplitudes (Figure 3.1-12A, C), thereby proving the FDSs to be mostly mediated by glutamatergic synaptic transmission. Since it is also known that GABAergic transmission plays an important role in the regulation of network activity within the amygdaloid complex, bicuculline methiodide (BIM) (2  $\mu\text{M}$ ), a GABA<sub>A</sub> receptor antagonist, was bath-applied. This resulted in a strong increase in FDS amplitudes (Figure 3.1-12B). This observation is in line with previous findings (Wang et al., 2001). Additionally, the stability of the FDSs over time was assessed (Figure 3.1-12D).

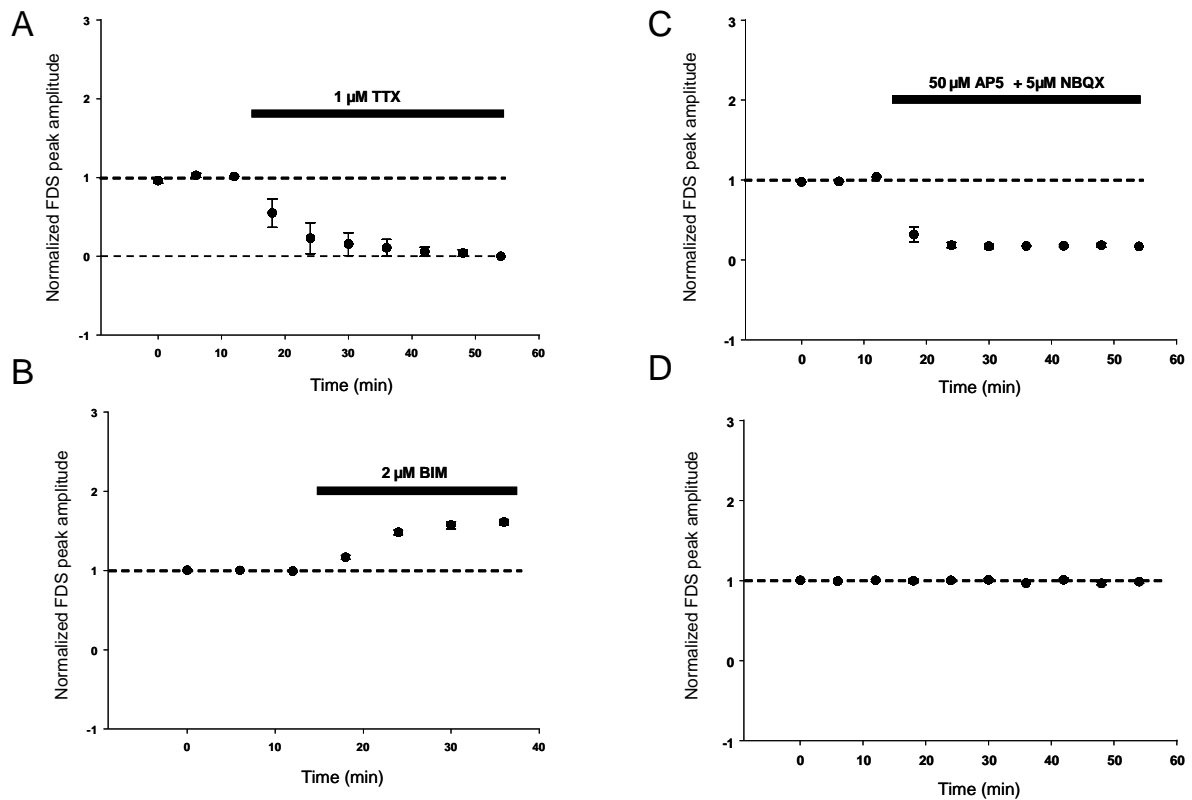


**Figure 3.1-12. Pharmacological characterization of VSD signal in the LA.** A, B, C, Pharmacological characterization of FDS after obtaining stable baseline responses by either bath application of 1  $\mu$ M TTX (3 slices/2 animals), 2  $\mu$ M BIM (6 slices/3 animals) or 50  $\mu$ M AP 5 and 5  $\mu$ M NBQX (3 slices/3 animals). D, Prove of stability of FDS over stimulation time (7 slices/4 animals). Data are presented as means  $\pm$  SEM. VSD = Voltage-sensitive dye, FDS = Fast depolarization-mediated signal, TTX = Tetrodotoxin, AP 5 = D(-)-2-Amino-5-phosphonopentanoic acid, NBQX = 2,3-dihydroxy-6-nitro-7-sulfamoyl-benzof[*f*]quinoxaline-2,3-dione, BIM = Bicuculline methiodide.

All characterizations were done for signals that arose in the LA and BLA (BLA data not shown).

## 3.2 Investigation of neuronal network dynamics

### 3.2.1 Field potential recordings

Prior to the investigation of neuronal network plasticity by means of VSDI, a stimulation protocol to induce LTP was validated for its usability in the amygdaloid network contained in the brain slices. The application of HFS to the EC induced LTP of excitatory field potentials recorded in the LA. The magnitude of LTP was significant ( $22.9 \pm 0.4\%$ ,  $n = 6$  slices/5 animals) compared to the last 10 min of baseline recordings (Figure 3.2.1-13).

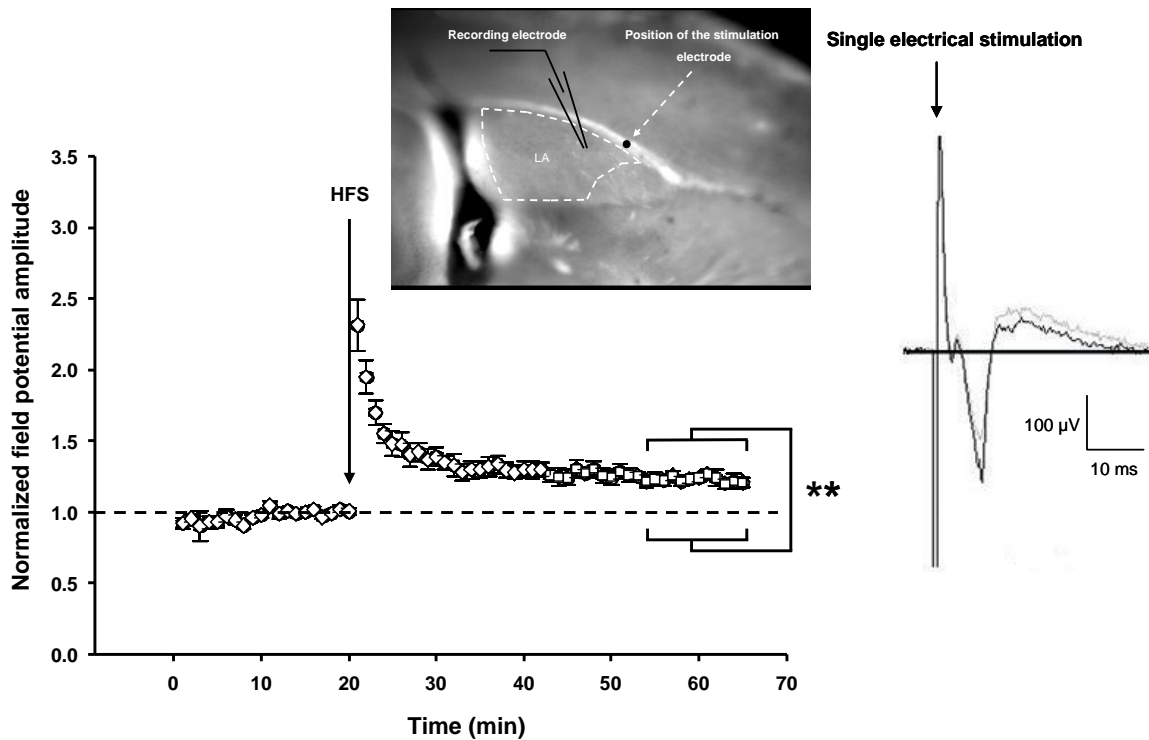


**Figure 3.2.1-13. Extracellular field potential recordings of LA responses upon single-pulse electrical stimulation of the EC before and after HFS.** HFS significantly (paired t-test,  $p = 0.001$ ) increased field potential amplitude within the LA in horizontal brain slices ( $n = 6$  slices/5 animals). Representative traces illustrate extracellular responses before (grey) and after (black) HFS. The scheme on the top shows of the location of the stimulation and recording electrodes. LA = Lateral amygdala, EC = External capsule, HFS = High-frequency stimulation.

### **3.2.2 Monitoring of network dynamics by means of VSDI and subsequent data processing**

To capture all HFS-induced changes in neuronal network excitability in the brain slice, advanced data analysis was applied to VSDI. First, network potentiation in the LA after HFS was monitored using VSDI. This approach was capable of reporting lasting changes in network activity (Figure 3.2.2-14A, B).

To gain more detailed insights into neuronal network dynamics, VSDI movies were imported into Matlab for further processing. Active Sites were defined (Figure 3.2.2-15) (for details see material and methods) and a ROI was set according to anatomical landmarks (Figure 3.2.2-14C).

The resultant images displayed changes in evoked network activity after HFS with a spatial resolution of  $36.4 \times 40 \mu\text{m}$ . By means of this analysis, it was possible to show that the LA is able to respond to the same HFS in opposite ways, spatially segregated: thus some sites showed potentiation whereas some other showed depression of the relative change in fluorescence after HFS compared to baseline level (Figure 3.2.2-14D, E). By use of anatomical landmarks, as described before, the BLA network, contained in the brain slice could also be analysed in this way (data not shown). Since the BLA was located in close proximity to the stimulation electrode, the resultant intense electrical excitation of the neurons of the BLA, most likely overrides depression of neuronal excitability. Therefore, BLA network dynamics were solely examined with respect to potentiation.

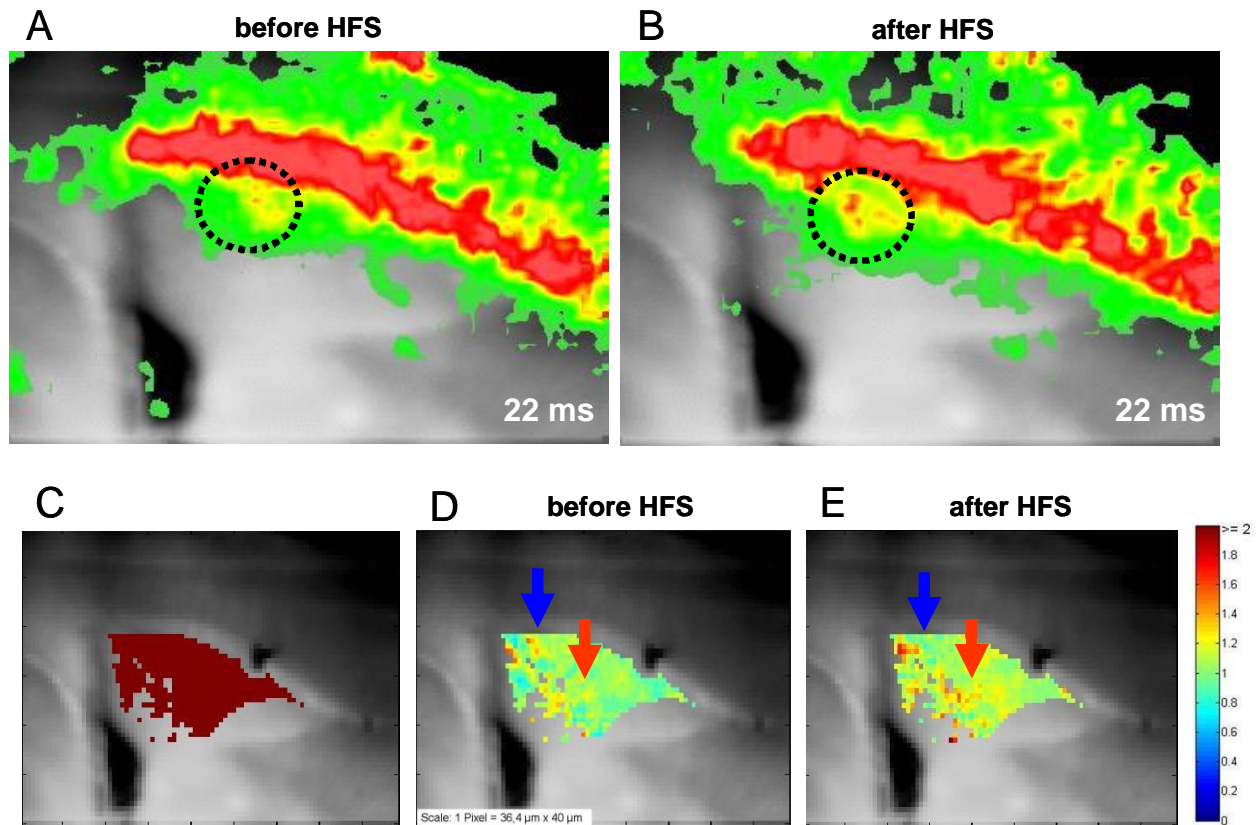


**Figure 3.2.2-14. Neuronal network plasticity in the LA monitored by means of VSDI and subsequent data processing.** A, Baseline response 22 ms after single-pulse stimulation. B, LA response 22 ms after single-pulse stimulation 36 min after HFS. Circle indicates network potentiation after HFS. C, "Active Site Filter" calculated by applying the "RMSThreshold" (for details see material and methods) to single-pixel maximum change in fluorescence of 25 consecutive frames after stimulus onset before HFS. The ROI was set according to anatomical landmarks excluding the portion of the BLA contained in the slice. D, Relative baseline responses of all active sites within the LA upon single-pulse electrical stimulation. E, Responses of all active sites 36 min after HFS within the LA upon single-pulse electrical stimulation. Arrows indicate a site of depression (blue) or potentiation (red) before and after HFS. Colour bar: relative change of  $\Delta F/F$ . LA = Lateral amygdala, BLA = Basolateral amygdala HFS = High-frequency stimulation, RMSThreshold = Root mean square threshold, ROI = Region of interest, VSDI = Voltage-sensitive dye imaging.

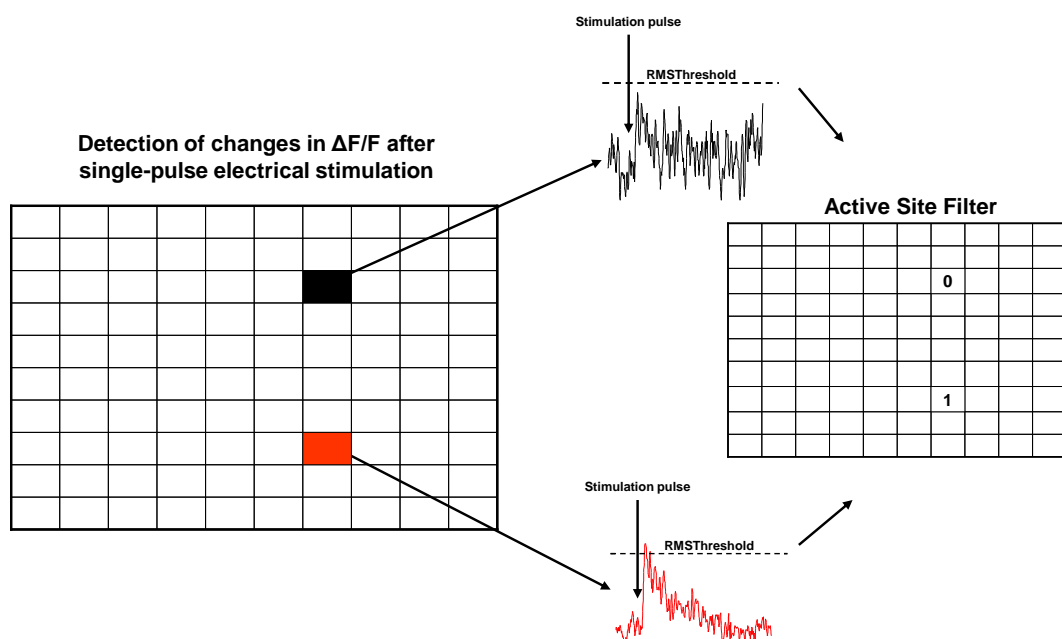


**Figure 3.2.2-15. Principle of the design of the Active Site Filter.** Maximum changes in  $\Delta F/F$  after single-pulse electrical stimulation can be distinguished from noise by use of the RMSThreshold operation. Sites with maximum  $\Delta F/F$  values  $\leq$  RMSThreshold (black trace) are set to 0, whereas sites with maximum  $\Delta F/F$  values  $>$  RMSThreshold (red trace) are set to 1. RMSThreshold = Root mean square threshold.

The FDS was captured through a maximum intensity projection operation of change in fluorescence within single sites over a defined course of frames (Figure 3.2.2-16).

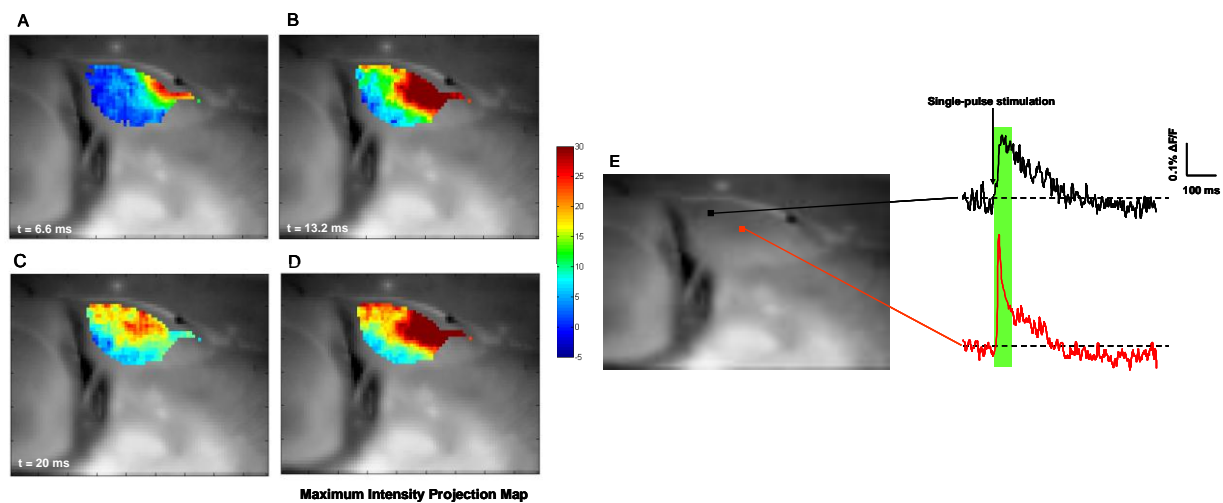


**Figure 3.2.2-16. Visualization of maximum intensity projection command output.** A,B,C, Time course of changes in fluorescence per pixel within the lateral amygdala shown for three different time points after single-pulse stimulation of the external capsule. D, Maximum intensity projection map of  $\Delta F/F$  values for each single pixel within 25 consecutive frames (Interval: 2.2 ms) after stimulus onset. Colour bar: changes in fluorescence intensity relative to background. E, Time course of FDSs after delivering a single electrical stimulation to the external capsule. Two traces depict different time courses of FDSs, dependent on the location of the ROI, here exemplified through black and red squares. To reliably capture the maximum amplitude of the FDS within the whole lateral amygdala within the slice, the maximum intensity projection map is computed in a certain time frame, illustrated by the green bar. FDSs = Fast depolarization-mediated signals, ROI = Region of interest.

The network dynamics analysis of the LA offered the whole spectrum of parameters which could be extracted from the same slice ( $n = 10$  slices/7 animals) (for details, see material and methods). In this way, it could be shown that, after HFS, VSD signals in the LA reliably reflected potentiation and depression of neuronal network activity on three levels. Mean values of relative strength of potentiation ( $15.7 \pm 1.7\%$ ) or depression ( $15.9 \pm 1.9\%$ ) were significant compared to baseline (Figure 3.2.2-17A). Additionally, the sum of total strength of potentiation ( $1946 \pm 515\%$ ) or depression ( $-1136 \pm 229\%$ ) over all active sites which reliably displayed changes in activity was significant, compared to baseline activity at these sites (Figure 3.2.2-17B). The third extracted parameter was the number of sites, in which potentiation ( $109 \pm 22$ ) or depression ( $69.9 \pm 13.3$ ) occurred (Figure 3.2.2-17C).

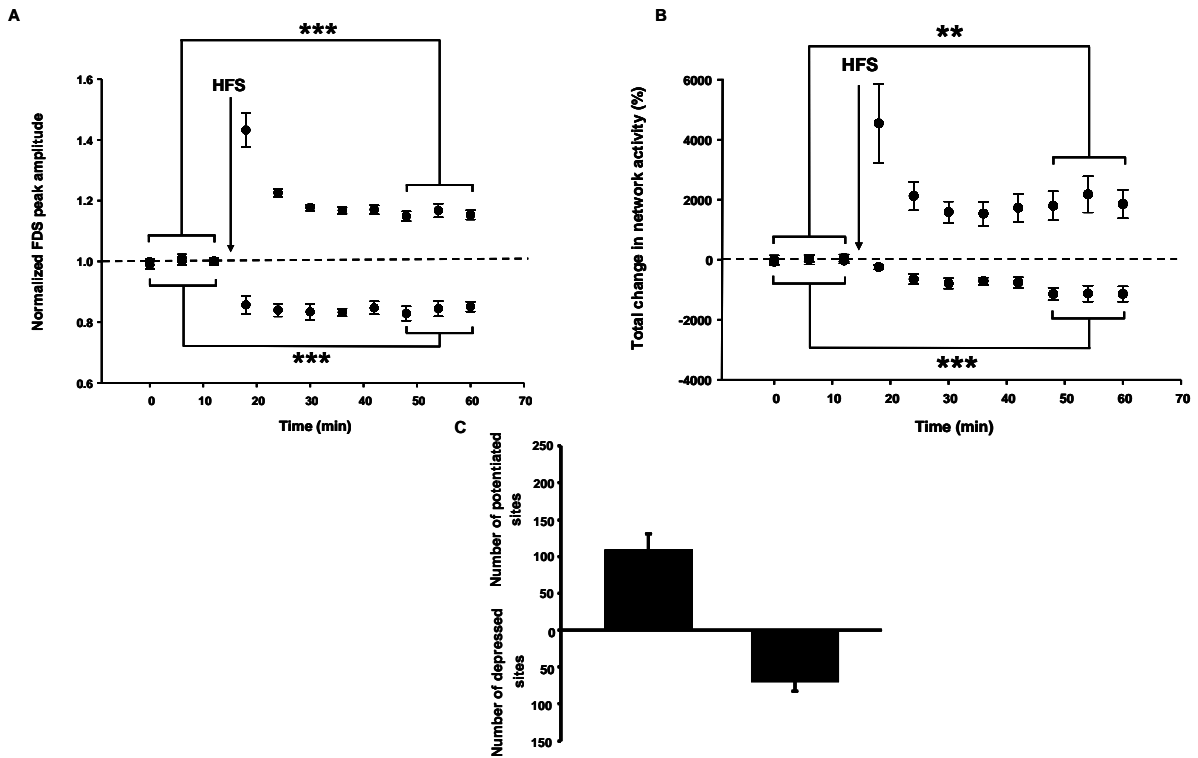


**Figure 3.2.2-17. Changes in network dynamics within the LA after HFS in C57BL/6N mice.** All measures were extracted from the same slices ( $n = 10$  slices/7 animals). A, Mean values of relative potentiation or depression of network activity. Mean values of potentiation during minutes 30-42 after HFS showed significant increase compared to baseline (paired t-test,  $p < 0.001$ ). Mean values of depression during minutes 30-42 after HFS showed significant decrease compared to baseline (paired t-test,  $p < 0.001$ ). B, Mean values of total potentiation or depression of network activity. Mean values of potentiation during minutes 30-42 after HFS showed significant increase compared to baseline (paired t-test,  $p = 0.004$ ). Mean values of depression during minutes 30-42 after HFS showed significant decrease compared to baseline (paired t-test,  $p < 0.001$ ). C, Number of sites within the LA ROI which showed potentiation or depression of network activity during minutes 30-42 after HFS. Data are presented as means  $\pm$  SEM. HFS = High-frequency stimulation, LA = Lateral amygdala, LA ROI = Lateral amygdala region of interest.

### 3.2.2.1 Pharmacological characterization of changes in network dynamics

The observed changes in network dynamics were pharmacologic characterized using AP 5 as a NMDA receptor antagonist and verapamil, a blocker for L-VGCCs. NMDA receptors and VGCCs were previously shown to contribute to the induction of neuronal plasticity in the amygdala (Grover and Teyler, 1990; Huang and Kandel, 1998; Bauer et al., 2002).

After bath application of AP 5 (50  $\mu$ M) or verapamil (50  $\mu$ M) and after obtaining stable baseline responses, HFS was applied and its effect on network dynamics in the LA was investigated.

The presence of verapamil significantly reduced the total strength of network potentiation ( $334 \pm 73\%$ ,  $n = 9$  slices/6 animals) in comparison to AP 5 treated slices ( $4820 \pm 1096\%$ ,  $n = 10$  slices/7 animals) (Figure 3.2.2.1-18A). Single-group comparison of the total strength in network potentiation of verapamil-treated slices with control slices ( $1946 \pm 515\%$ ,  $n = 10$  slices/7 animals) revealed that this treatment significantly (Mann-Whitney Rank Sum test,  $p = 0.002$ ) reduced HFS-induced potentiation. In contrast to that, the presence of AP 5 significantly (t-test,  $p = 0.029$ ) increased the strength of this parameter compared to control conditions.

Concerning the HFS-induced total network depression, AP 5-treated slices exhibited a significant decrease ( $-288 \pm 75\%$ ,  $n = 9$  slices/7 animals) of network depression compared to slices which were bathed in verapamil-containing nACSF ( $-2938 \pm 424\%$ ,  $n = 8$  slices/6 animals) (Figure 3.2.2.1-18B). Verapamil-treated slices showed a significant increase in strength of depression compared to control slices ( $-1136 \pm 229\%$ ,  $n = 10$  slices/7 animals) (Figure 3.2.2.1-18B).

Single-group comparison of HFS-induced total network depression between AP 5-treated slices and control slices showed a significant (Mann-Whitney Rank Sum test,  $p = 0.006$ ) decrease.

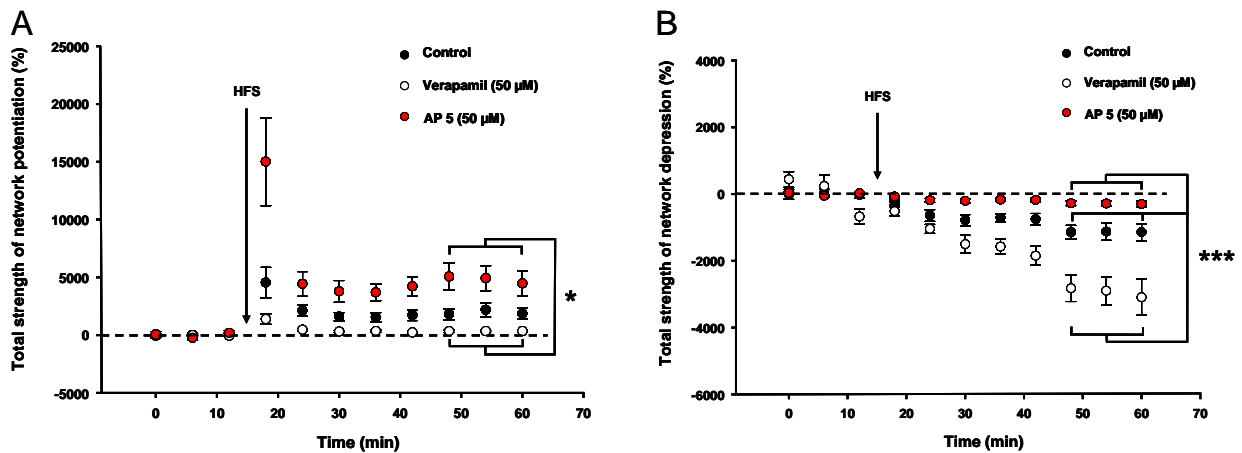


**Figure 3.2.2.1-18. Effects of verapamil or AP 5 on LA network dynamics.** A, The presence of 50  $\mu\text{M}$  verapamil (open circles) significantly (One-Way ANOVA on ranks,  $p < 0.001$ , followed by Dunn's test,  $p < 0.05$ ) reduced the total strength of network potentiation compared to 50  $\mu\text{M}$  AP 5 (red circles). Black circles depict total strength of network potentiation in untreated slices (verapamil:  $n = 9$  slices/6 animals, AP 5:  $n = 10$  slices/7 animals, control:  $n = 10$  slices/7 animals). B, The presence of 50  $\mu\text{M}$  verapamil significantly (One-Way ANOVA,  $p < 0.001$ , followed by Bonferroni *post hoc* test,  $p < 0.001$ ) increased the total strength of network depression after HFS compared to AP 5-treated slices. 50  $\mu\text{M}$  verapamil was capable of significantly (One-Way ANOVA,  $p < 0.001$ , followed by Bonferroni *post hoc* test,  $p < 0.001$ ) increasing the total strength of network depression compared to controls (verapamil:  $n = 8$  slices/6 animals, AP 5:  $n = 9$  slices/7 animals, control:  $n = 10$  slices/7 animals). Data are presented as means  $\pm$  SEM. AP 5 = D (-)-2-Amino-5-phosphonopentanoic acid, HFS = High-frequency stimulation, LA = Lateral amygdala.

As stated before, BLA network dynamics were solely investigated regarding potentiation of activity. The comparison of total strength of potentiation between control slices ( $486 \pm 125\%$ ,  $n = 10$  slices/7 animals) with the presence of verapamil ( $158 \pm 72\%$ ,  $n = 10$  slices/6 animals) or AP 5 ( $620 \pm 197\%$ ,  $n = 10$  slices/7 animals) showed that there was no significant effect on this parameter (data not shown). However, 50  $\mu\text{M}$  verapamil in the bathing solution significantly reduced the number of potentiated sites ( $4.70 \pm 1.96$ ,  $n = 10$  slices/6 animals) compared to control condition ( $27.4 \pm 5.9$ ,  $n = 10$  slices/7 animals) and AP 5-treatment ( $28.6 \pm 8.8$ ,  $n = 10$  slices/7 animals) (Figure 3.2.2.1-19).

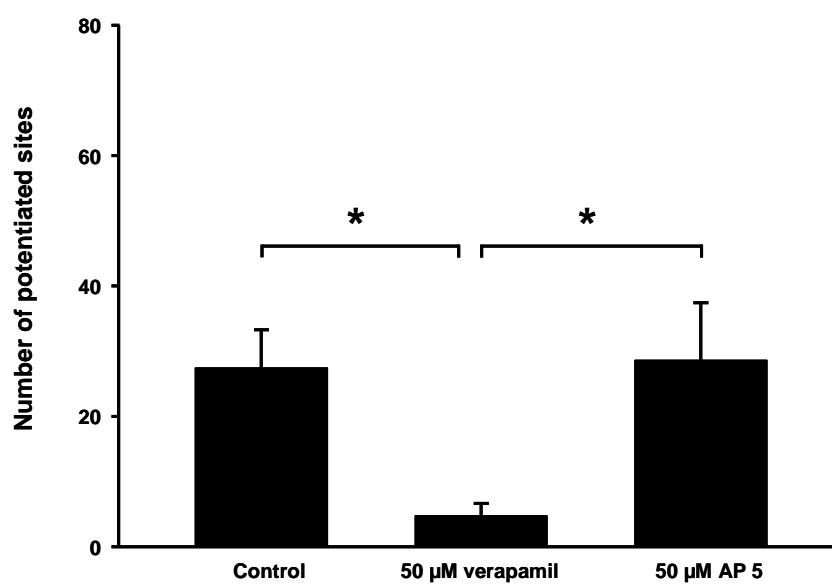


**Figure 3.2.2.1-19. Verapamil decreases the number of potentiated sites after HFS in the BLA.** Bath application of verapamil significantly (One-Way ANOVA on ranks,  $p = 0.005$ , followed by Dunn's test,  $p < 0.05$ ) reduced the number of potentiated sites after HFS comparing control conditions with the presence of verapamil and AP 5 conditions with the presence of verapamil (verapamil:  $n = 10$  slices/6 animals, AP 5:  $n = 10$  slices/7 animals, control:  $n = 10$  slices/7 animals). Data are presented as means  $\pm$  SEM. BLA = Basolateral amygdala, HFS = High-frequency stimulation, AP 5 = D (-)-2-Amino-5-phosphonopentanoic acid.

### 3.2.3 Investigation of the effect of CRH on network activity and dynamics in the LA and BLA

After the development of the VSDI assay for the examination of neuronal network activity and dynamics in the LA and BLA, the influence of mediators of stress response (CRH and Cort) on these electrophysiological measures was investigated.

Based on studies which showed that neurons of the LA and BLA express functional CRHR1 and since the CeA is a major source of extra-hypothalamic CRH which is capable of entering the LA and the BLA (Rooszendaal et al., 2002; Hubbard et al., 2007; Refojo et al., 2011), the effects of CRH on neuronal network activity and plasticity were examined.

Bath application of CRH (at the concentration of 125 or 250 nM) affected neuronal network activity reflected by changes in FDS amplitudes in the LA and BLA. Figure 3.2.3-20A, C depicts the effect of bath application of 125 nM CRH on FDS amplitudes in the LA and BLA. Although 125 nM CRH increased the FDS amplitudes in the BLA, this effect was not statistical significant ( $6.60 \pm 3.37\%$ ,  $n = 10$  slices/7 animals). Bath application of 250 nM CRH increased FDS amplitudes in the LA ( $3.20 \pm 2.33\%$ ,  $n = 8$  slices/5 animals) (Figure 3.2.3-20B), but again, this effect did not reach the level of significance. For statistical testing, the mean values of FDS amplitudes of the last 3 data points after CRH-application were compared to baseline. In contrast, the presence of 250 nM CRH in the bathing solution significantly increased FDS amplitudes in the BLA ( $6.50 \pm 2.06\%$ ,  $n = 8$  slices/5 animals) (Figure 3.2.3-20D).

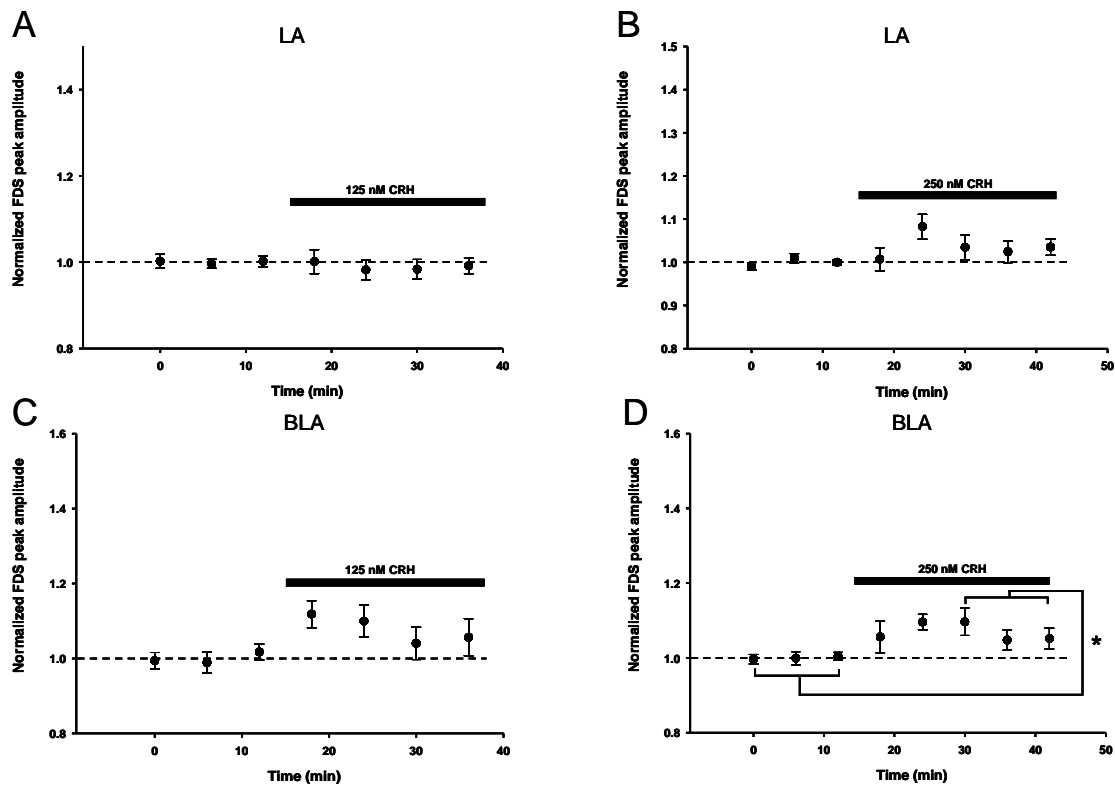


**Figure 3.2.3-20. Bath application of CRH affects FDS amplitudes in the LA and BLA in a concentration dependent manner.** A, C, Effects of 125 nM CRH on FDS amplitudes in the LA (A) and BLA (C). These effects did not reach the level of significance. (n = 10 slices/7 animals). B, D, Effects of 250 nM CRH on FDS amplitudes in the LA (B) and BLA (D). Within in the BLA, 250 nM CRH significantly (paired t-test, p = 0.016) increased FDS amplitudes (n = 8 slices/5 animals). Data are presented as means  $\pm$  SEM. CRH = Corticotropin-releasing hormone, FDS = Fast depolarization-mediated signal, LA = Lateral amygdala, BLA = Basolateral amygdala.

After obtaining stable baseline responses, HFS was applied in the same slices to investigate whether CRH affects network plasticity. In the LA, 125 nM CRH significantly increased the magnitude of HFS-induced relative potentiation ( $21.4 \pm 1.3\%$ , n = 10 slices/7 animals) compared to untreated control slices ( $15.7 \pm 1.7\%$ , n = 10 slices/7 animals) (Figure 3.2.3-21).

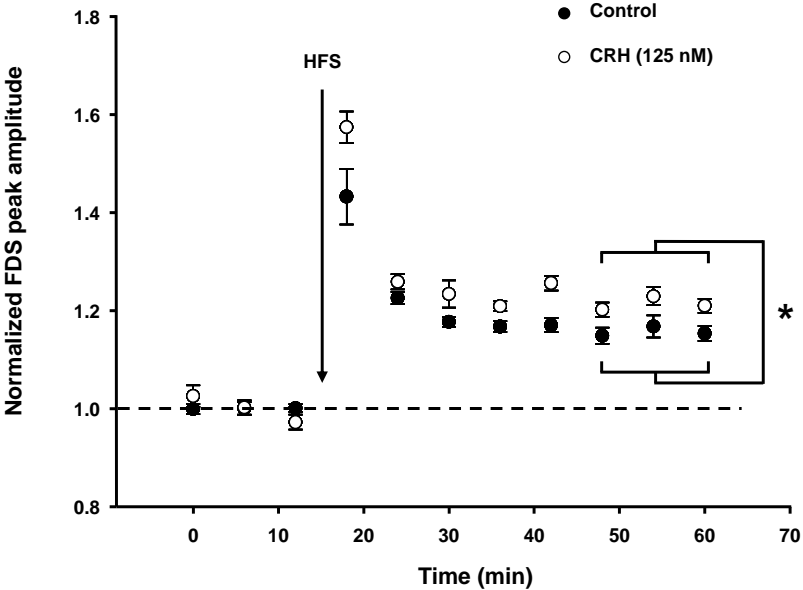


**Figure 3.2.3-21. 125 nM CRH increases HFS-induced network plasticity in the LA.** Bath application of 125 nM CRH (open circles) significantly (unpaired t-test;  $p = 0.016$ ) increased the magnitude of relative network potentiation compared to control conditions (black circles) (control:  $n = 10$  slices/7 animals, 125 nM CRH:  $n = 10$  slices/7 animals). Data are presented as means  $\pm$  SEM. CRH = Corticotropin-releasing hormone, HFS = High-frequency stimulation, LA = Lateral amygdala.

In contrast, bath application CRH (250 nM) impacted HFS-induced changes in neuronal network dynamics in the LA on three levels. Compared to control conditions ( $109 \pm 22$ ,  $n = 10$  slices/7 animals) and 125 nM CRH treatment ( $103 \pm 14$ ,  $n = 10$  slices/7 animals) the presence of 250 nM CRH significantly increased the number of potentiated sites ( $211 \pm 22$ ,  $n = 8$  slices/5 animals) (Figure 3.2.3-22A). Moreover, 250 nM CRH significantly reduced the number of depressed sites ( $16.3 \pm 8.1$ ,  $n = 8$  slices/5 animals) compared to control conditions ( $69.9 \pm 13.3$ ,  $n = 10$  slices/7 animals) (Figure 3.2.3-22B). Finally, the total strength of network potentiation was significantly enhanced ( $4102 \pm 653\%$ ,  $n = 8$  slices/5 animals) compared to control conditions ( $1946 \pm 515\%$ ,  $n = 10$  slices/7 animals) (Figure 3.2.3-22C). The comparison of the total strength of network potentiation in the presence of 125 nM CRH ( $2179 \pm 317\%$ ,  $n = 10$  slices/7 animals) with bathing solution containing 250 nM CRH ( $4103 \pm 653\%$ ,  $n = 8$  slices/5 animals) showed that there was a significant increase in total network potentiation (data not shown).

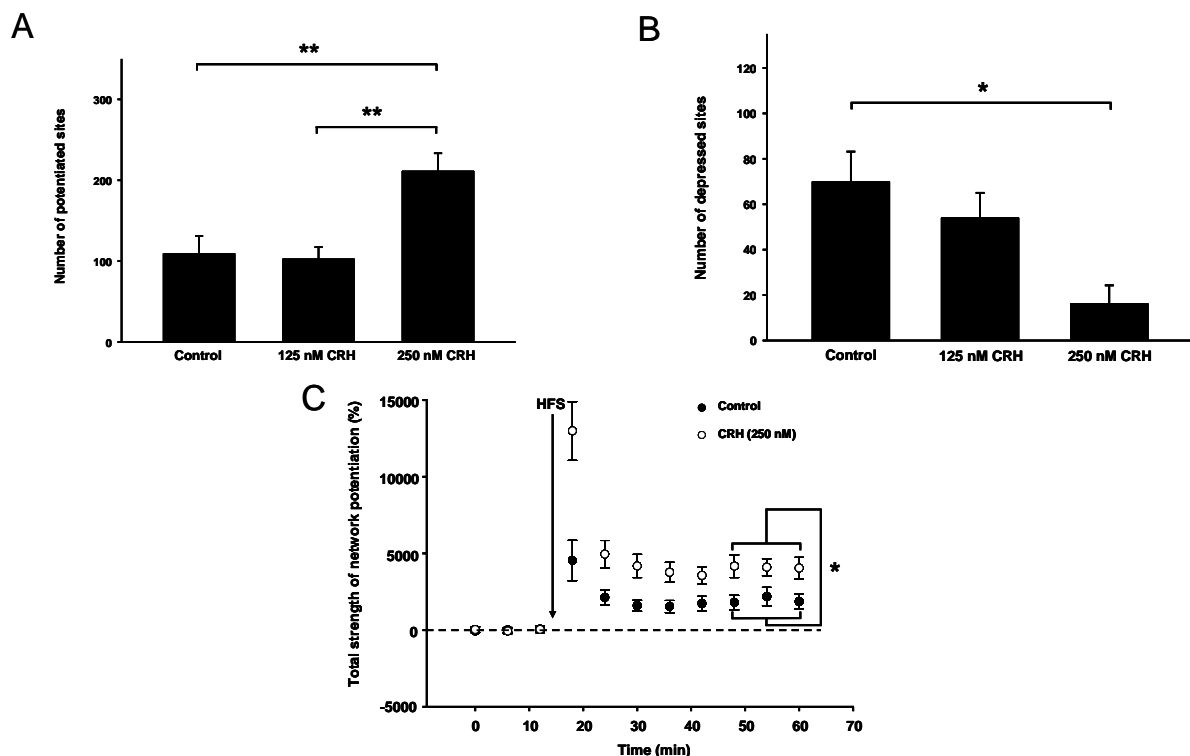


**Figure 3.2.3-22. CRH-induced changes in network dynamics after HFS in the LA.** A, The number of potentiated sites after HFS was significantly increased in 250 nM CRH-treated slices compared to control slices (One-Way ANOVA,  $p = 0.001$ , followed by Bonferroni *post hoc* test,  $p = 0.004$ ) and 125 nM CRH-treated slices (One-Way ANOVA,  $p = 0.001$ , followed by Bonferroni *post hoc* test,  $p = 0.002$ ). B, The number of depressed sites after HFS was significantly decreased in 250 nM CRH-treated slices compared to control slices (One-Way ANOVA,  $p = 0.011$ , followed by Bonferroni *post hoc* test,  $p = 0.010$ ). C, Slices treated with 250 nM CRH (open circles) exhibited a significant increase in HFS-induced total strength of network potentiation compared to control slices (black circles) (One-Way ANOVA,  $p = 0.012$ , followed by Bonferroni *post hoc* test,  $p = 0.017$ ) and to slices treated with 125 nM CRH (data not shown) (One-Way ANOVA,  $p = 0.012$ , followed by Bonferroni *post hoc* test,  $p = 0.038$ ) (control:  $n = 10$  slices/7 animals, 125 nM CRH:  $n = 10$  slices/7 animals, 250 nM CRH:  $n = 8$  slices/5 animals). Data are presented as means  $\pm$  SEM and all statistical comparisons were done for minutes 30-42 after HFS. LA = Lateral amygdala, HFS = High-frequency stimulation, CRH = Corticotropin-releasing hormone.

The investigation of network dynamics in the BLA indicated that neither 125 nM ( $14.7 \pm 3.8$ ,  $n = 10$  slices/7 animals) nor 250 nM ( $29.8 \pm 3.9$ ,  $n = 8$  slices/5 animals) significantly altered the number of sites at which potentiation occurred (Figure 3.2.3-23).

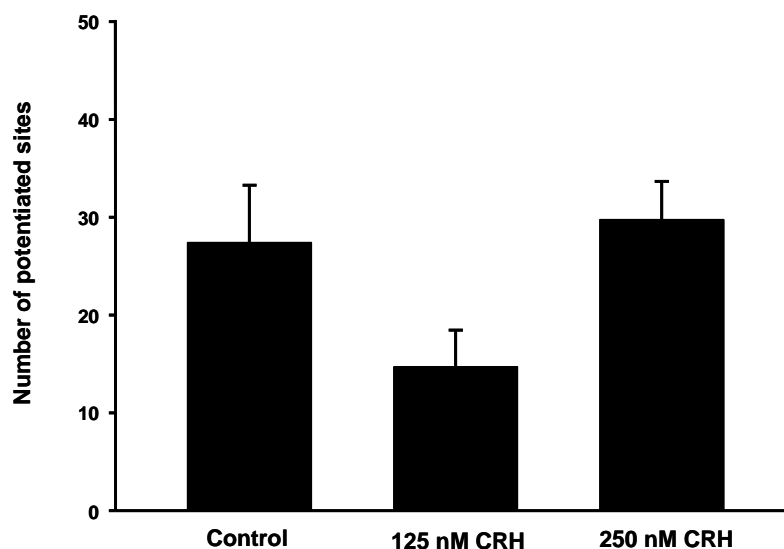


**Figure 3.2.3-23. CRH induces no changes in the number of potentiated sites in the BLA after HFS.** Bath application of 125 or 250 nM CRH did not significantly alter the number of potentiated sites after HFS (control:  $n = 10$  slices/7 animals, 125 nM CRH:  $n = 10$  slices/7 animals, 250 nM CRH:  $n = 8$  slices/5 animals). Data are presented as means  $\pm$  SEM. BLA = Basolateral amygdala, CRH = Corticotropin-releasing hormone, HFS = High-frequency stimulation.

### 3.2.3.1 Involvement of CRHR1 in CRH-induced changes in network activity and dynamics in the LA and BLA

By use of CKO mice and CTRL mice, it was investigated whether CRHR1 is involved in the mediation of the observed changes in network activity and dynamics. Since CRH in the concentration of 250 nM influenced network activity or dynamics in the LA or BLA to the highest amount, this concentration was used for subsequent experiments. Bath application of 250 nM CRH to slices from CTRL mice increased FDS amplitudes in the LA ( $5.10 \pm 2.63\%$ ,  $n = 10$  slices/6 animals) (Figure 3.2.3.1-24A). This effect did not reach the level of statistical significance. In contrast, 250 nM CRH significantly increased FDS amplitudes in the BLA ( $6.90 \pm 2.75\%$ ,  $n = 9$  slices/6 animals) (Figure 3.2.3.1-24B). Subsequently, slices from CKO mice were treated with CRH and VSDI recordings were analysed in the same way. FDS amplitudes in the LA were not significantly altered by 250 nM CRH in the bathing solution ( $7.60 \pm$

6.96%,  $n = 7$  slices/5 animals) (Figure 3.2.3.1-24C). However, the increase in FDS amplitudes induced by 250 nM CRH in the BLA was completely absent in brain slices from CKO mice ( $8.50 \pm 8.98\%$ ,  $n = 7$  slices/5 animals) (Figure 3.2.3.1-24D).

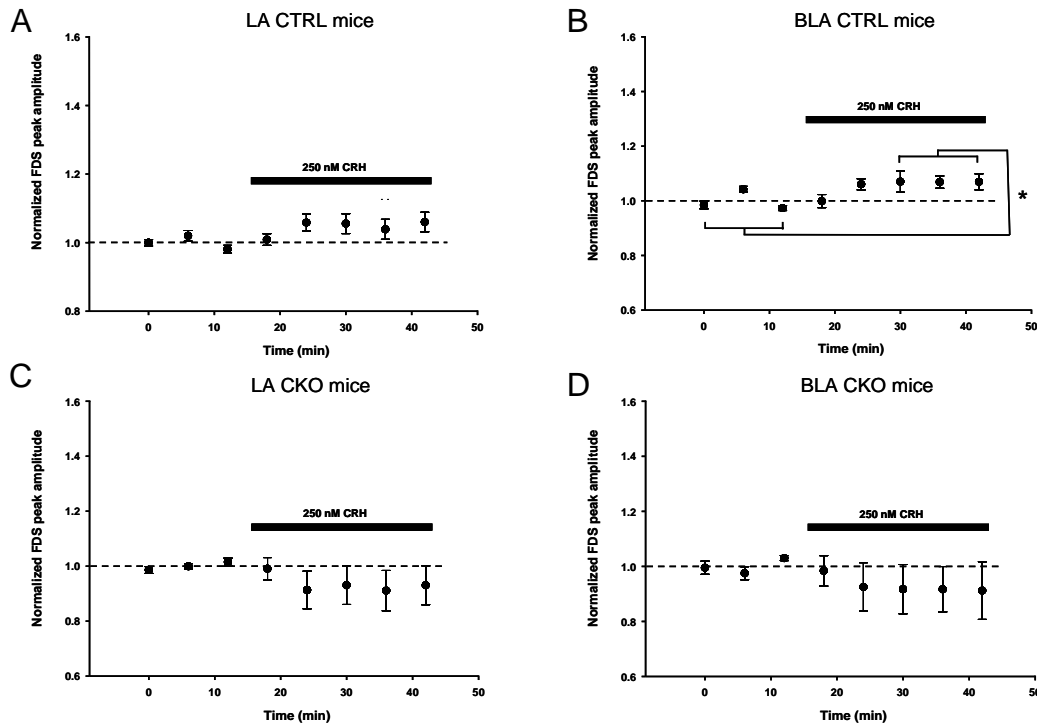


**Figure 3.2.3.1-24. Effects of bath application of 250 nM CRH on FDSs in the LA and BLA in brain slices from CKO and CTRL mice.** A, Bath application of 250 nM CRH increased FDS amplitudes in the LA in CTRL mice. This effect did not reach the level of significance ( $n = 10$  slices/6 animals). B, In brain slices from CTRL mice ( $n = 9$  slices/6 animals) 250 nM CRH significantly (paired t-test,  $p = 0.016$ ) increased FDS amplitudes in the BLA. C, 250 nM CRH had no significant effect on FDSs in the LA using CKO mice ( $n = 7$  slices/5 animals). D, The presence of 250 nM CRH in the bathing solution had no significant effect on the FDS amplitudes in the BLA of CKO mice ( $n = 7$  slices/5 animals). Data are presented as means  $\pm$  SEM. CRH = Corticotropin-releasing hormone, FDS = Fast depolarization-mediated signal, LA = Lateral amygdala, BLA = Basolateral amygdala, CTRL = *Crhr1<sup>loxP/loxP</sup>* mice, CKO = *Crhr1<sup>loxP/loxP</sup> Camk2 $\alpha$ -Cre* mice.

For the investigation of network dynamics in the LA, 250 nM CRH was bath applied and after obtaining stable baseline responses HFS was delivered to the EC.

In brain slices from CTRL mice, the presence of 250 nM CRH significantly increased the total strength of network potentiation ( $5024 \pm 1263\%$ ,  $n = 10$  slices/8 animals) compared to control conditions ( $1854 \pm 588\%$ ,  $n = 8$  slices/5 animals) (Figure 3.2.3.1-25A). In the same slices, quantification of sites of potentiation revealed that CTRL mice, in the presence of CRH, displayed a significant increase in number ( $211 \pm 38$ ) compared to controls ( $97.4 \pm 23.6$ ) (Figure 3.2.3.1-25B). The decrease of depressed sites (control:  $64.3 \pm 10.0$ , 250 nM CRH:  $34.7 \pm 11.0$ ) did not reach the level of significance (Figure 3.2.3.1-25C).

After these control experiments, CKO mice were used to investigate the role of CRHR1 in mediating the effects of CRH on network dynamics. With respect to the parameter total strength of network potentiation, there was no significant difference between the experiments performed in slices from CTRL (1854 ± 588%, n = 8 slices/5 animals) and CKO mice (4415 ± 1742%, n = 9 slices/5 animals). On the level of strength of network potentiation, the same untreated slices from CKO mice did not significantly differ from slices treated with 250 nM CRH (5480 ± 1102%, n = 7 slices/5 animals) (Figure 3.2.3.1-25D). Furthermore, quantification of the number of potentiated sites in the untreated slices (166 ± 48) vs. 250 nM CRH (237 ± 43) showed that there was no significant difference (Figure 3.2.3.1-25E). However in contrast, the application of 250 nM CRH led to a significant reduction of depressed sites (8.10 ± 6.50) compared to untreated slices (57.7 ± 19.3) (Figure 3.2.3.1-25F).

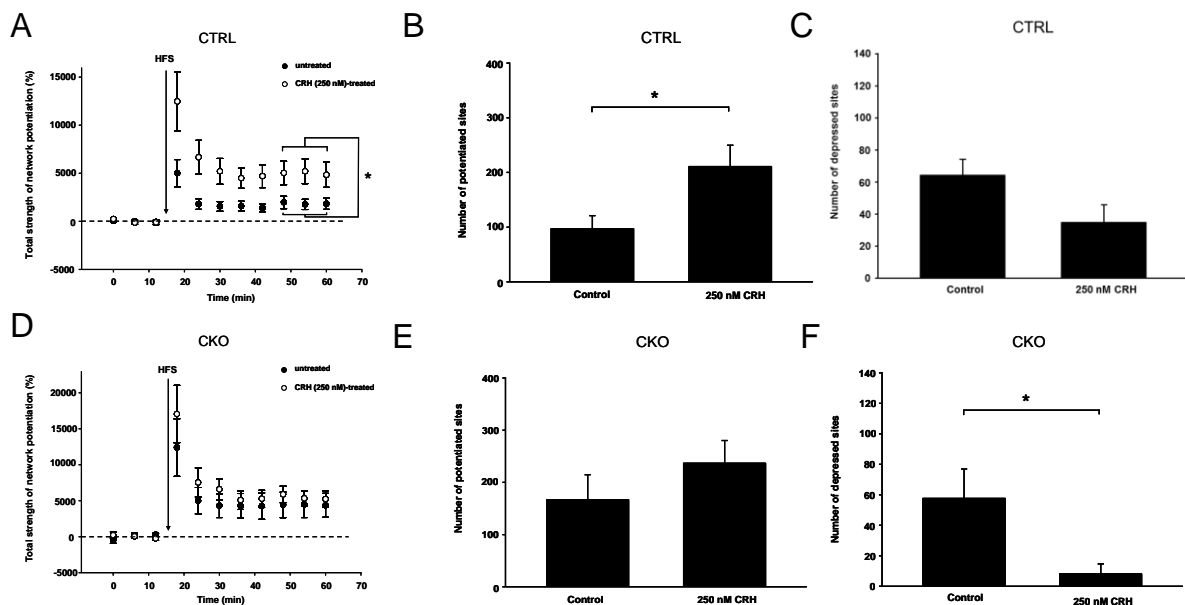


**Figure 3.2.3.1-25. CRH-induced changes in network dynamics after HFS in the LA are partially mediated by CRHR1.** A, Significant (Mann-Whitney Rank Sum test,  $p = 0.029$ ) increase of total strength of network potentiation in the presence of 250 nM CRH in slices from CTRL mice (untreated slices: black circles vs. CRH-treated slices: open circles). B, A Significant (Mann-Whitney Rank Sum test,  $p = 0.026$ ) increase in the number of potentiated sites after HFS was observed by application of 250 nM CRH. C, Reduction in number of depressed sites. D, The increase in total strength of network potentiation after HFS induced by 250 nM CRH in CTRL slices was abolished in CKO slices (untreated slices: black circles vs. CRH-treated slices: open circles). E, Similarly, the increase in the number of potentiated sites after HFS in CTRL slices after application of 250 nM CRH was also abolished in CKO slices. F, In CKO slices, 250 nM CRH induced a significant (t-test,  $p = 0.047$ ) decrease in the number of depressed sites after HFS compared to untreated slices (CTRL:  $n = 8$  slices/5 animals, CTRL presence of 250 nM CRH:  $n = 10$  slices/8 animals, CKO:  $n = 9$  slices/5 animals, CKO presence of 250 nM CRH:  $n = 7$  slices/5 animals). Data are presented as means ± SEM and all statistical comparisons were done for minutes 30-42 after HFS. CRH = Corticotropin-releasing hormone, CRHR1 = Corticotropin-releasing hormone receptor type 1, LA = Lateral amygdala, CTRL = *Crh1<sup>loxP/loxP</sup>* mice, CKO = *Crh1<sup>loxP/loxP</sup> Camk2a-Cre* mice, HFS = High-frequency stimulation.

Using this paradigm, the neuronal network of the BLA was also investigated with respect to the number of sites of potentiation after HFS. By this means slices obtained from CTRL mice and treated with 250 nM CRH ( $32.9 \pm 9.3$ ,  $n = 7$  slices/6 animals) displayed no significant difference compared to untreated slices ( $12.1 \pm 3.1$ ,

n = 8 slices/5 animals) (Figure 3.2.3.1-26A). Conversely, brain slices from CKO mice showed a significant increase in number of potentiated sites after HFS ( $50.4 \pm 10.0$ , n = 7 slices/5 animals) in the presence of 250 nM CRH compared to control conditions ( $22.7 \pm 6.2$ , n = 9 slices/5 animals) (Figure 3.2.3.1-26B).

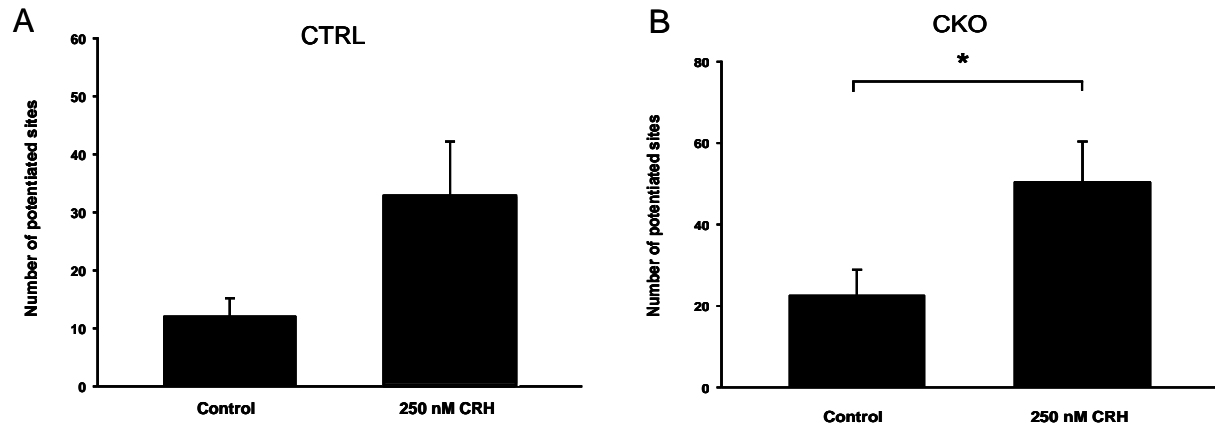


**Figure 3.2.3.1-26. CRHR1 is involved in mediating the effect of 250 nM CRH on network potentiation in the BLA after HFS.** A, In slices from CTRL mice, potentiated sites in the BLA did not significantly differ comparing the absence (n = 8 slices/5 animals) with the presence of 250 nM CRH (n = 7 slices/6 animals). B, Conversely, 250 nM CRH (n = 7 slices/5 animals) was capable of significantly (t-test,  $p = 0.027$ ) increasing the number of potentiated sites after HFS compared to control condition (n = 9 slices/5 animals) in brain slices from CKO mice. Data are presented as means  $\pm$  SEM. CTRL =  $Crhr1^{loxP/loxP}$ , CKO =  $Crhr1^{loxP/loxP} Camk2\alpha\text{-cre}$ , CRHR1 = Corticotropin-releasing hormone receptor type 1, CRH = Corticotropin-releasing hormone, BLA = Basolateral amygdala, HFS = High-frequency stimulation.

### **3.2.4 Investigation of the effect of Cort on network activity and dynamics in the LA and BLA**

CRH secretion from the hypothalamus triggers ACTH release from the anterior pituitary gland, which in turn stimulates the release of corticosteroids such as Cort, from the adrenals (Fink, 2006; Bonfiglio et al., 2011). The effect of bath application of Cort on neuronal network activity and dynamics in the LA and BLA was investigated. Bath application of 100 nM Cort significantly increased FDS amplitudes in the LA ( $5.90 \pm 1.40\%$ ,  $n = 8$  slices/6 animals). In the BLA, Cort also increased FDS amplitudes, but this effect was not significant ( $3.70 \pm 2.31\%$ ,  $n = 7$  slices/6 animals) (Figure 3.2.4-27A, B). The analysis of neuronal network dynamics after HFS revealed that the application of 100 nM Cort was capable of significantly increasing the total strength of network potentiation ( $5402 \pm 1259\%$ ,  $n = 8$  slices/6 animals) compared to control conditions ( $1946 \pm 515\%$ ,  $n = 10$  slices/7 animals) in the LA (Figure 3.2.4-27C). The total strength of network potentiation after HFS in the BLA was also significantly increased in the presence of 100 nM Cort ( $1073 \pm 224\%$ ,  $n = 7$  slices/6 animals) compared to control slices ( $486 \pm 125\%$ ,  $n = 10$  slices/7 animals) (Figure 3.2.4-27D).

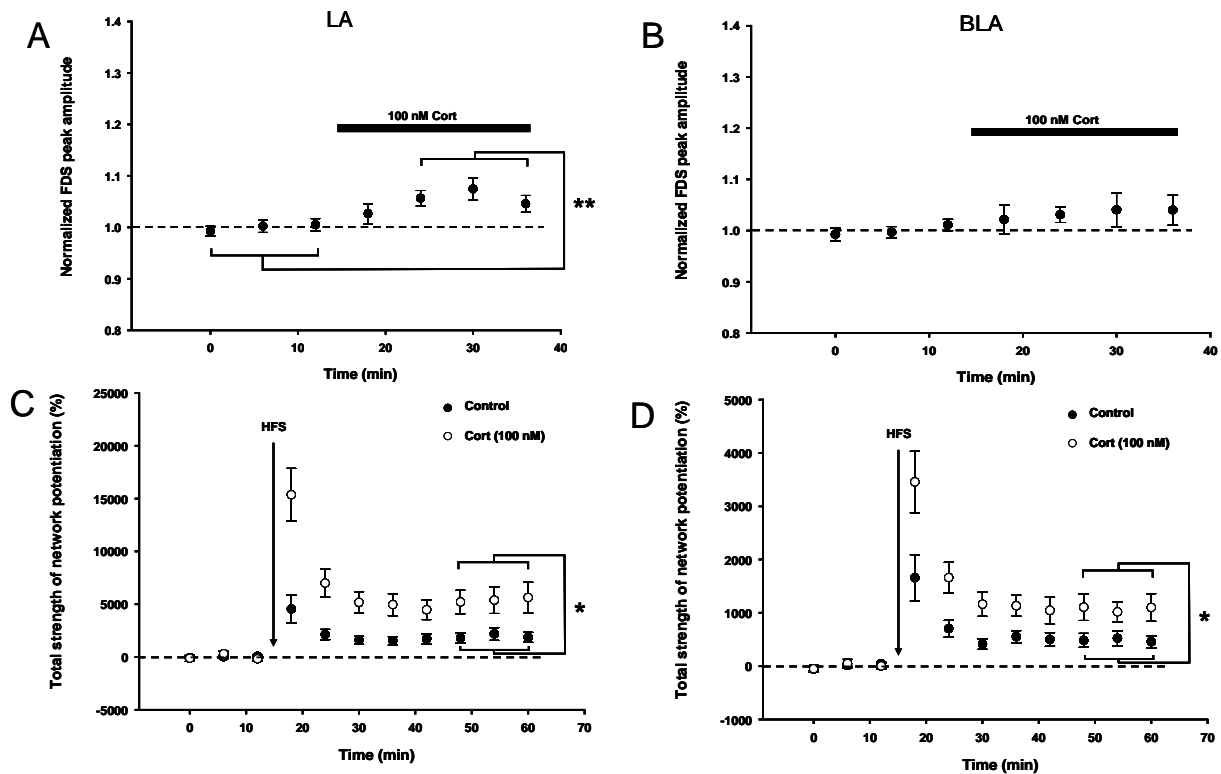


**Figure 3.2.4-27. Effects of bath application of 100 nM Cort on FDS amplitudes and total strength of network potentiation after HFS in brain slices containing the LA and BLA.** A, Bath application of 100 nM Cort significantly (paired t-test,  $p = 0.004$ ) increased FDS amplitudes in the LA. B, Although increasing the FDS amplitudes in the BLA, this effect of Cort did not reach the level of significance. C, Compared to control slices (black circles), the presence of 100 nM Cort (open circles) significantly (Mann-Whitney Rank Sum test,  $p = 0.023$ ) increased the total strength of network potentiation in the LA by comparing the mean values of total strength of potentiation minutes 30-42 after HFS to baseline. D, Using the same paradigm, a significant (t-test,  $p = 0.026$ ) increase of this parameter could be observed in the BLA. All data are presented as means  $\pm$  SEM (LA control:  $n = 10$  slices/7 animals, LA presence of Cort:  $n = 8$  slices/6 animals, BLA control:  $n = 10$  slices/7 animals, BLA presence of Cort:  $n = 7$  slices/6 animals). Cort = Corticosterone, FDS = Fast depolarization-mediated signal, LA = Lateral amygdala, BLA = Basolateral amygdala, HFS = High-frequency stimulation.

The quantification of the number of potentiated sites within the LA network showed a significant (t-test,  $p = 0.003$ ) increase comparing control slices ( $109 \pm 22$ ,  $n = 10$  slices/7 animals) with slices treated with 100 nM Cort ( $248 \pm 34$ ,  $n = 8$  slices/6 animals). In the same slices, the number of sites of depression was significantly (Mann-Whitney Rank Sum Test,  $p = 0.006$ ) reduced comparing control slices ( $69.9 \pm 13.3$ ,  $n = 10$  slices/7 animals) with the presence of 100 nM Cort ( $15.9 \pm 9.7$ ,  $n = 8$  slices/6 animals). The neuronal network of the BLA responded with a significant (t-test,  $p = 0.004$ ) increase in the number of potentiated sites after HFS comparing control condition ( $27.4 \pm 5.9$ ,  $n = 10$  slices/7 animals) to 100 nM Cort treatment ( $61.3 \pm 8.4$ ,  $n = 7$  slices/6 animals) (data not shown).

### 3.2.5 Comparison of network dynamics in amygdalar slices obtained from HAB and NAB mice

Since it was shown that HAB and NAB mice exhibit different levels of freezing in a contextual fear-conditioning paradigm (Yen et al., 2012), these mouse strains were tested with respect to differences in total strength of network potentiation in the LA and BLA after HFS.

The comparison of network dynamics revealed that there was no significant difference between HAB ( $3600 \pm 675\%$ ,  $n = 10$  slices/6 animals) and NAB ( $3365 \pm 656\%$ ,  $n = 11$  slices/6 animals) (Figure 3.2.5-28A) in the magnitude of total strength of network potentiation within the LA. Conversely, total strength of network potentiation in the BLA was significantly increased in HAB ( $863 \pm 149\%$ ,  $n = 10$  slices/6 animals) compared to NAB ( $511 \pm 83\%$ ,  $n = 10$  slices/6 animals) mice (Figure 3.2.5-28B).

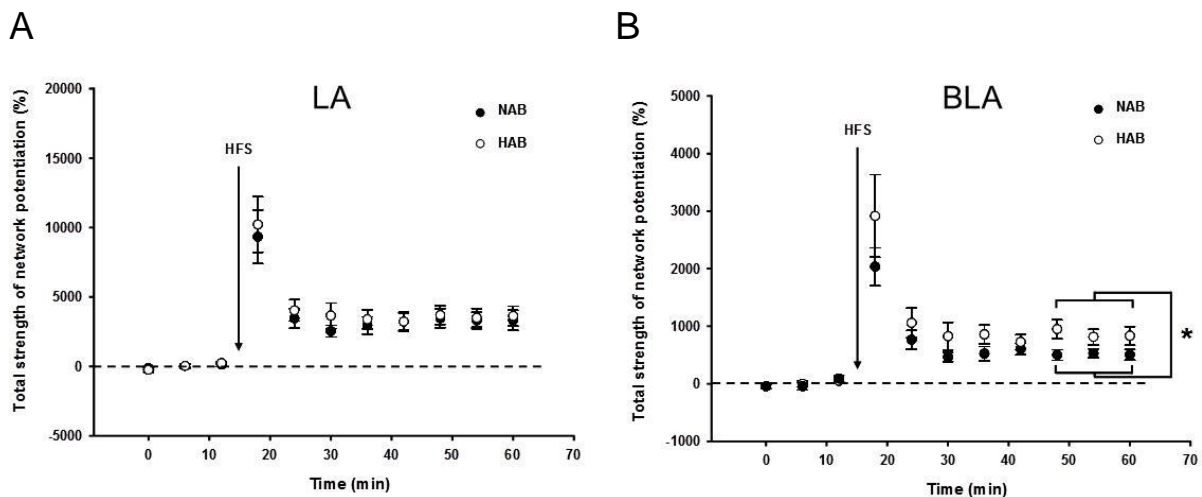


**Figure 3.2.5-28. Investigation of total strength of network potentiation after HFS comparing NAB and HAB mice.** A, After delivering a HFS, total strength of network potentiation did not significantly differ comparing NAB (black circles) with HAB (open circles) in the LA. B, Using the same paradigm, HAB mice showed a significant (t-test,  $p = 0.048$ ) increase compared to NAB mice in the BLA. All data are presented as means  $\pm$  SEM (NAB:  $n = 11$  slices/6 animals, HAB:  $n = 10$  slices/6 animals). HFS = High-frequency stimulation, NAB = Normal anxiety-related behaviour, HAB = High anxiety-related behaviour, LA = Lateral amygdala, BLA = Basolateral amygdala.

### 3.3 Pharmaceutical treatment

Based on the observations that the strength and synchrony of neuronal activity in the LA and to some extent in the BLA can be related to fear (Pare and Collins, 2000; Repa et al., 2001; An et al., 2012; Ryan et al., 2012), chemical compounds which might mediate their anxiolytic effects in part by regulating neuronal activity in the LA or BLA, were bath applied to show their putative role in the regulation of neuronal network activity in these brain regions.

Bath application of 1  $\mu$ M diazepam, a positive allosteric modulator of the GABA<sub>A</sub> receptor (Whiting, 2006) was capable of significantly reducing LA network activity, reflected through a decrease in FDS amplitudes compared to baseline ( $13.3 \pm 2.9\%$ ,  $n = 6$  slices/3 animals) (Figure 3.3-29A). By use of the same paradigm, a significant reduction of the FDSs could also be observed in the BLA ( $13.0 \pm 3.8\%$ ,  $n = 6$  slices/3 animals) (Figure 3.3-29B).

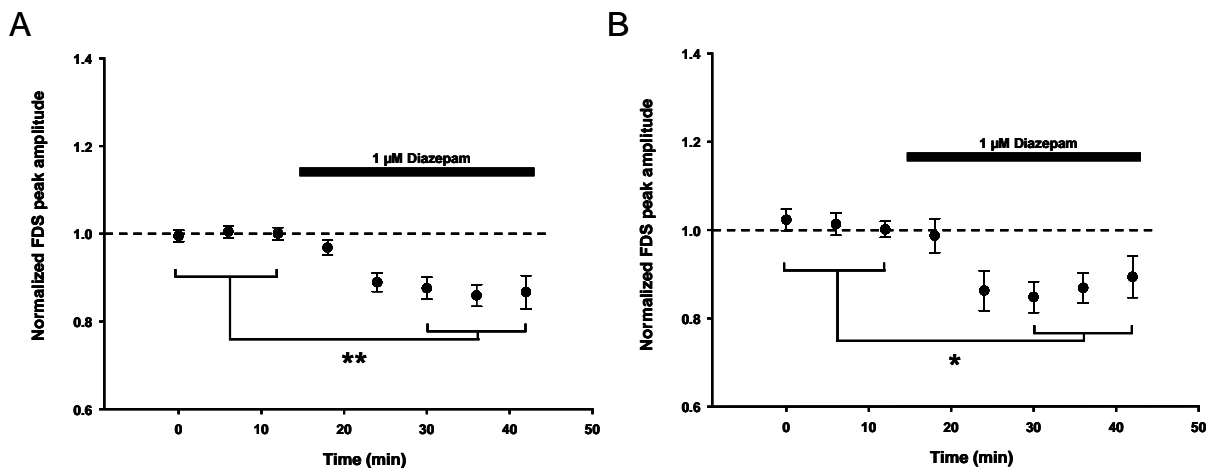


**Figure 3.3-29. Diazepam reduces FDS amplitudes in the LA and BLA.** A, Significant (paired t-test,  $p = 0.006$ ) reduction of FDSs after bath application of 1  $\mu$ M diazepam (6 slices/3 animals) in the LA. B, In the BLA, bath application of 1  $\mu$ M diazepam was capable of significantly (paired t-test,  $p = 0.019$ ) reducing FDSs (6 slices/3 animals). Data are presented as means  $\pm$  SEM. FDS = Fast depolarization-mediated signal, LA = Lateral amygdala, BLA = Basolateral amygdala.

Conversely, AM 404, an inhibitor of the uptake of endocannabinoids, which was shown to facilitate the extinction of contextual fear memory and might be a novel target for the treatment of anxiety disorders (Patel et al., 2004; Bitencourt et al., 2008) exerted circuit-specific effects on FDSs. The application of 10  $\mu$ M AM 404 had no significant effect on the FDSs in the LA ( $2.70 \pm 2.86\%$ ,  $n = 5$  slices/3 animals) (Figure 3.3-30A). In contrast, in the same slices, this treatment led to a significant reduction of FDSs in the BLA ( $5.90 \pm 1.30\%$ ) (Figure 3.3-30B).

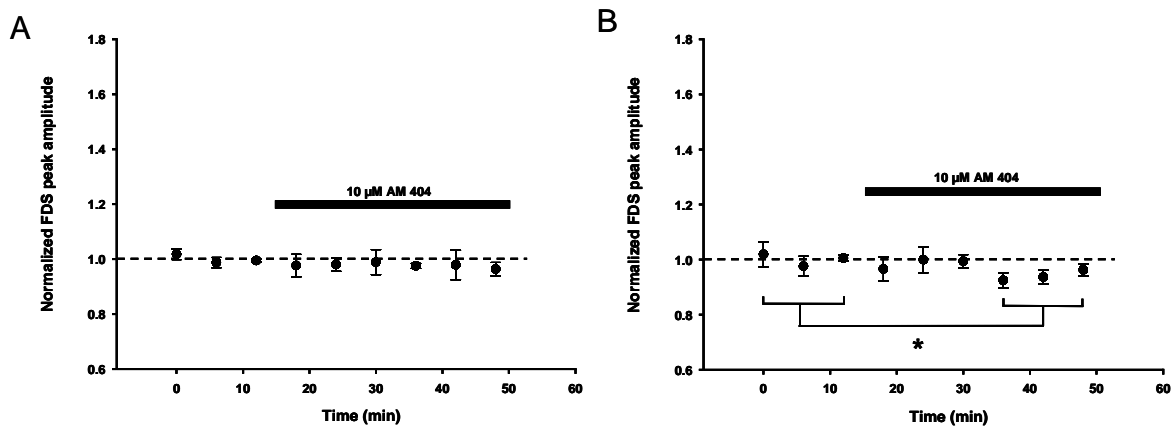


**Figure 3.3-30. Brain region-specific effects of AM 404 on FDS amplitudes in the LA and BLA.** A, Bath application of 10  $\mu\text{M}$  AM 404 had no significant effect on FDSs in the LA ( $n = 5$  slices/3 animals). B, Significant (paired t-test,  $p = 0.011$ ) reduction of FDSs caused by wash in of 10  $\mu\text{M}$  AM 404 in the BLA. Data are presented as means  $\pm$  SEM. FDS = Fast depolarization-mediated signal, LA = Lateral amygdala, BLA = Basolateral amygdala, AM 404 = N-(4-Hydroxyphenyl)arachidonylamide.

SSRIs are a class of antidepressants which are widely used for the treatment of affective and anxiety disorders (Vaswani et al., 2003). One example of this class of medications is fluvoxamine. Bath application of 20  $\mu\text{M}$  fluvoxamine did not significantly alter FDSs both in the LA ( $1.30 \pm 3.43\%$ ,  $n = 5$  slices/3 animals) and the BLA ( $2.90 \pm 2.25\%$ ,  $n = 5$  slices/3 animals) (Figure 3.3-31).

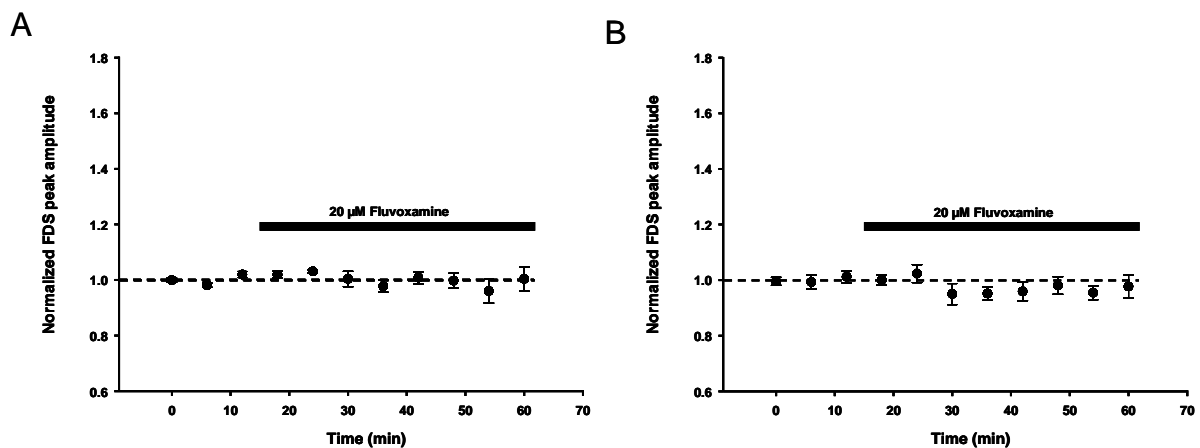


**Figure 3.3-31. Effects of bath application of fluvoxamine on FDSs in the LA and BLA.** Wash in of 20  $\mu\text{M}$  fluvoxamine had no significant effects on FDSs in the LA (A) or BLA (B) ( $n = 5$  slices/3 animals). Data are presented as means  $\pm$  SEM. FDS = Fast depolarization-mediated signal, LA = Lateral amygdala, BLA = Basolateral amygdala.

Among the class of SSRIs, citalopram represents the drug which has the highest efficacy in inhibiting the uptake of serotonin (Vaswani et al., 2003). On the one hand, bath application of 15  $\mu\text{M}$  citalopram significantly decreased FDSs in the LA ( $5.20 \pm 1.64\%$ ,  $n = 9$  slices/6 animals) (Figure 3.3-32A). On the other hand, the same treatment was not capable of significantly changing the FDSs in the BLA ( $1.00 \pm 3.13\%$ ,  $n = 9$  slices/6 animals) (Figure 3.3-32B).

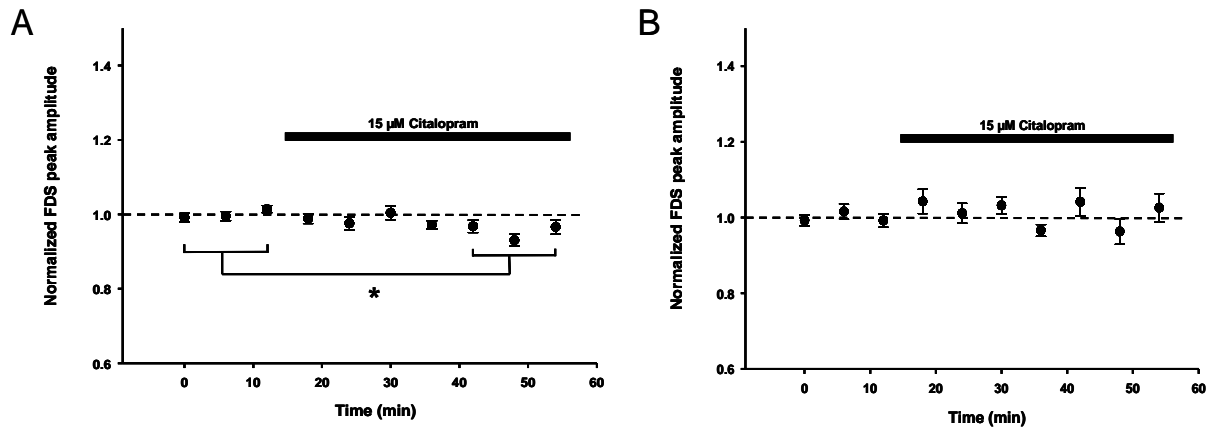


**Figure 3.3-32. Changes in FDSs in the LA or BLA upon bath application of citalopram.** A, 15  $\mu\text{M}$  citalopram was capable of significantly (paired t-test,  $p = 0.013$ ) reducing FDS amplitudes in the LA ( $n = 9$  slices/6 animals). B, Conversely, bath application of 15  $\mu\text{M}$  citalopram had no significant effects on FDSs in the BLA ( $n = 9$  slices/6 animals). Data are presented as means  $\pm$  SEM. FDS = Fast depolarization-mediated signal, LA = Lateral amygdala, BLA = Basolateral amygdala.

Venlafaxine, which is indicated for the treatment of a broad spectrum of anxiety disorders, is a SNRI (Katzman, 2004). Bath application of 5  $\mu\text{M}$  venlafaxine significantly reduced the FDS amplitudes compared to baseline in the LA ( $10.5 \pm 2.0\%$ ,  $n = 7$  slices/4 animals) and in the BLA ( $8.80 \pm 1.30\%$ ,  $n = 7$  slices/4 animals) (Figure 3.3-33).

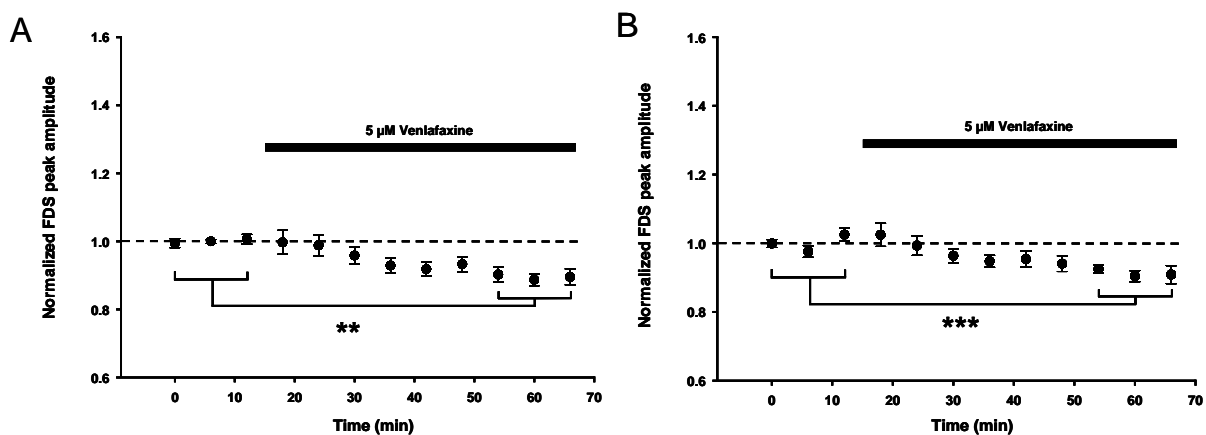


**Figure 3.3-33. Effects of bath application of venlafaxine on FDSs in the LA and BLA.** A, 5  $\mu\text{M}$  venlafaxine was capable of significantly (paired t-test,  $p = 0.002$ ) reducing the FDSs in the LA ( $n = 7$  slices/4 animals). B, FDSs in the BLA were significantly (paired t-test,  $p < 0.001$ ) reduced by bath application of 5  $\mu\text{M}$  venlafaxine ( $n = 7$  slices/4 animals). Data are presented as means  $\pm$  SEM. FDS = Fast depolarization-mediated signal, LA = Lateral Amygdala, BLA = Basolateral amygdala.

The third class of antidepressant which was investigated here was a tricyclic antidepressant (TCA). This class of substances is used for the treatment of various forms of anxiety disorders (Zohar and Westenberg, 2000). To test their effects on the FDSs in the LA and BLA, 15  $\mu\text{M}$  clomipramine was bath applied. Both, the LA and BLA were influenced by this treatment, reflected through a significant reduction of the

FDS amplitudes compared to baseline: in the LA ( $6.80 \pm 1.42\%$ ,  $n = 6$  slices/4 animals); in the BLA ( $7.20 \pm 1.43\%$ ,  $n = 6$  slices/4 animals) (Figure 3.3-34).

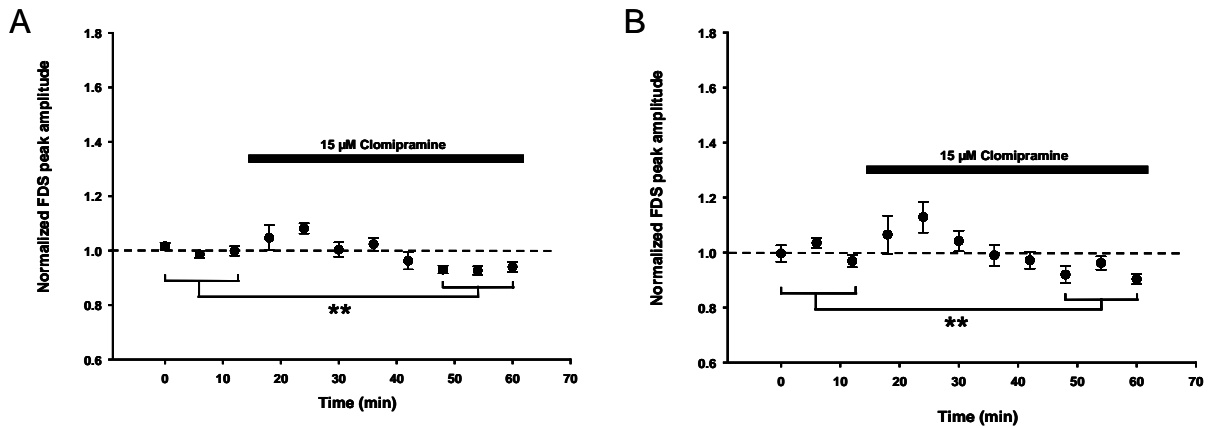


**Figure 3.3-34. Clomipramine affects basal neuronal network activity reflected by a decrease of FDSs in the LA and BLA.** A, 15  $\mu\text{M}$  clomipramine significantly (paired t-test,  $p = 0.005$ ) decreased FDSs in the LA upon bath application ( $n = 6$  slices/4 animals). B, The FDS amplitudes were significantly (paired t-test,  $p = 0.004$ ) decreased by bath application of 15  $\mu\text{M}$  clomipramine ( $n = 6$  slices/4 animals). Data are presented as means  $\pm$  SEM. FDS = Fast depolarization-mediated signal, LA = Lateral amygdala, BLA = Basolateral amygdala.

A disturbed regulation of activity in the LA and BLA might lead to an increase of activity in these nuclei as response to stress and as a result, probably, to an elevated incidence of psychiatric diseases such as schizophrenia (Grace, 2006). Therefore, the antipsychotic haloperidol at a concentration of 20  $\mu\text{M}$  was bath applied and neuronal activity in the LA and BLA was monitored. The relative FDS amplitudes were significantly reduced ( $4.20 \pm 1.10\%$ ,  $n = 7$  slices/4 animals) in the LA and BLA ( $7.00 \pm 1.69\%$ ,  $n = 7$  slices/4 animals) (Figure 3.3-35).

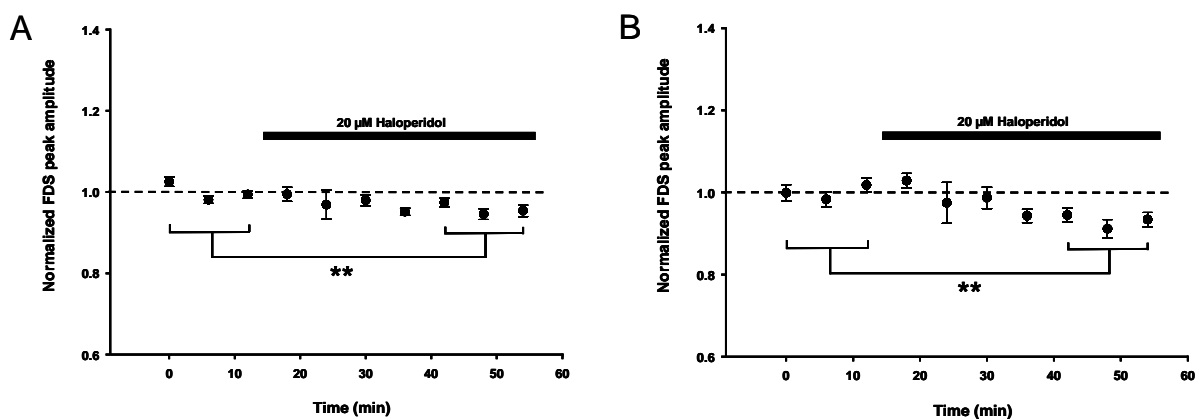


**Figure 3.3-35. Haloperidol is capable of reducing basal neuronal network activity in the LA and BLA.** A, Significant (paired t-test,  $p = 0.009$ ) reduction of FDSs by bath application of 20  $\mu\text{M}$  haloperidol in the LA ( $n = 7$  slices/4 animals). B, Basal neuronal network activity in the BLA was also significantly (paired t-test,  $p = 0.006$ ) reduced by bath application of 20  $\mu\text{M}$  haloperidol ( $n = 7$  slices/4 animals). Data are presented as means  $\pm$  SEM. FDS = Fast depolarization-mediated signal, LA = Lateral amygdala, BLA = Basolateral amygdala.

## **4 Discussion**

### **4.1 Slicing procedure and qualitative/quantitative investigation of signal propagation within the amygdalar neuronal network**

The neuronal network of the LA and BLA contained in horizontal brain slices was investigated in other studies performed in mice and rats (von Bohlen und Halbach and Albrecht, 1998; Drephal et al., 2006; Kulisch et al., 2011). Therefore, the anatomical landmarks described for the rat brain could be used for the mouse brain slice preparation employed in this study. To preserve similar neuronal networks across the slices, the important landmarks were the CA1 region of the intermediate hippocampus, the stria terminalis, and the lateral ventricle as anatomically well-defined brain structures (von Bohlen und Halbach and Albrecht, 1998). An additional and less well described landmark was a fibre bundle separating the BLA from the CeA. A tracing study in cats attributed this fibre bundle to parts of the intercalated cell masses, which regulate information flow from the BLA to the CeA via GABAergic inhibition (Pare and Smith, 1993). This fibre bundle can also be found in rat brain slices (von Bohlen und Halbach and Albrecht, 1998).

To ensure inter-nuclear connectivity in the brain slice preparation used here, the spread of neuronal activity was qualitatively examined by either stimulation of the EC or fibres in the LA. The course of neuronal activity propagation followed the tendency to travel from lateral to medial and along previously described axonal projections, thereby validating the slicing protocol to be well suited for the investigations conducted here (Krettek and Price, 1978; Sah et al., 2003; LeDoux, 2007; Ehrlich et al., 2009; Pare and Duvarci, 2012). Additionally, the level of the LA and BLA within this horizontal slice preparation along the dorso-ventral axis made this neuronal network suitable for the study of plastic changes in neuronal excitability which might be associated with fear conditioning (Schafe et al., 2000; Müller et al., 2009; Wilson and Murphy, 2009; Orsini and Maren, 2012; Coyner et al., 2013).

The time course of the change in fluorescence after single-pulse stimulation of the EC showed a FDS in the LA and BLA, which in the LA was followed by a slow hyperpolarisation-mediated component. The capability of Di-4-ANEPPS to report cellular de- and hyperpolarisation in neuronal networks has already been reported in

previous studies (Tominaga et al., 2000; von Wolff et al., 2011). The observation that slow components of the VSDI signals are affected by bath application of the GABA<sub>B</sub> receptor antagonist CGP 55845 is in line with electrophysiological studies that pointed to the occurrence of GABA<sub>B</sub> receptor-mediated currents in BLA neurons in rat brain slices (Rainnie et al., 1991; Washburn and Moises, 1992). Consistently with these observations, the GABA<sub>B</sub>R1 receptor subunits could be immunocytochemically localised in the LA and BLA in rat brain slices (McDonald et al., 2004).

Bath application of voltage-gated sodium channel and ionotropic glutamate receptor blockers (Hille, 2001) proved the FDS mediated by electrical neuronal activity and the prevalence of glutamatergic neurotransmission within the LA and BLA. The latter finding is in accordance with reports that revealed a dominance of glutamate signalling in the LA and BLA, which is also emphasised by the high portion of pyramidal-like projection neurons in these nuclei (McDonald, 1982; Sah et al., 2003). The small (~20% of baseline response) remaining VSDI signal after bath application of NBQX and AP 5 could be attributed to electrical activity of stimulated afferents.

Abolishing fast inhibitory signalling, which is mediated via GABA<sub>A</sub> receptors in the LA and BLA (Rainnie et al., 1991; Wang et al., 2001), strongly increased FDS peak-amplitude (~50% of baseline response), thus emphasizing the importance of GABAergic inhibition in the regulation of neuronal activity in the amygdala (Ehrlich et al., 2009).

As a prerequisite for the study of activity and plasticity in subsequent experiments, the FDSs in the LA and BLA remained constant upon repeated evocation.

## 4.2 Investigation of neuronal network dynamics

### 4.2.1 Verification of induction protocol

It has been shown that delivery of HFS to the EC is capable of inducing LTP in the LA, reflected by a lasting increase in the amplitude of excitatory post-synaptic potentials in brain slices obtained from rats (Chapman et al., 1990). Accordingly, extracellular recordings of excitatory field potential in the LA *in vitro* showed that HFS, as a well-established stimulation protocol for the induction of LTP in the hippocampus and the amygdala (Maren, 1999; Albenzi et al., 2007), succeeded in reliably and long-lastingly increasing evoked neuronal network activity.

By use of a horizontal brain slice preparation, bath application of GABA<sub>A</sub> receptor antagonists (e.g. picrotoxin) to allow for LTP formation in the LA (Huang et al., 2000; Fourcaudot et al., 2009; Krishnan et al., 2010) could be circumvented.

This finding is in line with the results of previous work done in horizontal brain slices prepared from rats (Drephal et al., 2006; Kulisch et al., 2011).

### 4.2.2 Detection of amygdalar network dynamics by means of VSDI and data processing of VSDI movies

After proving the validity of HFS as an induction protocol for long-lasting changes in evoked neuronal network activity in the LA, these changes were qualitatively investigated by means of VSDI. It was shown that after HFS stimulus-triggered network activity in the LA, in a spatially restricted manner, is sustained enhanced, reflected by a prolonged increase in FDS peak amplitude. Studies that employed hippocampal slices demonstrated the capacity of VSDI as a valuable tool to quantitatively examine changes in the strength of neuronal activity by use of different stimulation intensities, pharmacological intervention, and neuroplasticity-inducing electrical stimulation (Tominaga et al., 2000; von Wolff et al., 2011; Stepan et al., 2012).

The advanced processing of VSDI movies in Matlab, accounting for VSD and camera chipset mediated-noise, via the "Active Site Filter", enabled the restriction of further analysis steps to pixels, that reliably displayed depolarization-induced changes in

fluorescence. The fast depolarization-mediated change in fluorescence throughout the slice was captured by the computation of a maximum intensity projection map and the use of anatomical landmarks allowed for a signal detection restricted to the LA or BLA.

The mean of all single relative values of these changes reflected the overall change in potentiation or depression.

Since the investigation of neuronal network dynamics on the level of mean values of changes over all sites, which display these changes, bears the risk that the actual strength of changes is lost by the averaging, two other parameters were additionally introduced.

First, the number of sites that displayed depression or potentiation of network activity was quantified.

The second measure took both parameters into account and was calculated by summing up the single percentage values of sites at which potentiation or depression occurred.

The quantification of neuronal network dynamics revealed that the LA responded spatially segregated to the same HFS with depression or potentiation.

Due to its proximity to the stimulation electrode the network of the BLA was solely examined regarding potentiation. This proximity and the resultant intensive excitation of the BLA upon single-pulse electrical stimulation most likely override depression of neuronal excitability. These findings exemplify the stimulus-dependent information-encoding capacity of the LA and the BLA on the level of the modulation of neuronal network activity. The observation that HFS, besides being an intensively used stimulation paradigm for LTP induction (Maren, 1999; Albenis et al., 2007), is also capable of triggering LTD of LA network activity via cortical afferents additionally highlights the methodological value of the VSDI assay developed here. In line with this observation, it has been shown on the single-cell level that projection neurons in the LA responded to the same stimulus with LTP or LTD of excitatory postsynaptic potential slope in coronal slices from mice. The authors found that these differential responses depended on the timing and location of synaptic activity and postsynaptic calcium spikes (Humeau and Lüthi, 2007). However, since the experimental approach developed in the present study monitors spatio-temporally restricted neuronal network dynamics, the observed changes in signalling might also be mediated by indirect signalling routes, e. g. fast feedback circuits.

#### 4.2.2.1 Pharmacological characterization of changes in network dynamics

Changes in amygdalar network dynamics after HFS were pharmacologically investigated.

For this purpose, AP 5 or verapamil, blockers of NMDA receptors or L-VGCCs, respectively, were bath applied. In these studies, in which whole-cell patch-clamp and extracellular recordings were used, the authors could show that these treatments were capable of decreasing the magnitude of LTP or LTD in the LA in horizontal or coronal brain slices from mice (Bauer et al., 2002; Fourcaudot et al., 2009; Müller et al., 2009).

On the neuronal network level within this study, AP 5 and verapamil conversely influenced the magnitude of LTP and LTD in the LA in a way that AP 5 increased network potentiation and decreased network depression. Verapamil in turn decreased network potentiation and increased network depression.

On the behavioural level, infusions of AP 5 into the LA/BLA were capable of preventing the fear memory-enhancing effect of a stressful event in rats (Shors and Mathew, 1998). AP 5 was also shown to prevent the extinction of fear memory upon its administration to the amygdala, a process that can also be related to the formation of new memories (Davis et al., 2003).

One study highlighted the presence of NMDA receptors both at pre- and postsynaptic membranes in the LA. By interference with calcium signalling via blockade of NMDA receptors or VGCCs, the authors demonstrated intracellular calcium signalling in pre- and postsynaptic components to be involved in the regulation of auditory fear conditioning (Tsvetkov et al., 2002). Together with the finding that LTP and LTD are differentially regulated at the level of single projection neurons, dependent on the intracellular calcium concentration (Humeau and Lüthi, 2007), the observed alterations in evoked neuronal network activity might reflect a bidirectional modulation of LA network dynamics by the blockade of either NMDA receptors or L-VGCCs.

In the BLA, verapamil decreased the number of potentiated sites in comparison to control conditions and the presence of AP 5. This observation is in line with a study pointing to a minor contribution of NMDA receptors to LTP induction in the BLA. The authors showed that AP 5, at a concentration that is able to abolish LTP formation in

the CA1 region of the hippocampus and cortex, did not impact on the magnitude of LTP in the BLA as revealed by intracellular recordings (Chapman and Bellavance, 1992). Conversely, a study conducted in rats demonstrated NMDA receptor antagonism in the BLA to be capable of blocking the acquisition of contextual fear memory (Fanselow and Kim, 1994).

The finding that verapamil reduces the number of sites at which potentiation occurred can be related to a study in rats, in which infusions of verapamil in the BLA prevented the formation of extinction memory (Davis and Bauer, 2012). Putting these observations together, the present *in vitro* investigation of the processing units LA and BLA offers a promising approach to dissect network activity and dynamics under distinct conditions.

#### **4.2.3 Effect of CRH on LA and BLA network activity and dynamics**

Bath application of 125 nM or 250 nM CRH differentially influenced neuronal network activity and dynamics in the amygdala.

The CRH concentrations employed were in the range that has previously been shown to elicit an increase in spike frequency in pyramidal cells of the hippocampus in rat brain slices (Aldenhoff et al., 1983). Such an enhancement in spiking activity could also be observed in the hippocampus (Kratzer et al., 2013). Moreover, in coronal brain slices from mice containing the BLA, bath application of 125 nM CRH significantly increased the amplitude of field potentials evoked by stimulation of the LA. This effect was mediated via CRHR1 (Refojo et al., 2011).

On the level of neuronal network activity, bath application of CRH, concentration-dependently increased FDS amplitudes in the LA and BLA. This effect might arise from a CRH-induced alteration in the responsiveness of neurons to neurotransmitters, an altered release probability of neurotransmitters, a decrease in GABAergic inhibition and elevated intrinsic spiking capacities of neurons (Rainnie et al., 2004; Gallagher et al., 2008; Kratzer et al., 2013). The observation that 250 nM CRH significantly increase FDS amplitudes in the BLA offers a circuit-level description of the effect of this stress hormone on the activity of this neuronal network. A similar action of 125 CRH was previously found on the level of evoked neuronal activity, reflected by excitatory field potentials recorded in brain slices from mice (Refojo et al., 2011). Although, in this study, neuronal activity in coronal slices

containing the BLA was evoked by intra-nuclear stimulation of the LA, in contrast to EC stimulation in horizontal slices as done in the present work, the same tendency in change of activity could be observed.

In the context of fear conditioning, it has been previously reported that the presentation of once learned fear-associated cues elevates *in vivo* levels of CRH in the BLA. Thereby, the authors related the behavioural expression of fear to an increase in CRH levels in this circuitry (Mountney et al., 2011).

After induction of plastic changes by HFS it was observed that the presence of CRH concentration-dependently affected neuronal network plasticity in the LA.

Several *in vivo* studies point to the involvement of endogenous CRH, probably released by neurons of the CeA, in the regulation of fear memory consolidation within the LA and BLA (Roosendaal et al., 2002; Shekhar et al., 2005; Hubbard et al., 2007; Isogawa et al., 2013). In this study, bath application of CRH before HFS possibly mimics the release of CRH from the CeA in the LA and BLA during stressful conditions (Roosendaal et al., 2002; Isogawa et al., 2013).

By use of the developed VSDI assay, in conjunction with advanced data processing, CRH-mediated changes after HFS could be observed on different levels. 125 nM CRH was capable of significantly increasing the mean relative change of network potentiation, but not of affecting the number of potentiated or depressed sites. In contrast, in the presence of 250 nM CRH, the network dynamics after HFS were reshaped. This was reflected by a significant increase in the number of potentiated sites and a significant reduction in the number of depressed sites. As a consequence, total potentiation, which reflects both the strength of potentiation and the number of sites at which the changes occur, was significantly increased.

Conversely, the presence of 125 nM or 250 nM CRH had no significant influence on the formation of potentiated sites after HFS in the BLA.

The enhancing effect of CRH on network plasticity within the LA is in line with a study in which the authors showed that 125 nM CRH enhanced the magnitude of population spike LTP in the hippocampus *in vitro* (Blank et al., 2002). Other studies correlated CRH effects and LTP on the level of their partial share in regulating intracellular signalling cascades in the dentate gyrus of the hippocampus, which included the enhancement of adenylyl-cyclase activity and a higher rate of protein phosphorylation (Dave et al., 1985; Hung et al., 1992; Wang et al., 2000).

Experiments performed in rat coronal brain slices showed that the presence of 25 nM CRH in the bathing solution leads to an increased magnitude of HFS-induced LTP of excitatory field potentials in the LA. The authors conducted these experiments in animals that had a history of cocaine consumption and were withdrawn from this drug. In this respect, this study points to an involvement of dopamine receptors in the enhancing effect of CRH on LTP, namely mediated via a decrease in neuronal inhibition (Krishnan et al., 2010). Accordingly, an involvement of dopamine-gated inhibitory circuits in the control of LA excitability was shown by a study that employed coronal slices from mice (Marowsky et al., 2005). Furthermore, urocortin, a potent CRH receptor agonist, was infused into the BLA in rats, and 5 days after this treatment the animals exhibited enhanced anxiety-related behaviour, which persisted for >30 days and could be correlated with a decrease in the amplitude of spontaneous and evoked inhibitory post-synaptic potentials as revealed by whole-cell patch-clamp recordings in coronal brain slices. The authors also showed that this lasting reduction could be blocked by the NMDA receptor antagonist AP 5 and CaMKII inhibition by 1-[N, O,-bis-(5-isoquinolinesulfonyl)-N-methyl-L-tyrosyl]-4-phenylpiperazine (Rainnie et al., 2004).

In addition to these observations, it has been reported that *in vivo* administration of CRH into mouse brains results in a phosphorylation of the ERK 1/2, intracellular kinases of the MAPK superfamily, in the LA and BLA, pointing to an increased activity of these kinases (Refojo et al., 2005).

Moreover, infusions of CRH into the BLA of rats and subsequent behavioural testing in an inhibitory avoidance test revealed that CRH enhances the memory retention latency. By treatment with the  $\beta$ -adrenoceptor antagonist atenolol the authors could link the CRH effect with this receptor type and its downstream intracellular target cAMP (Roozendaal et al., 2008).

From the studies described above it becomes likely that the magnitude of LA LTP in the presence of CRH can be modulated by several molecular pathways and also critically depends on the balance between excitation and inhibition.

The observed increase in basal neuronal activity reflected by the enhancement of FDS amplitudes by 250 nM CRH can also be interpreted in such a way that a larger portion of neurons is included in the pool of neurons, which can be potentiated in their excitability by HFS. This interpretation fits to a biophysical model, which correlates the intrinsic excitability of LA neurons with their capability to be integrated

into a fear memory trace. Although this study pointed to a relatively constant number of neurons within such traces (Kim et al., 2013), CRH concentrations used *in vitro* might counteract the mechanisms that balance this system. The finding that 250 nM significantly reduces the number of depressed sites in the LA can be brought in line with a study performed in mice. This study employed safety learning paradigms by pairing a CS with a safe environment. *In vivo* electrophysiological recordings demonstrated a CS-evoked long-term depression of LA single unit activity, which was accompanied by the behavioural expression of a positive affect (Rogan et al., 2005). Taking this data together with the effect of CRH on the enhancement of retention latency of fear memories in rats (Roosendaal et al., 2008), unrevealed alterations in LA dynamics may provide a circuit-level mechanism for the impact of CRH on fear memory modulation.

The finding that CRH had no significant effect on the number of potentiated sites in the BLA after HFS might be interpreted in that way that, although EC stimulation directly provokes neuronal activity in the BLA along the known connectivity (Sah et al., 2003), GABAergic projections from the LA could in addition indirectly modulate BLA activity. In this way BLA FDS amplitudes could be decreased and, thereby, a significant increase in the number of potentiated sites after HFS could be prevented in the presence of 250 nM CRH.

All findings regarding the effect of CRH on network dynamics should be interpreted cautiously with respect to fear conditioning since a study in rats shows that infusions of this peptide into the LA differentially impacts on fear memory acquisition and expression, depending on the timing of its administration relative to the conditioning procedure (Isogawa et al., 2013).

#### **4.2.3.1 Dissection of the involvement of CRHR1 in the observed changes in network activity and dynamics**

250 nM CRH was capable of increasing FDSs in the LA and BLA in CTRL mice. These effects were abolished in CKO mice. This finding is in line with studies having provided evidence for an involvement of CRHR1 in the regulation of excitatory neurotransmission (Ugolini et al., 2008; Refojo et al., 2011).

Next, HFS was applied in the presence of 250 nM CRH to the EC in brain slices from CTRL mice and similar results as in Bl 6 mice were obtained with respect to the total

strength of network potentiation and the number of potentiated sites. Although the decrease in the number of sites of depression in the presence of 250 nM CRH did not reach the level of significance, the observed effect followed the same tendency as in brain slices from Bl 6 mice. An explanation for this difference might be slight variations in the LA circuitry preserved in the brain slices. This explanation is favoured by a p-value of 0.05 in the respective statistical comparison.

The use of brain slices, in which the CRHR1 gene was selectively deleted in projection neurons in the forebrain, revealed that CRHR1 was involved in CRH-induced changes in network potentiation in the LA after HFS, whereas the reduction of depressed sites in the presence of CRH was unchanged.

In the BLA from CTRL mice, no significant differences in the number of potentiated sites after HFS in the presence of 250 nM CRH could be found, but, on the contrary, CKO mice showed a significant increase in the number of potentiated sites.

Influence of CRHR1 on LA network potentiation could possibly be related to its function as class "B" G-protein-coupled receptor. Thereby, this receptor may modulate various intracellular signalling cascades, some of which were also shown to be involved in the regulation of synaptic plasticity in the LA (Gallagher et al., 2008; Johansen et al., 2011).

The reduction of depressed sites in the LA within slices from KO mice could point to an involvement of CRHR2, the function of which was attributed to a depression of glutamatergic neurotransmission (Gallagher et al., 2008). The CRH-induced significant increase in the number of potentiated sites after HFS in the BLA within brain slices from CKO mice could be due to a decrease in inhibition arising from CRHR1-expressing neuronal circuits in the LA, which, in the presence of CRH, increase their inhibitory output.

On the behavioural level, forebrain deletion of the CRHR1 gene could be related to a reduction of anxiety-related behaviour and infusions of a specific CRHR1 antagonist ([9-41]- $\alpha$ -helical CRH) into the BLA of rats, immediately after fear conditioning impaired the retention of fear memory (Roosendaal et al., 2002; Refojo et al., 2011).

Moreover, elevated anxiety-related behaviour in the presence of a molecule that binds to CRHR1, namely urocortin (infused into the BLA), was prevented by co-application of the CRHRs antagonist astressin in rats (Sajdyk and Gehlert, 2000). Altogether, the findings of the present work provide additional evidence for CRHR1

antagonists being promising therapeutics for the treatment of anxiety disorders (Holsboer and Ising, 2008; Kehne and Cain, 2010).

#### 4.2.4 Effect of Cort on LA and BLA network activity and dynamics

Bath application of Cort at a concentration of 100 nM, which lies in the range of other doses used in *in vitro* studies (Karst et al., 2002; Duvarci and Pare, 2007; Stepan et al., 2012) increased FDS amplitudes in the LA and BLA. Moreover, both nuclei exhibited an enhancement in network potentiation, reflected by an increase in total potentiation and the number of potentiated sites. In addition, Cort decreased the number of sites of depression in the LA. Due to its rapid onset (Makara and Haller, 2001), the increase in FDS amplitudes after wash in of 100 nM Cort probably reflects non-genomic effects. *In vitro* studies performed in the BLA contained in rat brain slices showed that bath application of Cort is able to increase the excitability of principal neurons. This increase was partly mediated by a depolarized resting membrane potential and indirectly through a reduction of GABA<sub>A</sub> receptor-mediated IPSPs. The latter effect was attributed to a positive shift in the reversal potential of chloride (Duvarci and Pare, 2007).

Genomic effects of *in vitro* administration of Cort, which were linked to a modulation of ion channel endowment of BLA principal neurons, could be related to an alteration in the transcription of the  $\alpha_1$  subunit of L-VGCCs. These observations were made in coronal brain slices from rats (Karst et al., 2002).

On the behavioural level, several observations point to an involvement of Cort in the amygdala in the modulation of fear- and anxiety-related behaviour. Experiments conducted in rats showed that infusions of Cort into the BLA increase anxiety-related behaviour as revealed by a decreased percentage of time spent in the open arm of the elevated-plus maze (Mitra and Sapolsky, 2008). The specific involvement of the BLA in the mediation of Cort-induced enhancement of fear memory was postulated by a study performed in rats (Quirarte et al., 1997). *In vivo* testing of the influence of post-training infusions of Cort within an auditory fear-conditioning paradigm into the BLA of rats revealed that this treatment is capable of increasing the retention latency of acquired fear memory. The authors further related this enhancement to the activation of  $\beta_1$  adrenoceptors (Roosendaal et al., 2006).

In the light of these findings, the changes observed here in neuronal network activity and dynamics in the LA and BLA could reflect non-genomic effects of Cort application. Interestingly, on the level of investigation of electrical activity, 100 nM Cort, similar to 250 nM CRH, increased network potentiation and decreased network depression in the LA. This effect might be due to a modulation of L-VGCCs and the concomitant alteration of calcium influx into neurons which at least in part might underlie the changes in network dynamics, and thus, contribute differentially to LTP and LTD formation in the LA (Humeau and Lüthi, 2007).

#### **4.2.5 Differences in network dynamics in the LA and BLA of HAB/NAB mice**

The use of brain slices from HAB or NAB mice and concomitant investigation of network dynamics in the LA and BLA revealed that these amygdaloid circuits differentially responded to HFS. LA total strength of network potentiation was not significantly altered after HFS, whereas the circuitry of the BLA displayed a significant increase in network potentiation in HAB mice compared to NAB mice.

On the molecular level, this observation is in line with a study which reported an increase in the phosphorylation of PKB in the BLA after contextual fear conditioning in brain tissue from HAB compared to NAB mice (Yen et al., 2012). By referring to observations that the activation of PKB can be involved in cellular processes triggered by fear conditioning and *in vitro* LTP induction (Lin et al., 2001), the dissociation on the level of network potentiation between the LA and BLA in the present work with respect to HAB/NAB mice may partly be governed by such mechanisms. Additionally, in another study, mice were selected and bidirectionally bred with respect to their magnitude of freezing within an auditory fear conditioning paradigm. Mice that showed elevated freezing behaviour upon the presentation of the CS also showed an increase in molecular markers reflecting neuronal activity, such as ERK1/2 in the dorsal part of the LA compared to the medial and ventral part of the LA (Coyner et al., 2013).

Moreover, a study in humans compared the startle potentiation of subjects with high trait anxiety with low trait anxiety personalities by use of a fear conditioning paradigm. The authors could show that high-anxious individuals tended to acquire conditioned cues associated with a certain context much faster than less anxious subjects (Glotzbach-Schoon et al., 2013). Taken these observations together, the observed

differences in LA and BLA network dynamics between HAB and NAB mice could reflect a functional dissociation of these nuclei in their fear memory-encoding capacity, dependent on the basal anxiety level.

### 4.3 Pharmaceutical treatment

Bath application of distinct pharmaceuticals and subsequent investigation of their influence on LA and BLA network activity, revealed their potential to differentially affect these electrophysiological measures.

A medication, whose mechanism action has been elucidated on the level of synaptic transmission, is diazepam (Whiting, 2006). As a positive allosteric modulator of GABA<sub>A</sub> receptors bath application of diazepam is capable of reducing FDS amplitudes both in the LA and BLA. These findings are in line with the prominent role of inhibitory neurotransmission in the regulation of LA and BLA activity and, from a clinical point of view, the use of this substance as an anxiolytic (Whiting, 2006; Ehrlich et al., 2009).

The endocannabinoid uptake inhibitor (Giuffrida et al., 2001) AM 404 differentially influenced neuronal network activity in the LA and BLA. LA neuronal network activity was not significantly altered, FDS amplitudes in the BLA were significantly reduced. Given the observations that LA and BLA circuits differentially contribute to distinct forms of fear conditioning (Yen et al., 2012; Coyner et al., 2013) and that AM 404 is able to facilitate the extinction of contextual fear memory (de Bitencourt et al., 2008), the observed effect of AM 404 on BLA network activity might reflect a circuit level mechanism for the influence of this drug on fear memory.

Bath application of fluvoxamine or citalopram as member of the SSRIs (Burghardt and Bauer, 2013) affected FDS amplitudes in that way that only citalopram decreased network activity in the LA. These antidepressants were reported to affect different stages of amygdala-dependent fear memory formation. Acute treatment with SSRIs facilitated the acquisition and expression of fear memory, whereas chronic treatment impaired its expression (Burghardt and Bauer, 2013).

The observation that fluvoxamine failed to affect LA and BLA network activity could be related to a study demonstrating that this substance only effectively inhibited conditioned freezing in rats in the presence of a serotonin receptor agonist (Li et al.,

2001). Furthermore, with respect to its use in humans, fluvoxamine is not explicitly recommended for the treatment of anxiety disorders (Benkert and Hippus, 2011).

Belonging to the same class of pharmaceuticals, citalopram significantly reduced FDS amplitudes in the LA but failed to exert an effect on the BLA. Several studies provided evidence that citalopram changes amygdalar plasticity, as reflected by the outcome of fear conditioning paradigms. For instance, chronic intraperitoneal injections of citalopram in rats led to an impairment in the acquisition of extinction memory (Burghardt et al., 2013). Conversely, microinjections of citalopram into the amygdala of rats and subsequent behavioural testing of the animals by means of a contextual fear-conditioning paradigm revealed that this treatment was capable of significantly reducing freezing behaviour (Inoue et al., 2004).

Despite these contradictory observations there is a consensus that chronic SSRI treatment affects the electrical activity in the LA and BLA by regulating glutamatergic signalling (Burghardt and Bauer, 2013).

The observed reduction of FDS amplitudes in the LA by citalopram might possibly reflect a dampening of LA signalling as response to sensory inputs, which in turn could influence downstream signalling in the amygdaloid complex, leading to a reduction of fear and anxiety. This putative mechanism of action in the amygdala was also recently stated by Outhred et al (2013). The frequent use of citalopram for the treatment of anxiety disorders in humans also speaks in favour of this hypothesis (Benkert and Hippus, 2011).

Bath application of venlafaxine as an exponent of the class of SNRIs (Katzman, 2004) exerted a significant reduction of LA and BLA FDS amplitudes. Acute intraperitoneal injections of venlafaxine in rats before extinction training of auditory fear memory facilitated the reduction of freezing behaviour. In the same study, chronic venlafaxine treatment prevented the recovery of once extinguished fear memory (Yang et al., 2012). Venlafaxine is widely approved in pharmacotherapy of anxiety disorders in humans. (Katzman, 2004; Katzman, 2009; Ravindran and Stein, 2010; Benkert and Hippus, 2011). Thus the observed changes in network activity in the LA and BLA might point to a circuit-level mechanism of action by which venlafaxine contributes to ameliorate the symptoms of these disorders.

Clomipramine as a TCA (Zohar and Westenberg, 2000) was capable of significantly reducing FDS amplitude in the LA and BLA. Interestingly, there is a report demonstrating that delivering clomipramine chronically with the drinking water to rats,

which were afterwards subjected to repeated restraint stress, increased their levels of anxiety. The authors point to an altered regulation of Na<sup>+</sup>/K<sup>+</sup>-ATPase activity in the cerebral cortex, which they associated with putatively occurring side effects of this substance during chronic treatment (Balk Rde et al., 2011). Nevertheless, the observed changes within the present study point to a dampening of neuronal network activity in the LA and BLA by this substance, an effect by which patients suffering from anxiety disorders might benefit from this treatment. This is also emphasised by its therapeutic employment (Zohar and Westenberg, 2000; Benkert and Hippus, 2011).

The widely used antipsychotic haloperidol (Mailman and Murth, 2010) was capable of significantly decreasing FDS amplitudes, both in the LA and BLA. Several studies point to an involvement of the glutamatergic system in schizophrenia, possibly on the level of diminished NMDA receptor function (Tsai and Coyle, 2002). In this context it is worth mentioning a study employing a mouse model in which a ketamine-induced hypofunction of the glutamatergic system was elicited by injection of this substance into mice. As a consequence, the animals showed a disruption of fear-conditioned responses, which was related to schizophrenia-associated emotional blunting. The authors further report that injections of haloperidol intraperitoneally partially rescued the ketamine-induced decrease in neuronal activity as indirectly revealed by c-fos immunolabelling (Pietersen et al., 2007).

In the context of fear memory, there are studies describing an inhibitory influence of subcutaneous haloperidol injections in rats on the acquisition of the contextual cue, reflected by a decrease in freezing behaviour after conditioning (Inoue et al., 1996; Inoue et al., 2005). Therefore, the observed reduction in FDS amplitudes in the LA and BLA in response to haloperidol treatment could be interpreted that this would counteract the enhancement of neuronal activity through putative miss-associated fear-memory formation. Efforts to develop new strategies for pharmaceuticals for the treatment of schizophrenia underscore this finding (Mailman and Murthy, 2010).

In conclusion, the observed changes in BLA and LA activity upon pharmacological intervention confirm this experimental approach as being useful to gain further insights into the action profile of various neuroactive substances. Based on the emerging role of the glutamatergic system governing parts of the mechanisms of action of some of these pharmaceuticals, the observed changes possibly reflect the

sum of all cellular events regulating the excitability of the processing units LA and BLA.

## **5. Conclusion**

The development of an *in vitro* VSDI assay in conjunction with advanced data processing have succeeded in providing a method by which neuronal network activity in the LA and BLA can specifically and reliably be investigated with high spatial and temporal resolution. The detection capacity achieved by the data-processing algorithms and the resultant tracing of lasting changes in network excitability resembles an "optical multi-electrode array". By this means, new insights into the information-encoding capacity of the LA, and in part the BLA, could be gained. These data point to the ability of these circuits to dynamically respond to incoming signals in distinct ways, a scenario supported by findings from previous studies performed on the single-cell level but, until now, has not been systematically examined on the whole network level. The uncovered changes in neuronal network dynamics could be correlated with known cellular mechanisms, thereby underpinning the methodological value of this assay. By application of mediators of the stress response, it could be shown that the processing units LA and BLA respond with an increase in neuronal network activity and a shift in the tuning of these nuclei towards a potentiation of excitability. This finding could be related to a circuit-level mechanism for the modulation of fear, fear memory, and anxiety-related behaviour by stress and also correlated in part with an involvement of CRHR1.

Observed differences in information-encoding capacities of animals that differ in anxiety-related behaviour within distinct amygdalar circuitries could provide new insights into the differential information-encoding capacity of amygdalar nuclei.

Finally, substances frequently used in the pharmacotherapy of anxiety disorders were found to dampen the excitability of LA and BLA circuits. Therefore, a novel mechanism of action could be elucidated.

## **6. References**

- Adolphs R (2010) Emotion. *Curr Biol* 20:R549-552.
- Adolphs R (2013) The biology of fear. *Curr Biol* 23:R79-93.
- Aggleton JP (2000) *The Amygdala: A functional analysis*. Second Edition, Oxford Univ. Pr.
- Airan RD, Meltzer LA, Roy M, Gong Y, Chen H, Deisseroth K (2007) High-speed imaging reveals neurophysiological links to behavior in an animal model of depression. *Science* 317:819-823.
- Albensi BC, Oliver DR, Toupin J, Odero G (2007) Electrical stimulation protocols for hippocampal synaptic plasticity and neuronal hyper-excitability: Are they effective or relevant? *Exp Neurol* 204:1-13.
- Aldenhoff JB, Gruol DL, Rivier J, Vale W, Siggins GR (1983) Corticotropin releasing factor decreases postburst hyperpolarizations and excites hippocampal neurons. *Science* 221:875-877.
- An B, Hong I, Choi S (2012) Long-term neural correlates of reversible fear learning in the lateral amygdala. *J Neurosci* 32:16845-16856.
- Andersen P, Morris R, Amaral D, Bliss T, O'Keefe J (2007) *The Hippocampus Book*. Oxford Univ. Pr..
- Apergis-Schoute AM, Debiec J, Doyere V, LeDoux JE, Schafe GE (2005) Auditory fear conditioning and long-term potentiation in the lateral amygdala require ERK/MAP kinase signaling in the auditory thalamus: a role for presynaptic plasticity in the fear system. *J Neurosci* 25:5730-5739.
- Balk Rde S, Silva MH, Bridi JC, Carvalho NR, Portella Rde L, Dobrachinski F, Amaral GP, Barcelos R, Dias GR, Rocha JB, Barbosa NB, Soares FA (2011) Effect of repeated restraint stress and clomipramine on Na<sup>+</sup>/K<sup>+</sup>-ATPase activity and behavior in rats. *Int J Dev Neurosci* 29:909-916.
- Baratta MV, Lucero TR, Amat J, Watkins LR, Maier SF (2008) Role of the ventral medial prefrontal cortex in mediating behavioral control-induced reduction of later conditioned fear. *Learn Mem* 15:84-87.
- Bauer EP, Schafe GE, LeDoux JE (2002) NMDA receptors and L-type voltage-gated calcium channels contribute to long-term potentiation and different components of fear memory formation in the lateral amygdala. *J Neurosci* 22:5239-5249.
- Benkert O, Hippus H (2011) *Kompendium der Psychiatrischen Pharmakotherapie*. 8. Auflage, Springer Verlag, Heidelberg.

- Bitencourt RM, Pamplona FA, Takahashi RN (2008) Facilitation of contextual fear memory extinction and anti-anxiogenic effects of AM404 and cannabidiol in conditioned rats. *Eur Neuropsychopharmacol* 18:849-859.
- Blair HT, Schafe GE, Bauer EP, Rodrigues SM, LeDoux JE (2001) Synaptic plasticity in the lateral amygdala: a cellular hypothesis of fear conditioning. *Learn Mem* 8:229-242.
- Blank T, Nijholt I, Eckart K, Spiess J (2002) Priming of long-term potentiation in mouse hippocampus by corticotropin-releasing factor and acute stress: implications for hippocampus-dependent learning. *J Neurosci* 22:3788-3794.
- Bonfiglio JJ, Inda C, Refojo D, Holsboer F, Arzt E, Silberstein S (2011) The corticotropin-releasing hormone network and the hypothalamic-pituitary-adrenal axis: molecular and cellular mechanisms involved. *Neuroendocrinology* 94:12-20.
- Bourin M, Petit-Demouliere B, Dhonnchadha BN, Hascoet M (2007) Animal models of anxiety in mice. *Fundam Clin Pharmacol* 21:567-574.
- Buffalari DM, Grace AA (2009) Anxiogenic modulation of spontaneous and evoked neuronal activity in the basolateral amygdala. *Neuroscience* 163:1069-1077.
- Burghardt NS, Bauer EP (2013) Acute and chronic effects of selective serotonin reuptake inhibitor treatment on fear conditioning: implications for underlying fear circuits. *Neuroscience* 247:253-272.
- Burghardt NS, Sigurdsson T, Gorman JM, McEwen BS, LeDoux JE (2013) Chronic antidepressant treatment impairs the acquisition of fear extinction. *Biol Psychiatry* 73:1078-1086.
- Chapman PF, Bellavance LL (1992) Induction of long-term potentiation in the basolateral amygdala does not depend on NMDA receptor activation. *Synapse* 11:310-318.
- Chapman PF, Kairiss EW, Keenan CL, Brown TH (1990) Long-term synaptic potentiation in the amygdala. *Synapse* 6:271-278.
- Ciocchi S, Herry C, Grenier F, Wolff SB, Letzkus JJ, Vlachos I, Ehrlich I, Sprengel R, Deisseroth K, Stadler MB, Müller C, Lüthi A (2010) Encoding of conditioned fear in central amygdala inhibitory circuits. *Nature* 468:277-282.
- Cisler JM, Olatunji BO (2012) Emotion regulation and anxiety disorders. *Curr Psychiatry Rep* 14:182-187.
- Collingridge GL, Bliss TV (1995) Memories of NMDA receptors and LTP. *Trends Neurosci* 18:54-56.

- Coyner J, McGuire JL, Parker CC, Ursano RJ, Palmer AA, Johnson LR (2013) Mice selectively bred for High and Low fear behavior show differences in the number of pMAPK (p44/42 ERK) expressing neurons in lateral amygdala following Pavlovian fear conditioning. *Neurobiol Learn Mem*.
- Cryan JF, Holmes A (2005) The ascent of mouse: advances in modelling human depression and anxiety. *Nat Rev Drug Discov* 4:775-790.
- Dalton GL, Wang YT, Floresco SB, Phillips AG (2008) Disruption of AMPA receptor endocytosis impairs the extinction, but not acquisition of learned fear. *Neuropsychopharmacology* 33:2416-2426.
- Dalton GL, Wu DC, Wang YT, Floresco SB, Phillips AG (2012) NMDA GluN2A and GluN2B receptors play separate roles in the induction of LTP and LTD in the amygdala and in the acquisition and extinction of conditioned fear. *Neuropharmacology* 62:797-806.
- Damasio A, Carvalho GB (2013) The nature of feelings: evolutionary and neurobiological origins. *Nat Rev Neurosci* 14:143-152.
- Darwin C (1871) *The Descent of Man*. John Murray, London.
- Dave JR, Eiden LE, Eskay RL (1985) Corticotropin-releasing factor binding to peripheral tissue and activation of the adenylate cyclase-adenosine 3',5'-monophosphate system. *Endocrinology* 116:2152-2159.
- Davis M, Rainnie D, Cassell M (1994) Neurotransmission in the rat amygdala related to fear and anxiety. *Trends Neurosci* 17:208-214.
- Davis M, Walker DL, Myers KM (2003) Role of the amygdala in fear extinction measured with potentiated startle. *Ann N Y Acad Sci* 985:218-232.
- Davis SE, Bauer EP (2012) L-type voltage-gated calcium channels in the basolateral amygdala are necessary for fear extinction. *J Neurosci* 32:13582-13586.
- de Bitencourt RM, Pamplona FA, Takahashi RN (2013) A current overview of cannabinoids and glucocorticoids in facilitating extinction of aversive memories: potential extinction enhancers. *Neuropharmacology* 64:389-395.
- Drephal C, Schubert M, Albrecht D (2006) Input-specific long-term potentiation in the rat lateral amygdala of horizontal slices. *Neurobiol Learn Mem* 85:272-282.
- Duvarci S, Pare D (2007) Glucocorticoids enhance the excitability of principal basolateral amygdala neurons. *J Neurosci* 27:4482-4491.
- Ehrlich I, Humeau Y, Grenier F, Ciocchi S, Herry C, Lüthi A (2009) Amygdala inhibitory circuits and the control of fear memory. *Neuron* 62:757-771.

- Fanselow MS, Kim JJ (1994) Acquisition of contextual Pavlovian fear conditioning is blocked by application of an NMDA receptor antagonist D,L-2-amino-5-phosphonovaleric acid to the basolateral amygdala. *Behav Neurosci* 108:210-212.
- Felix-Ortiz AC, Beyeler A, Seo C, Leppla CA, Wildes CP, Tye KM (2013) BLA to vHPC Inputs Modulate Anxiety-Related Behaviors. *Neuron* 79:658-664.
- Fink G (2006) *The Encyclopedia of Stress*. Second Edition, Academic Press, London.
- Fourcaudot E, Gambino F, Casassus G, Poulain B, Humeau Y, Lüthi A (2009) L-type voltage-dependent Ca(2+) channels mediate expression of presynaptic LTP in amygdala. *Nat Neurosci* 12:1093-1095.
- Gallagher JP, Orozco-Cabal LF, Liu J, Shinnick-Gallagher P (2008) Synaptic physiology of central CRH system. *Eur J Pharmacol* 583:215-225.
- Giuffrida A, Beltramo M, Piomelli D (2001) Mechanisms of endocannabinoid inactivation: biochemistry and pharmacology. *J Pharmacol Exp Ther* 298:7-14.
- Glotzbach-Schoon E, Tadda R, Andreatta M, Troger C, Ewald H, Grillon C, Pauli P, Muhlberger A (2013) Enhanced discrimination between threatening and safe contexts in high-anxious individuals. *Biol Psychol* 93:159-166.
- Goosens KA, Hobin JA, Maren S (2003) Auditory-evoked spike firing in the lateral amygdala and Pavlovian fear conditioning: mnemonic code or fear bias? *Neuron* 40:1013-1022.
- Grace AA (2006) Disruption of cortical-limbic interaction as a substrate for comorbidity. *Neurotox Res* 10:93-101.
- Groeneweg FL, Karst H, de Kloet ER, Joels M (2012) Mineralocorticoid and glucocorticoid receptors at the neuronal membrane, regulators of nongenomic corticosteroid signalling. *Mol Cell Endocrinol* 350:299-309.
- Grover LM, Teyler TJ (1990) Two components of long-term potentiation induced by different patterns of afferent activation. *Nature* 347:477-479.
- Hille B (2001) *Ion Channels of Excitable Membranes*. 3rd Edition, Sinauer Associates.
- Ho VM, Lee JA, Martin KC (2011) The cell biology of synaptic plasticity. *Science* 334:623-628.
- Holsboer F, Ising M (2008) Central CRH system in depression and anxiety--evidence from clinical studies with CRH1 receptor antagonists. *Eur J Pharmacol* 583:350-357.
- Hostetler CM, Ryabinin AE (2013) The CRF system and social behavior: a review. *Front Neurosci* 7:92.

- Huang YY, Kandel ER (1998) Postsynaptic induction and PKA-dependent expression of LTP in the lateral amygdala. *Neuron* 21:169-178.
- Huang YY, Martin KC, Kandel ER (2000) Both protein kinase A and mitogen-activated protein kinase are required in the amygdala for the macromolecular synthesis-dependent late phase of long-term potentiation. *J Neurosci* 20:6317-6325.
- Hubbard DT, Nakashima BR, Lee I, Takahashi LK (2007) Activation of basolateral amygdala corticotropin-releasing factor 1 receptors modulates the consolidation of contextual fear. *Neuroscience* 150:818-828.
- Humeau Y, Lüthi A (2007) Dendritic calcium spikes induce bi-directional synaptic plasticity in the lateral amygdala. *Neuropharmacology* 52:234-243.
- Humeau Y, Shaban H, Bissiere S, Lüthi A (2003) Presynaptic induction of heterosynaptic associative plasticity in the mammalian brain. *Nature* 426:841-845.
- Hung HC, Chou CK, Chiu TH, Lee EH (1992) CRF increases protein phosphorylation and enhances retention performance in rats. *Neuroreport* 3:181-184.
- Inoue T, Tsuchiya K, Koyama T (1996) Effects of typical and atypical antipsychotic drugs on freezing behavior induced by conditioned fear. *Pharmacol Biochem Behav* 55:195-201.
- Inoue T, Izumi T, Li XB, Kitaichi Y, Nakagawa S, Koyama T (2005) Effect of a dopamine D1/5 receptor antagonist on haloperidol-induced inhibition of the acquisition of conditioned fear. *Eur J Pharmacol* 519:253-258.
- Inoue T, Li XB, Abekawa T, Kitaichi Y, Izumi T, Nakagawa S, Koyama T (2004) Selective serotonin reuptake inhibitor reduces conditioned fear through its effect in the amygdala. *Eur J Pharmacol* 497:311-316.
- Isogawa K, Bush DE, LeDoux JE (2013) Contrasting effects of pretraining, posttraining, and pretesting infusions of corticotropin-releasing factor into the lateral amygdala: attenuation of fear memory formation but facilitation of its expression. *Biol Psychiatry* 73:353-359.
- Jasnow AM, Ehrlich DE, Choi DC, Dabrowska J, Bowers ME, McCullough KM, Rainnie DG, Ressler KJ (2013) Thy1-expressing neurons in the basolateral amygdala may mediate fear inhibition. *J Neurosci* 33:10396-10404.
- Johansen JP, Cain CK, Ostroff LE, LeDoux JE (2011) Molecular mechanisms of fear learning and memory. *Cell* 147:509-524.
- Johansen JP, Wolff SB, Lüthi A, LeDoux JE (2012) Controlling the elements: an optogenetic approach to understanding the neural circuits of fear. *Biol Psychiatry* 71:1053-1060.

- Johansen JP, Hamanaka H, Monfils MH, Behnia R, Deisseroth K, Blair HT, LeDoux JE (2010) Optical activation of lateral amygdala pyramidal cells instructs associative fear learning. *Proc Natl Acad Sci U S A* 107:12692-12697.
- Johnson LR, Farb C, Morrison JH, McEwen BS, LeDoux JE (2005) Localization of glucocorticoid receptors at postsynaptic membranes in the lateral amygdala. *Neuroscience* 136:289-299.
- Karst H, Berger S, Erdmann G, Schutz G, Joels M (2010) Metaplasticity of amygdalar responses to the stress hormone corticosterone. *Proc Natl Acad Sci U S A* 107:14449-14454.
- Karst H, Nair S, Velzing E, Rumpff-van Essen L, Slagter E, Shinnick-Gallagher P, Joels M (2002) Glucocorticoids alter calcium conductances and calcium channel subunit expression in basolateral amygdala neurons. *Eur J Neurosci* 16:1083-1089.
- Katzman MA (2004) Venlafaxine in the treatment of anxiety disorders. *Expert Rev Neurother* 4:371-381.
- Katzman MA (2009) Current considerations in the treatment of generalized anxiety disorder. *CNS Drugs* 23:103-120.
- Kehne JH, Cain CK (2010) Therapeutic utility of non-peptidic CRF1 receptor antagonists in anxiety, depression, and stress-related disorders: evidence from animal models. *Pharmacol Ther* 128:460-487.
- Kim D, Pare D, Nair SS (2013) Assignment of model amygdala neurons to the fear memory trace depends on competitive synaptic interactions. *J Neurosci* 33:14354-14358.
- Kim MJ, Loucks RA, Palmer AL, Brown AC, Solomon KM, Marchante AN, Whalen PJ (2011) The structural and functional connectivity of the amygdala: from normal emotion to pathological anxiety. *Behav Brain Res* 223:403-410.
- Kjelstrup KG, Tuvnes FA, Steffenach HA, Murison R, Moser EI, Moser MB (2002) Reduced fear expression after lesions of the ventral hippocampus. *Proc Natl Acad Sci U S A* 99:10825-10830.
- Kratzer S, Mattusch C, Metzger MW, Dedic N, Noll-Hussong M, Kafitz KW, Eder M, Deussing JM, Holsboer F, Kochs E, Rammes G (2013) Activation of CRH receptor type 1 expressed on glutamatergic neurons increases excitability of CA1 pyramidal neurons by the modulation of voltage-gated ion channels. *Front Cell Neurosci* 7:91.
- Krettek JE, Price JL (1978) A description of the amygdaloid complex in the rat and cat with observations on intra-amygdaloid axonal connections. *J Comp Neurol* 178:255-280.

- Krishnan B, Centeno M, Pollandt S, Fu Y, Genzer K, Liu J, Gallagher JP, Shinnick-Gallagher P (2010) Dopamine receptor mechanisms mediate corticotropin-releasing factor-induced long-term potentiation in the rat amygdala following cocaine withdrawal. *Eur J Neurosci* 31:1027-1042.
- Krömer SA, Kessler MS, Milfay D, Birg IN, Bunck M, Czibere L, Panhuysen M, Putz B, Deussing JM, Holsboer F, Landgraf R, Turck CW (2005) Identification of glyoxalase-I as a protein marker in a mouse model of extremes in trait anxiety. *J Neurosci* 25:4375-4384.
- Kühne C, Puk O, Graw J, Hrabe de Angelis M, Schutz G, Wurst W, Deussing JM (2012) Visualizing corticotropin-releasing hormone receptor type 1 expression and neuronal connectivities in the mouse using a novel multifunctional allele. *J Comp Neurol* 520:3150-3180.
- Kulisch C, Eckers N, Albrecht D (2011) Method of euthanasia affects amygdala plasticity in horizontal brain slices from mice. *J Neurosci Methods* 201:340-345.
- LeDoux J (2007) The amygdala. *Curr Biol* 17:R868-874.
- LeDoux JE, Farb CR, Romanski LM (1991) Overlapping projections to the amygdala and striatum from auditory processing areas of the thalamus and cortex. *Neurosci Lett* 134:139-144.
- Lehner M, Wislowska-Stanek A, Taracha E, Maciejak P, Szyndler J, Skorzewska A, Turzynska D, Sobolewska A, Hamed A, Bidzinski A, Plaznik A (2010) The effects of midazolam and D-cycloserine on the release of glutamate and GABA in the basolateral amygdala of low and high anxiety rats during extinction trial of a conditioned fear test. *Neurobiol Learn Mem* 94:468-480.
- Li XB, Inoue T, Hashimoto S, Koyama T (2001) Effect of chronic administration of flesinoxan and fluvoxamine on freezing behavior induced by conditioned fear. *Eur J Pharmacol* 425:43-50.
- Lin CH, Yeh SH, Lu KT, Leu TH, Chang WC, Gean PW (2001) A role for the PI-3 kinase signaling pathway in fear conditioning and synaptic plasticity in the amygdala. *Neuron* 31:841-851.
- Mahan AL, Ressler KJ (2012) Fear conditioning, synaptic plasticity and the amygdala: implications for posttraumatic stress disorder. *Trends Neurosci* 35:24-35.
- Mailman RB, Murthy V (2010) Third generation antipsychotic drugs: partial agonism or receptor functional selectivity? *Curr Pharm Des* 16:488-501.
- Makara GB, Haller J (2001) Non-genomic effects of glucocorticoids in the neural system. Evidence, mechanisms and implications. *Prog Neurobiol* 65:367-390.
- Maren S (1999) Long-term potentiation in the amygdala: a mechanism for emotional learning and memory. *Trends Neurosci* 22:561-567.

- Maren S (2008) Pavlovian fear conditioning as a behavioral assay for hippocampus and amygdala function: cautions and caveats. *Eur J Neurosci* 28:1661-1666.
- Maren S, Quirk GJ (2004) Neuronal signalling of fear memory. *Nat Rev Neurosci* 5:844-852.
- Marowsky A, Yanagawa Y, Obata K, Vogt KE (2005) A specialized subclass of interneurons mediates dopaminergic facilitation of amygdala function. *Neuron* 48:1025-1037.
- McDonald AJ (1982) Neurons of the lateral and basolateral amygdaloid nuclei: a Golgi study in the rat. *J Comp Neurol* 212:293-312.
- McDonald AJ, Mascagni F (2001) Localization of the CB1 type cannabinoid receptor in the rat basolateral amygdala: high concentrations in a subpopulation of cholecystinin-containing interneurons. *Neuroscience* 107:641-652.
- McDonald AJ, Mascagni F, Muller JF (2004) Immunocytochemical localization of GABABR1 receptor subunits in the basolateral amygdala. *Brain Res* 1018:147-158.
- McEwen BS, Chattarji S, Diamond DM, Jay TM, Reagan LP, Svenningsson P, Fuchs E (2010) The neurobiological properties of tianeptine (Stablon): from monoamine hypothesis to glutamatergic modulation. *Mol Psychiatry* 15:237-249.
- McGaugh JL (2004) The amygdala modulates the consolidation of memories of emotionally arousing experiences. *Annu Rev Neurosci* 27:1-28.
- McKernan MG, Shinnick-Gallagher P (1997) Fear conditioning induces a lasting potentiation of synaptic currents in vitro. *Nature* 390:607-611.
- Mechoulam R, Parker LA (2013) The endocannabinoid system and the brain. *Annu Rev Psychol* 64:21-47.
- Minichiello L, Korte M, Wolfer D, Kuhn R, Unsicker K, Cestari V, Rossi-Arnaud C, Lipp HP, Bonhoeffer T, Klein R (1999) Essential role for TrkB receptors in hippocampus-mediated learning. *Neuron* 24:401-414.
- Miserendino MJ, Sananes CB, Melia KR, Davis M (1990) Blocking of acquisition but not expression of conditioned fear-potentiated startle by NMDA antagonists in the amygdala. *Nature* 345:716-718.
- Mitra R, Sapolsky RM (2008) Acute corticosterone treatment is sufficient to induce anxiety and amygdaloid dendritic hypertrophy. *Proc Natl Acad Sci U S A* 105:5573-5578.
- Morgan MA, LeDoux JE (1995) Differential contribution of dorsal and ventral medial prefrontal cortex to the acquisition and extinction of conditioned fear in rats. *Behav Neurosci* 109:681-688.

- Morozov A, Sukato D, Ito W (2011) Selective Suppression of Plasticity in Amygdala Inputs from Temporal Association Cortex by the External Capsule. *J Neurosci* 31:339-345.
- Mountney C, Anisman H, Merali Z (2011) In vivo levels of corticotropin-releasing hormone and gastrin-releasing peptide at the basolateral amygdala and medial prefrontal cortex in response to conditioned fear in the rat. *Neuropharmacology* 60:410-417.
- Müller T, Albrecht D, Gebhardt C (2009) Both NR2A and NR2B subunits of the NMDA receptor are critical for long-term potentiation and long-term depression in the lateral amygdala of horizontal slices of adult mice. *Learn Mem* 16:395-405.
- Myers KM, Davis M (2007) Mechanisms of fear extinction. *Mol Psychiatry* 12:120-150.
- Neumann ID, Wegener G, Homberg JR, Cohen H, Slattery DA, Zohar J, Olivier JD, Mathe AA (2011) Animal models of depression and anxiety: What do they tell us about human condition? *Prog Neuropsychopharmacol Biol Psychiatry* 35:1357-1375.
- Orsini CA, Maren S (2012) Neural and cellular mechanisms of fear and extinction memory formation. *Neurosci Biobehav Rev* 36:1773-1802.
- Orsini CA, Kim JH, Knapska E, Maren S (2011) Hippocampal and prefrontal projections to the basal amygdala mediate contextual regulation of fear after extinction. *J Neurosci* 31:17269-17277.
- Outhred T, Hawkshead BE, Wager TD, Das P, Malhi GS, Kemp AH (2013) Acute neural effects of selective serotonin reuptake inhibitors versus noradrenaline reuptake inhibitors on emotion processing: Implications for differential treatment efficacy. *Neurosci Biobehav Rev* 37:1786-1800.
- Papadimitriou A, Priftis KN (2009) Regulation of the hypothalamic-pituitary-adrenal axis. *Neuroimmunomodulation* 16:265-271.
- Pare D, Smith Y (1993) The intercalated cell masses project to the central and medial nuclei of the amygdala in cats. *Neuroscience* 57:1077-1090.
- Pare D, Collins DR (2000) Neuronal correlates of fear in the lateral amygdala: multiple extracellular recordings in conscious cats. *J Neurosci* 20:2701-2710.
- Pare D, Duvarci S (2012) Amygdala microcircuits mediating fear expression and extinction. *Curr Opin Neurobiol* 22:717-723.
- Patel S, Roelke CT, Rademacher DJ, Cullinan WE, Hillard CJ (2004) Endocannabinoid signaling negatively modulates stress-induced activation of the hypothalamic-pituitary-adrenal axis. *Endocrinology* 145:5431-5438.

- Paxinos G (2004) *The Rat Nervous System*. Academic Press, San Diego.
- Pietersen CY, Bosker FJ, Doorduyn J, Jongsma ME, Postema F, Haas JV, Johnson MP, Koch T, Vladusich T, den Boer JA (2007) An animal model of emotional blunting in schizophrenia. *PLoS One* 2:e1360.
- Pillai AG, Anilkumar S, Chattarji S (2012) The same antidepressant elicits contrasting patterns of synaptic changes in the amygdala vs hippocampus. *Neuropsychopharmacology* 37:2702-2711.
- Price JL (2003) Comparative aspects of amygdala connectivity. *Ann N Y Acad Sci* 985:50-58.
- Price JL, Drevets WC (2010) Neurocircuitry of mood disorders. *Neuropsychopharmacology* 35:192-216.
- Quirarte GL, Roozendaal B, McGaugh JL (1997) Glucocorticoid enhancement of memory storage involves noradrenergic activation in the basolateral amygdala. *Proc Natl Acad Sci U S A* 94:14048-14053.
- Quirk GJ, Pare D, Richardson R, Herry C, Monfils MH, Schiller D, Vicentic A (2010) Erasing fear memories with extinction training. *J Neurosci* 30:14993-14997.
- Radley JJ, Gosselink KL, Sawchenko PE (2009) A discrete GABAergic relay mediates medial prefrontal cortical inhibition of the neuroendocrine stress response. *J Neurosci* 29:7330-7340.
- Rainnie DG, Asprodini EK, Shinnick-Gallagher P (1991) Inhibitory transmission in the basolateral amygdala. *J Neurophysiol* 66:999-1009.
- Rainnie DG, Bergeron R, Sajdyk TJ, Patil M, Gehlert DR, Shekhar A (2004) Corticotrophin releasing factor-induced synaptic plasticity in the amygdala translates stress into emotional disorders. *J Neurosci* 24:3471-3479.
- Ramirez S, Liu X, Lin PA, Suh J, Pignatelli M, Redondo RL, Ryan TJ, Tonegawa S (2013) Creating a false memory in the hippocampus. *Science* 341:387-391.
- Ravindran LN, Stein MB (2010) The pharmacologic treatment of anxiety disorders: a review of progress. *J Clin Psychiatry* 71:839-854.
- Refojo D, Holsboer F (2009) CRH signaling. Molecular specificity for drug targeting in the CNS. *Ann N Y Acad Sci* 1179:106-119.
- Refojo D, Echenique C, Müller MB, Reul JM, Deussing JM, Wurst W, Sillaber I, Paez-Pereda M, Holsboer F, Arzt E (2005) Corticotropin-releasing hormone activates ERK1/2 MAPK in specific brain areas. *Proc Natl Acad Sci U S A* 102:6183-6188.

- Refojo D, Schweizer M, Kuehne C, Ehrenberg S, Thoeringer C, Vogl AM, Dedic N, Schumacher M, von Wolff G, Avrabos C, Touma C, Engblom D, Schutz G, Nave KA, Eder M, Wotjak CT, Sillaber I, Holsboer F, Wurst W, Deussing JM (2011) Glutamatergic and dopaminergic neurons mediate anxiogenic and anxiolytic effects of CRHR1. *Science* 333:1903-1907.
- Repa JC, Muller J, Apergis J, Desrochers TM, Zhou Y, LeDoux JE (2001) Two different lateral amygdala cell populations contribute to the initiation and storage of memory. *Nat Neurosci* 4:724-731.
- Rodrigues SM, Farb CR, Bauer EP, LeDoux JE, Schafe GE (2004) Pavlovian fear conditioning regulates Thr286 autophosphorylation of Ca<sup>2+</sup>/calmodulin-dependent protein kinase II at lateral amygdala synapses. *J Neurosci* 24:3281-3288.
- Rogan MT, Staubli UV, LeDoux JE (1997) Fear conditioning induces associative long-term potentiation in the amygdala. *Nature* 390:604-607.
- Rogan MT, Leon KS, Perez DL, Kandel ER (2005) Distinct neural signatures for safety and danger in the amygdala and striatum of the mouse. *Neuron* 46:309-320.
- Roosendaal B, Schelling G, McGaugh JL (2008) Corticotropin-releasing factor in the basolateral amygdala enhances memory consolidation via an interaction with the beta-adrenoceptor-cAMP pathway: dependence on glucocorticoid receptor activation. *J Neurosci* 28:6642-6651.
- Roosendaal B, Brunson KL, Holloway BL, McGaugh JL, Baram TZ (2002) Involvement of stress-released corticotropin-releasing hormone in the basolateral amygdala in regulating memory consolidation. *Proc Natl Acad Sci U S A* 99:13908-13913.
- Roosendaal B, Hui GK, Hui IR, Berlau DJ, McGaugh JL, Weinberger NM (2006) Basolateral amygdala noradrenergic activity mediates corticosterone-induced enhancement of auditory fear conditioning. *Neurobiol Learn Mem* 86:249-255.
- Ryan SJ, Ehrlich DE, Jasnow AM, Daftary S, Madsen TE, Rainnie DG (2012) Spike-timing precision and neuronal synchrony are enhanced by an interaction between synaptic inhibition and membrane oscillations in the amygdala. *PLoS One* 7:e35320.
- Sah P, Faber ES, Lopez De Armentia M, Power J (2003) The amygdaloid complex: anatomy and physiology. *Physiol Rev* 83:803-834.
- Sajdyk TJ, Gehlert DR (2000) Astressin, a corticotropin releasing factor antagonist, reverses the anxiogenic effects of urocortin when administered into the basolateral amygdala. *Brain Res* 877:226-234.

- Samson RD, Pare D (2006) A spatially structured network of inhibitory and excitatory connections directs impulse traffic within the lateral amygdala. *Neuroscience* 141:1599-1609.
- Samson RD, Dumont EC, Pare D (2003) Feedback inhibition defines transverse processing modules in the lateral amygdala. *J Neurosci* 23:1966-1973.
- Schafe GE, Atkins CM, Swank MW, Bauer EP, Sweatt JD, LeDoux JE (2000) Activation of ERK/MAP kinase in the amygdala is required for memory consolidation of pavlovian fear conditioning. *J Neurosci* 20:8177-8187.
- Schmitt O, Eipert P, Philipp K, Kettlitz R, Fuellen G, Wree A (2012) The intrinsic connectome of the rat amygdala. *Front Neural Circuits* 6:81.
- Shekhar A, Truitt W, Rainnie D, Sajdyk T (2005) Role of stress, corticotrophin releasing factor (CRF) and amygdala plasticity in chronic anxiety. *Stress* 8:209-219.
- Shors TJ, Mathew PR (1998) NMDA receptor antagonism in the lateral/basolateral but not central nucleus of the amygdala prevents the induction of facilitated learning in response to stress. *Learn Mem* 5:220-230.
- Sigurdsson T, Doyere V, Cain CK, LeDoux JE (2007) Long-term potentiation in the amygdala: a cellular mechanism of fear learning and memory. *Neuropharmacology* 52:215-227.
- Sotres-Bayon F, Quirk GJ (2010) Prefrontal control of fear: more than just extinction. *Curr Opin Neurobiol* 20:231-235.
- Stein MB, Steckler T (2010) *Behavioral Neurobiology of Anxiety and Its Treatment*. Springer Verlag, Heidelberg.
- Stepan J, Dine J, Fenzl T, Polta SA, von Wolff G, Wotjak CT, Eder M (2012) Entorhinal theta-frequency input to the dentate gyrus trisynaptically evokes hippocampal CA1 LTP. *Front Neural Circuits* 6:64.
- Stout SC, Owens MJ, Nemeroff CB (2002) Regulation of corticotropin-releasing factor neuronal systems and hypothalamic-pituitary-adrenal axis activity by stress and chronic antidepressant treatment. *J Pharmacol Exp Ther* 300:1085-1092.
- Szinyei C, Heinbockel T, Montagne J, Pape HC (2000) Putative cortical and thalamic inputs elicit convergent excitation in a population of GABAergic interneurons of the lateral amygdala. *J Neurosci* 20:8909-8915.
- Thompson BL, Erickson K, Schulkin J, Rosen JB (2004) Corticosterone facilitates retention of contextually conditioned fear and increases CRH mRNA expression in the amygdala. *Behav Brain Res* 149:209-215.

- Tominaga T, Tominaga Y, Yamada H, Matsumoto G, Ichikawa M (2000) Quantification of optical signals with electrophysiological signals in neural activities of Di-4-ANEPPS stained rat hippocampal slices. *J Neurosci Methods* 102:11-23.
- Tsai G, Coyle JT (2002) Glutamatergic mechanisms in schizophrenia. *Annu Rev Pharmacol Toxicol* 42:165-179.
- Tsvetkov E, Carlezon WA, Benes FM, Kandel ER, Bolshakov VY (2002) Fear conditioning occludes LTP-induced presynaptic enhancement of synaptic transmission in the cortical pathway to the lateral amygdala. *Neuron* 34:289-300.
- Tye KM, Prakash R, Kim SY, Fenno LE, Grosenick L, Zarabi H, Thompson KR, Gradinaru V, Ramakrishnan C, Deisseroth K (2011) Amygdala circuitry mediating reversible and bidirectional control of anxiety. *Nature* 471:358-362.
- Ugolini A, Sokal DM, Arban R, Large CH (2008) CRF1 receptor activation increases the response of neurons in the basolateral nucleus of the amygdala to afferent stimulation. *Front Behav Neurosci* 2:2.
- van Gaalen MM, Stenzel-Poore MP, Holsboer F, Steckler T (2002) Effects of transgenic overproduction of CRH on anxiety-like behaviour. *Eur J Neurosci* 15:2007-2015.
- Vaswani M, Linda FK, Ramesh S (2003) Role of selective serotonin reuptake inhibitors in psychiatric disorders: a comprehensive review. *Prog Neuropsychopharmacol Biol Psychiatry* 27:85-102.
- Veening JG, Swanson LW, Sawchenko PE (1984) The organization of projections from the central nucleus of the amygdala to brainstem sites involved in central autonomic regulation: a combined retrograde transport-immunohistochemical study. *Brain Res* 303:337-357.
- von Bohlen und Halbach O, Albrecht D (1998) Tracing of axonal connectivities in a combined slice preparation of rat brains--a study by rhodamine-dextran-amine-application in the lateral nucleus of the amygdala. *J Neurosci Methods* 81:169-175.
- von Wolff G, Avrabos C, Stepan J, Wurst W, Deussing JM, Holsboer F, Eder M (2011) Voltage-sensitive dye imaging demonstrates an enhancing effect of corticotropin-releasing hormone on neuronal activity propagation through the hippocampal formation. *J Psychiatr Res* 45:256-261.
- Walker DL, Miles LA, Davis M (2009) Selective participation of the bed nucleus of the stria terminalis and CRF in sustained anxiety-like versus phasic fear-like responses. *Prog Neuropsychopharmacol Biol Psychiatry* 33:1291-1308.
- Wallisch P, Lusignan M, Benayoun M, Baker TI, Dickey AS, Hatsopoulos NG (2009) *Matlab for Neuroscientists*. Academic Press, San Diego.

- Wang C, Wilson WA, Moore SD (2001) Role of NMDA, non-NMDA, and GABA receptors in signal propagation in the amygdala formation. *J Neurophysiol* 86:1422-1429.
- Wang HL, Tsai LY, Lee EH (2000) Corticotropin-releasing factor produces a protein synthesis--dependent long-lasting potentiation in dentate gyrus neurons. *J Neurophysiol* 83:343-349.
- Washburn MS, Moises HC (1992) Inhibitory responses of rat basolateral amygdaloid neurons recorded in vitro. *Neuroscience* 50:811-830.
- Weisskopf MG, LeDoux JE (1999) Distinct populations of NMDA receptors at subcortical and cortical inputs to principal cells of the lateral amygdala. *J Neurophysiol* 81:930-934.
- Whiting PJ (2006) GABA-A receptors: a viable target for novel anxiolytics? *Curr Opin Pharmacol* 6:24-29.
- Wilson YM, Murphy M (2009) A discrete population of neurons in the lateral amygdala is specifically activated by contextual fear conditioning. *Learn Mem* 16:357-361.
- Yang CH, Shi HS, Zhu WL, Wu P, Sun LL, Si JJ, Liu MM, Zhang Y, Suo L, Yang JL (2012) Venlafaxine facilitates between-session extinction and prevents reinstatement of auditory-cue conditioned fear. *Behav Brain Res* 230:268-273.
- Yen YC, Mauch CP, Dahlhoff M, Micale V, Bunck M, Sartori SB, Singewald N, Landgraf R, Wotjak CT (2012) Increased levels of conditioned fear and avoidance behavior coincide with changes in phosphorylation of the protein kinase B (AKT) within the amygdala in a mouse model of extremes in trait anxiety. *Neurobiol Learn Mem* 98:56-65.
- Zohar J, Westenberg HG (2000) Anxiety disorders: a review of tricyclic antidepressants and selective serotonin reuptake inhibitors. *Acta Psychiatr Scand Suppl* 403:39-49.

<b>Chemical</b>	<b>Solvent</b>	<b>Fabricant</b>
D (-)-2-Amino-5-phosphonopentanoic acid (AP 5)	Distilled water	Abcam
N-(4-Hydroxyphenyl)arachidonylamide (AM 404)	DMSO	Tocris
Bicuculline methiodide (BIM)	Distilled water	Sigma
Citalopram hydrobromide	Distilled water	Sigma
Corticosterone (Cort)	DMSO	Sigma
Corticotropin-releasing hormone (CRH)	Distilled water	Abcam
Clomipramine	Distilled water	Sigma
(2S)-3-[[[(1S)-1-(3,4-Dichlorophenyl)ethyl]amino-2-hydroxypropyl](phenylmethyl)phosphinic acid hydrochloride (CGP 55845)	DMSO	Tocris
Dimethylsulfoxide (dry) (DMSO)		Sigma
4-(2-(6-(Dibutylamino)-2-naphtalenyl)-1-(3-sulfopropyl) pyridinium hydroxide inner salt (Di-4-ANEPPS)	DMSO	Sigma
Diazepam	DMSO	Sigma
Fluvoxamine maleat	Distilled water	Sigma
Haloperidol	Distilled water	Sigma
2,3-dihydroxy-6-nitro-7-sulfamoyl-benzo[f]quinoxaline-2,3-dione (NBQX)	DMSO	Abcam

Salts for ACSF- solutions	Distilled Water	Sigma
Tetrodotoxin (TTX)	Distilled water	Sigma
Venlafaxine hydrochloride	Distilled water	Sigma
Verapamil	Distilled water	Sigma

## **8. Abbreviations**

nACSF = Artificial cerebrospinal fluid

sACSF = Sucrose-based artificial cerebrospinal fluid

ACTH = Adrenocorticotrophic hormone

AMPA =  $\alpha$ -amino-3-hydroxy-5-methyl-4-isoxazolepropionic acid

AM 404 = N-(4-Hydroxyphenyl) arachidonylamide

AP 5 = D(-)-2-Amino-5-phosphopentanoic acid

AVP = Arginine vasopressin

BLA = Basolateral amygdala

BIM = Bicuculline methiodide

BI 6 = C57BL/6N mice

CaMKII = Calcium/calmodulin protein kinase

cAMP = Cyclic adenosine monophosphate

CCD = Charge-coupled device

CeA = Central amygdala

ICe = Centrolateral amygdala

mCe = Centromedial amygdala

CGP 55845 = (2S)-3-[[[(1S)-1-(3,4-Dichlorophenyl)-ethyl]amino-2-hydroxypropyl](phenylmethyl)phosphinic acid hydrochloride

CKO =  $Crhr1^{loxP/loxP}$  *Camk2 $\alpha$ -Cre* mice

Cort = Corticosterone

CRH = Corticotropin-releasing hormone

CRHR1 = Corticotropin-releasing hormone receptor type 1

CRHR2 = Corticotropin-releasing hormone receptor type 2

CS = Conditioned stimulus

CTRL =  $Crhr1^{loxP/loxP}$  mice

Di-4-ANEPPS = 4-(2-(6-(Dibutylamino)-2-naphthalenyl)-1-(3-sulfopropyl) pyridinium hydroxide inner salt

DMSO = Dimethylsulfoxide

EC = External capsule

ERK = Extracellular-signal regulated kinase

FDS = Fast depolarization-mediated signal

GABA = Gamma-aminobutyric acid

GR = Glucocorticoid receptor

HAB = High anxiety-related behaviour

HFS = High-frequency stimulation

HPA = Hypothalamic-pituitary-adrenal

IC = Internal capsule

LA = Lateral amygdala

L-VGCC = L-type voltage-gated calcium channel

LTD = Long-term depression

LTP = Long-term potentiation

MAP Kinases = Mitogen-activated protein kinases

MR = Mineralocorticoid receptor

NAB = Normal anxiety-related behaviour

NBQX = 2,3-dihydroxy-6-nitro-7-sulfamoyl-benzo[f]quinoxaline-2,3-dione

NMDA = N-methyl-D-aspartate

NO = Nitric oxide

PKA = Protein kinase A

PKB = Protein kinase B

PKC = Protein kinase C

PLC = Phospholipase C

PVN = Paraventricular nucleus

RMS = Root-mean square

ROI = Region of interest

RT = Room temperature

SNRI = Serotonin noradrenalin reuptake inhibitor

SSRI = Selective serotonin reuptake inhibitor

TCA = Tricyclic antidepressant

TTX = Tetrodotoxine

US = Unconditioned stimulus

VGCC = Voltage-gated calcium channel

VSD = Voltage-sensitive dye

VSDI = Voltage-sensitive dye imaging

## **9. List of Figures**

**Figure 1.2.-1. Basic scheme of the limbic brain system with known connectivity as indicated through black lines (page 2)**

**Figure 1.5.2-2. Key nuclei, cell groups, and fibre tracts within the amygdaloid complex and their anatomical location along the dorsal/ventral and lateral/medial axes (page 10)**

**Figure 1.5.3-3. Functional connectivity of amygdala key nuclei and cell groups (page 12)**

**Figure 2.3-4. Principle of VSDI (page 23)**

**Figure 2.3-5. Data acquisition using the Brain Vision software and averaging steps to reduce noise (page 23)**

**Figure 2.3-6. Baseline correction of FDSs (page 24)**

**Figure 2.3-7. Principle of the adjustment of FDSs for subsequent VSDI experiments in the LA and BLA (page 25)**

**Figure 3.1-8. Different planes of horizontal brain slices which contain distinct nuclei of the amygdaloid complex (page 31)**

**Figure 3.1-9. Overview of amygdaloid nuclei contained in the horizontal brain slice and location of the stimulation electrode (page 32)**

**Figure 3.1-10. Overview of amygdaloid nuclei contained in the horizontal brain slice and location of the stimulation electrode (page 33)**

**Figure 3.1-11. Detection of VSD signal in specific ROIs after single electrical stimulation of the external capsule (page 34)**

**Figure 3.1-12. Pharmacological characterization of VSD signal in the LA (page 35)**

**Figure 3.2.1-13. Extracellular field potential recordings of LA responses upon single-pulse electrical stimulation of the EC before and after HFS (page 36)**

**Figure 3.2.2-14. Neuronal network plasticity in the LA monitored by means of VSDI and subsequent data processing (page 38)**

**Figure 3.2.2-15. Principle of the design of the Active Site Filter (page 38)**

**Figure 3.2.2-16. Visualization of maximum intensity projection command output (page 39)**

**Figure 3.2.2-17. Changes in network dynamics within the LA after HFS in C57BL/6N mice (page 40)**

**Figure 3.2.2.1-18. Effects of verapamil or AP 5 on LA network dynamics (page 42)**

**Figure 3.2.2.1-19. Verapamil decreases the number of potentiated sites after HFS in the BLA (page 43)**

**Figure 3.2.3-20. Bath application of CRH affects FDS amplitudes in the LA and BLA in a concentration dependent manner (page 45)**

**Figure 3.2.3-21. 125 nM CRH increases HFS-induced network plasticity in the LA (page 46)**

**Figure 3.2.3-22. CRH-induced changes in network dynamics after HFS in the LA (page 47)**

**Figure 3.2.3-23. CRH induces no changes in the number of potentiated sites in the BLA after HFS (page 48)**

**Figure 3.2.3.1-24. Effects of bath application of 250 nM CRH on FDSs in the LA and BLA in brain slices from CKO and CTRL mice (page 49)**

**Figure 3.2.3.1-25. CRH-induced changes in network dynamics after HFS in the LA are partially mediated by CRHR1 (page 50)**

**Figure 3.2.3.1-26. CRHR1 is involved in mediating the effect of 250 nM CRH on network potentiation in the BLA after HFS (page 51)**

**Figure 3.2.4-27. Effects of bath application of 100 nM Cort on FDS amplitudes and total strength of network potentiation after HFS in brain slices containing the LA and BLA (page 53)**

**Figure 3.2.5-28. Investigation of total strength of network potentiation after HFS comparing NAB and HAB mice (page 54)**

**Figure 3.3-29. Diazepam reduces FDS amplitudes in the LA and BLA (page 55)**

**Figure 3.3-30. Brain region-specific effects of AM 404 on FDS amplitudes in the LA and BLA (page 56)**

**Figure 3.3-31. Effects of bath application of fluvoxamine on FDSs in the LA and BLA (page 56)**

**Figure 3.3-32. Changes in FDSs in the LA or BLA upon bath application of citalopram (page 57)**

**Figure 3.3-33. Effects of bath application of venlafaxine on FDSs in the LA and BLA (page 57)**

**Figure 3.3-34. Clomipramine affects basal neuronal network activity reflected by a decrease of FDSs in the LA and BLA (page58)**

**Figure 3.3-35. Haloperidol is capable of reducing basal neuronal network activity in the LA and BLA (page 58)**

## **10. Publications**

### **Masterarbeit**

Hladky F (2009) **Characterization of neural stem / progenitor cells of embryonic mouse by means of Immunocytochemistry, Whole Cell Patch Clamp and Single Cell RT-PCR** (Paris-Lodron Universität Salzburg, Masterarbeit).

### **Poster Abstracts in Tagungsbänden**

Hladky F, Gehwolf R, Tempfer H, Hermann A, Weiger T M, Bauer H C **Characterization of neural progenitor cells by means of single cell PCR, whole cell patch clamp and immunocytochemistry** (ANA 2009).

Hladky F, Avrabos C, Eder M **Towards the elucidation of fear memories: investigating whole-network long-term potentiation in the lateral amygdala using voltage-sensitive dye imaging** (Institutssymposium 2011; MPI für Psychiatrie).

Stepan J \*, Hladky F \*, von Wolff G, Avrabos C, Eder M **Neuronal network profiling of antidepressant drug action** (\* equal contribution) (Institutssymposium 2011; MPI für Psychiatrie).

Hladky F, Avrabos C, Eder M **Insights into antidepressant drug action: Regulation of network activity in the amygdala by distinct classes of antidepressants** (Institutssymposium 2012; MPI für Psychiatrie).

Stepan J, Hladky F, Eder M **Antidepressants enhance neuronal activity flow through the hippocampus** (Institutssymposium 2012; MPI für Psychiatrie).

Hladky F, Avrabos C, Eder M **Studying neuronal network plasticity in the lateral amygdala using voltage-sensitive dye imaging** (FENS 2012).

Hladky F, Kühne C, Deussing JM, Eder M **CRH-induced changes in neuronal network dynamics in the lateral amygdala revealed by an “optical” multi-electrode array** (Institutssymposium 2013; MPI für Psychiatrie).

Hladky F, Eder M **Regulation of network activity in the amygdala by distinct classes of antidepressants** (AGNP 2013).

## Danksagung

Ich möchte mich bei Prof. Landgraf für seine Bereitschaft bedanken mein Doktorvater zu sein. Er stand mir bei der Vorbereitung dieser Arbeit jederzeit als Ansprechpartner zur Seite und hat mir geholfen diese Arbeit termingerecht einzureichen. Darüber hinaus hat er mir HAB/NAB Mäuse zur Verfügung gestellt, mit denen ich sehr interessante Daten für meine Arbeit gewinnen konnte.

Mein Dank gilt Dr. Matthias Eder für die Möglichkeit mich in seiner Arbeitsgruppe auf meine Promotion vorzubereiten. Die Diskussionen mit ihm haben meinen wissenschaftlichen Horizont erweitert. Er hatte stets ein Auge darauf, dass ich in der Planung meiner Experimente den Fokus richtig setze und mir trotzdem den Freiraum gegeben, eigene Ideen und Projekte zu verfolgen.

Ich möchte mich bei Prof. Boyan bedanken, dass er sich sofort bereit erklärt hat als Zweitgutachter dieser Arbeit mitzuwirken.

Bei Prof. Holsboer möchte ich mich für die finanzielle Unterstützung meiner Projekte bedanken.

Ich danke Dr. Dine für inspirierende wissenschaftliche Diskussionen und seine Anregungen dieses Manuskript betreffend.

Ich möchte mich bei meinen Kollegen in der „AG Dynamik neuronaler Netzwerke“ für die gute Zusammenarbeit bedanken.

Innerhalb des MPI für Psychiatrie möchte ich mich bei Dr. Wotjak und Dr. Deussing für die erfolgreiche Zusammenarbeit bedanken.

Ich danke Frau Carola Hetzel für ihre Anregungen bezüglich der englischen Sprache in diesem Manuskript.

**Erklärung**

Hiermit erkläre ich an Eides statt, dass die vorgelegte Dissertation von mir selbstständig und ohne unerlaubte Hilfsmittel angefertigt wurde.

Alle Ausführungen, die wörtlich oder sinngemäß übernommen wurden, sind als solche gekennzeichnet.

Des Weiteren erkläre ich, dass ich nicht anderweitig ohne Erfolg versucht habe, eine Dissertation einzureichen oder mich der Doktorprüfung zu unterziehen. Die vorliegende Dissertation liegt weder ganz, noch in wesentlichen Teilen einer anderen Prüfungskommission vor.

München, den 07.11.2013



Florian Hladky